UNIVERSITY OF CALIFORNIA, SAN DIEGO

SAN DIEGO STATE UNIVERSITY

First X-ray crystal structure of an insect muscle myosin

A dissertation submitted in partial satisfaction of the

requirements for the degree Doctor of Philosophy

in

Chemistry

by

James Tore Caldwell

Committee in charge:

San Diego State University

Professor Tom Huxford, Chair
Professor Sanford Bernstein
Professor Peter van der Geer

University of California, San Diego

Professor Ju Chen
Professor Simpson Joseph
Professor Andrew Kummel

2013

The dissertation of James Tore Caldwell is approved, and it is acceptable in quality and form for publication on microfilm and electronically:

Chair

University of California, San Diego

San Diego State University

2013

Dedication

In recognition of the time spent for my college education, away from my wonderful mother, Virginia Caldwell, and my son, Andrew Caldwell, I dedicate this dissertation to them. They have been a wonderful source of support and encouragement throughout the years living in California while working on my degree.

Table of Contents

List of Figures

List of Tables

Acknowledgements

I acknowledge Professor Tom Huxford for his support as the chair of my committee. His hard won knowledge, encouragement, and guidance has been invaluable. I acknowledge Professor Sanford Bernstein for his leadership, wisdom, and support. Our collaboration has made this dissertation possible.

I acknowledge Jennifer Suggs, who taught me many lab procedures during my collaboration in the Bernstein lab. Her knowledge and practical experience with fly husbandry and molecular biology was the most valuable. She helped me understand many concepts and protocols through my sometimes relentless questioning. Her patience in answering hundreds of my questions was without a doubt stoic!

I acknowledge Bill Kronert, his knowledge was a great asset with the molecular biology strategy and he completed several ligations that proved extremely difficult, moving the project forward when I could not.

Girish Melkani lent his expertise in purification of myosin and proteolysis of myosin to S1. He provided data for myosin ATPase experiments. Tony Cammarato produced electron micrographs of single molecule honeybee myosin and gave guidance in myosin purification. Anju Melkani provided technical instruction for microdissection and fly husbandry. She provided results from the *in vitro* sliding motility assay. Norm Zhu and Art Hauenstein provided great

conversations and shared their practical knowledge of HPLC and X-ray crystallography techniques. I acknowledge B. Cudney for advice, encouragement and Hampton Research product samples, J. Jenkins of TTP LabTech for the demo day with the Mosquito crystallization robot, J. Schuermann of NE CAT for assistance with synchrotron data collection, J. Headd for help with Molprobity and KiNG refinement software, and J. Vertrees for help with PyMOL software.

Chapter 4, in full, is a reprint of the material as it appears in Methods: Focusing on Rapidly Developing Techniques, Volume 56, Issue 1, January 2012, pages 25-32. Caldwell, JT., Melkani, G.C., Huxford, T., Bernstein, S.I. The dissertation author was the primary investigator and author of this paper.

Curriculum Vita and Publications

EDUCATION

2006 - 2013 **Doctor of Philosophy Degree: Chemistry**
Department of Chemistry and Biochemistry
Joint Doctoral Program between San Diego State University and University of California, San Diego

2010 **Master of Arts Degree: Chemistry**
San Diego State University

2005 - 2006 **Masters Student: Department of Chemistry and Biochemistry**
San Diego State University

2004 **Bachelors Degree: Biology with a minor in Chemistry**
Northern Illinois University

2004 - 2002 **Bachelors Student: Biology and Chemistry**
Northern Illinois University

1999 - 2000 **Bachelors Student: Biology**
Rockford College

PROFESSIONAL EXPERIENCE

2006 - 2013 **Doctoral Student: Structural Biology Lab**
Department of Chemistry and Biochemistry
San Diego State University and University of California, San Diego

2010 - 2013 **Research Associate,** Department of Biology
San Diego State University

2007 - 2009 **Graduate Teaching Assistant**
Department of Chemistry and Biochemistry
San Diego State University

2006 - 2007 **Graduate Teaching Assistant**
Department of Chemistry and Biochemistry
University of California, San Diego

2005 - 2006 **Graduate Teaching Assistant**
Department of Chemistry and Biochemistry
San Diego State University

AWARDS

2004 Graduated *Summa Cum Laude* (Northern Illinois University)

PUBLICATIONS

Caldwell JT, Melkani GC, Huxford T, and Bernstein SI. (2012). Transgenic expression and purification of myosin isoforms using the Drosophila melanogaster indirect flight muscle system. Methods. 56(1):25-32

Yasui LS, Chen K, Wang K, Jones TP, **Caldwell J**, Guse D, and Kassis AI. Using Hoechst 33342 to target radioactivity to the cell nucleus. Radiation Research 167(2):167-75.

PUBLICATIONS (IN PREPARATION)

Caldwell JT, Melkani GC, Bernstein SI and Huxford T. X-ray Structure Determination of the First Insect Muscle Myosin II (In Preparation)

CONFERENCE ABSTRACTS / POSTERS

1) **Caldwell JT**, Melkani GC, Huxford T, and Bernstein SI. (4/2012) A Method for the Transgenic Expression and Purification of Skeletal Muscle Cell and Molecular Biology Symposium, San Diego State University
2) **Caldwell JT**, Melkani GC, Huxford T, and Bernstein SI. (4/21-25/2012) Transgenic Expression and Purification of Myosin Isoforms Using the *Drosophila melanogaster* Indirect Flight Muscle System, Experimental Biology 2012, San Diego, CA
3) **Caldwell JT**, Melkani GC, Huxford T, and Bernstein SI. (2/25-29/2012) Muscle Myosin II Isoforms Using *Drosophila Melanogaster***.** *Biophysical Society 56th Annual Meeting*. San Diego, CA
4) **Caldwell JT**, Melkani GC, Lee C, Huxford T, and Bernstein SI. (3/4/2011) The application of *Drosophila melanogaster* as an expression system for transgenic myosin.
   Student Research Symposium, San Diego State University
5) **Caldwell, JT**, Huxford, T, Bernstein, SI. (April 24, 2009)
   Purification of Sub-fragment 1 of Indirect Flight Muscle Myosin II from *Apis mellifera*.
   Cell and Molecular Biology Symposium, San Diego State University

SDSU CHEMISTRY & BIOCHEMISTRY GRADUATE SEMINARS

1) Oct 18, 2013 X-ray Structure Determination of the First Insect Muscle Myosin II
2) Oct 5, 2012 Transgenic Expression and Purification of Skeletal Muscle Myosin II from *Drosophila melanogaster* for the Purpose of Producing a Molecular Model through X-ray Crystallography.
3) Sept 30, 2011 Transgenic Expression and Purification of Myosin Isoforms using the *Drosophila melanogaster* Indirect Flight Muscle System

4) Oct 1, 2010 Purification of Insect Muscle Myosin for X-ray Crystallography to Determine Molecular Mechanism
5) Sep 25, 2009 Purification of Insect Muscle Myosin for X-ray Crystallography to Determine Molecular Mechanism
6) Sept 12, 2008 Structural Studies on Insect Indirect Flight Muscle myosin.

Abstract of the Dissertation

First X-ray crystal structure of an insect muscle myosin

by

James Tore Caldwell

Doctor of Philosophy in Chemistry

University of California, San Diego, 2013
San Diego State University, 2013

Professor Tom Huxford, Chair

Variation in myosin heavy chain generates muscle fiber functional diversity. The results of 30 years of experimental investigation by the Bernstein lab and others provides evidence that supports many novel nuances in the mechanochemical mechanism of myosin due to the alternative exon splicing and mutations of the myosin gene in *Drosophila melanogaster.* Their *in vivo* and *in vitro* studies have characterized many functional differences. Biophysical and

structural studies on muscle myosin rely upon milligram quantities of extremely pure material. However, many biologically interesting myosin isoforms are expressed at levels that are too low for direct purification from primary tissues. Efforts aimed at recombinant expression of functional striated muscle myosin isoforms in bacterial or insect cell culture has largely met with failure, although high-level expression in muscle cell culture has recently been achieved at significant expense (Resnicow, Deacon et al. 2010). We have developed a novel method for the use of strains of the fruit fly *Drosophila melanogaster* genetically engineered to produce histidine-tagged recombinant muscle myosin isoforms (Caldwell, Melkani et al. 2012). This method takes advantage of the single muscle myosin heavy chain gene within the *Drosophila* genome, the high level of expression of accessible myosin in the thoracic indirect flight muscles, the ability to knock out endogenous expression of myosin in this tissue and the relatively low cost of fruit fly colony production and maintenance. We illustrate this method by expressing and purifying recombinant histidine-tagged variant of embryonic body wall skeletal muscle myosin II from an engineered fly strain. The recombinant protein shows the expected ATPase activity and is of sufficient purity and homogeneity for crystallization. The X-ray structure of the first insect muscle myosin is solved using this method. This system may prove useful for the expression and isolation of mutant myosins associated with skeletal muscle diseases and cardiomyopathies for their biochemical and structural characterization.

Chapter 1

Introduction

1.1. Purpose

Myosin II is one of the most abundant proteins in the body and is responsible for producing the contractile force in muscle movement and heart contractions. Myosin II mutations can cause severe human cardiomyopathies and skeletal myopathies. The purpose of this dissertation is to contribute to the understanding of myosin's molecular mechanism by developing a deeper understanding of the structure-function relationship. Much of science involves describing things we cannot see, and no method has revealed more about the hidden world of molecular structures than X-ray crystallography (Blow 2002). It is our goal to probe the molecular structure of *Drosophila melanogaster* skeletal muscle myosin II through X-ray crystallography to investigate the roles of specific amino acids or whole domains in the mechanochemical cycle of muscle contraction.

We set out to purify myosin for X-ray crystallography structural determination. Several goals needed to be reached to make this happen: milligram quantities of purified myosin were needed, a crystallization condition had to be found, and the structure needed to be solved. Initially, several problem areas arose and needed to be surpassed. First, the quantities of purified myosin needed for crystal trials were not accessible with the then current microdissection technology. Second, that even with refined, purified myosin, and the current state of macromolecular crystallization, while successful in perhaps 40% of

cases, was by no means a guarantee to produce diffraction quality crystals (McPherson 1995). Finally, that even with diffraction data in hand the phase problem must be solved to determine the crystal structure. This dissertation includes the achievements made to overcome the above problems in order to attain a high-resolution crystal structure of myosin. This introductory chapter provides a brief overview of muscle, muscle contraction, myosin heavy chain structure and X-ray crystal structures. In addition, the advantages of the *Drosophila melanogaster* model system are covered.

1.2. Muscle

Animation, defined as the quality of liveliness, vivacity, the condition of being alive- brings to mind one word, motion. Movement through space is fundamental to animal life, but of course there are many large life forms that do not have muscle, mainly plants. Animal movement is accomplished by muscle. Muscle acts simply by drawing its ends closer together or at least pulling on its ends trying to bring them closer.

Muscle makes up fully 40% of a human body that is in decent physical shape (Vogel and de Ferrari 2001). Humans have three types of muscle tissue: striated skeletal muscle, striated cardiac muscle and smooth muscle. Muscle disease can be caused by mutations in many different contractile proteins, including myosin. Numerous muscle and non-muscle myosin mutations have been identified in the myosin heavy chain and linked to diseases such as:

deafness, Freeman-Sheldon syndrome, Griscelli syndrome (characterized by defects in pigmentation and neuronal defects), hypertrophic and dilated cardiac myopathies (Hartman and Spudich 2012). Treatment of disease by improving myosin function is therefore a viable option. Omecamtiv mecarbil, a small molecule activator specific for cardiac myosin is currently in clinical trails for treatment of systolic heart failure (Malik, Hartman et al. 2011, Kull and Endow 2013).

A wide range of physiological tasks is accomplished by a vast array of different types of muscle. The two main categories are striated or smooth, depending on the appearance of the muscle cell (myocyte) with light microscopy. The striated myocyte appears striped with light and dark bands due to overlapping filaments regularly arranged in the cell. In smooth muscle these myofilaments are not arranged regularly but rather in a spiral fashion (Hill and Olson 2012).

There are two types of striated muscle: cardiac and skeletal. Skeletal muscle cells are long multi-nucleate fibers formed from the fusion of many cells during development. In humans, a single cell or muscle fiber, can be a several centimeters long with hundreds of nuclei. Each fiber contains many myofibrils arranged longitudinally. There may be a few hundred to thousands of myofibrils in a single cell. The myofibrils run the length of the cell and are 1-2 μM in diameter. The myofibrils are further comprised of two types of much smaller interdigitating myofilaments. Thick filaments are made mainly of myosin

arranged in an antiparallel bundle. Thin filaments are made mainly of a double strand of actin.

In the animal kingdom, muscle creates movement with a variety of highly specialized forms of skeletal muscle. All types of muscle have the common feature of actin and myosin myofilaments sliding past one another during a muscle contraction. However, “muscle contraction” is not as an appropriate term as “muscle shortening” would be, especially when a “contracted” muscle looks thicker and perhaps larger! Since the time of the ancient Greeks (300 BC), muscle was thought to be filled with fluid during a contraction. In 1667, Jan Swammerdam, a Dutch anatomist (famous for demonstrating that the various forms of an insect, the egg, larva, pupa, and adult, were all the same organism undergoing metamorphosis), placed a frog thigh muscle in a glass syringe filled with water and “irritated” the nerve causing a contraction and the level of water surrounding the muscle did not change, thereby disproving the fluid filled contraction theory and supporting his hypothesis that the volume of the muscle was constant during contraction (Cobb 2002). Isovolumetric muscle has been studied intensively ever since.

1.3. The mechanism of muscle contraction

> Since antiquity, motion has been looked upon as the index of life. The organ of motion is muscle. Our present understanding of the mechanism of contraction is based on three fundamental discoveries, all arising from studies on striated muscle. The modern era began with the demonstration that contraction is the result of the interaction of two proteins, actin and myosin with ATP, and that contraction can

> be reproduced *in vitro* with purified proteins. The second fundamental advance was the sliding filament theory, which established that shortening and power production are the result of interactions between actin and myosin filaments, each containing several hundreds of molecules and that this interaction proceeds by sliding without any change in filament lengths. Third, the atomic structures arising from the crystallization of actin and myosin now allow one to search for the changes in molecular structure that account for force production. (Szent-Gyorgyi 2004)

The basic myofibril structural unit of striated muscle contraction is the sarcomere (Figure 1.1). The sarcomere has lateral boundaries called Z-discs, also known as Z-lines or Z-bands ("Z" for "Zwischenscheibe", *the disc in between* the I-bands). The thin filaments (+) "barbed" ends are anchored in the Z-discs and their (-) ends project inward towards the center of the sarcomere and the M-line (M for "Mittelscheibe", the disc in the *middle* of the sarcomere). The light area next to the Z-disc is known as the I-band (called *I* band because they are *i*sotropic when viewed with polarized light), this is where the thick filaments do not reach at rest (relaxed muscle). The dark area, known as the A-band (*A*-band for *a*nisotropic), in the central region of the sarcomere corresponds to the length of the thick filaments. The thick filaments interdigitate with the thin filaments in a highly ordered macromolecular array. Since the 1950s, it was determined that the length of the myofilaments do not change during contraction but rather they slide past each other drawing the Z-discs closer together thereby shortening the sarcomere, which originated the sliding filament model of muscle contraction (Huxley and Niedergerke 1954, Huxley and Hanson 1954).

At the single molecule level of muscle contraction, myosin does the work.

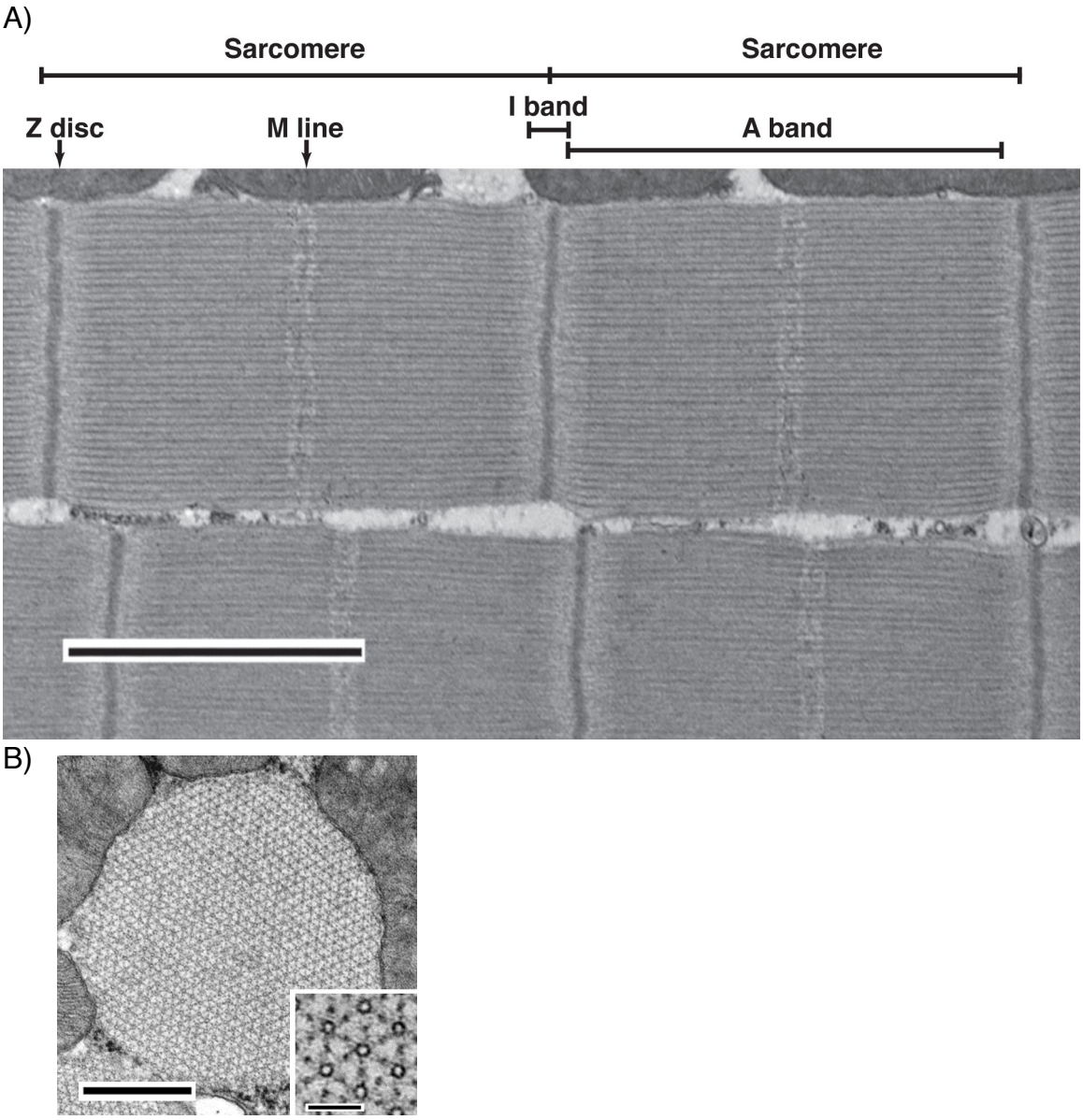

Figure 1.1: Ultrastructure of *Drosophila* indirect flight muscle

A) Transmission electron micrograph of the striated myofibrils showing sarcomeric structure. The sarcomeres are bounded on either end by the Z-discs and are bisected by the M-line. The thick filaments in the A-band stretch nearly the entire length of the sarcomere so that very small I-bands are present. Bar = 2.00 μm
B) Cross section through the indirect flight muscle myofibril. The higher power photo inset shows the double hexagonal array of thick (hollow) and thin filaments. Bar = 0.500 μm. Bar = 0.050 μm in inset of Panel B. (Figure 1.1A and 1.1B provided by J. Suggs)

Myosin is a molecular motor that converts chemical energy, stored in adenosine triphosphate, to directed movement. In 1954, myosin was observed by electron microscopy and with X-ray diffraction (Huxley and Hanson 1954). The relative sliding of thick and thin filaments is brought about by the macromolecular interaction of myosin and actin. This interaction, visualized with electron microscopy, was termed “cross-bridge” by A.F. Huxley to describe the relationship between filaments and the mechanical properties of muscle (Huxley 1957).

In 1971, Lymn and Taylor proposed a simple kinetic scheme of myosin ATP hydrolysis activated by actin from which they postulated a contraction cycle with 4 states (Lymn and Taylor 1971). In state 1 (rigor-like), the contractile proteins myosin.ADP.Pi (myosin with adenosine diphosphate and inorganic phosphate bound) and actin form contacts called cross-bridges when the swinging head of myosin binds to the exposed actin. In state 2 (post-rigor), the kinetic studies they carried out had shown that ATP (adenosine triphosphate) dissociated actin from myosin. In state 3 (pre-power stroke), the recovery stroke then takes place where the myosin head resets due to ATP hydrolysis. In state 4 (top of power stroke), the subsequent rebinding of actin is followed by Pi release, the “power stroke” where a 10 nm movement takes place, and finally with ADP release (Szent-Gyorgyi 2004).

1.4. Advantages of the *Drosophila melanogaster* model system

In order to understand the mechanochemical mechanism of myosin and to investigate the affects of MHC (myosin heavy chain) isoforms on the physiological function of skeletal muscle, we have chosen the common fruit fly, *Drosophila melanogaster*. It is one of the most intensively studied organisms known. The high fecundity, short life cycle, extensive genetic tools, and availability of thousands of mutants from stock centers make *Drosophila* the best organism to serve as a model system for the investigation of many developmental and cellular processes common to humans. *Drosophila* genetics papers have been published for over 100 years and include the discovery of the chromosomal theory of heredity. It was the first major complex organism to have its genome sequenced. The 120 Mb genome encodes ~13,600 genes (Adams, Celniker et al. 2000). A few years after the fly genome, the human genome was sequenced and with the observed homologies between the two genomes, it became clearly established that Drosophila is, and always was, an excellent model to understand human disease and biology. There are known *Drosophila* orthologs for 77% of 929 human disease genes (Reiter, Potocki et al. 2001). Recently, it was established that the fly can even be effectively used for low to high throughput drug screens as well as in target discovery (Pandey and Nichols 2011).

Fly muscles are an excellent model system to tease apart the biological details of human disease. For example, the one-chambered tubular heart of the

fly has human cardiomyopathy models, which currently are being investigated by the Bernstein lab and many others (Cammarato, Ahrens et al. 2011, Qian and Bodmer 2012, Na, Musselman et al. 2013). Several new, sophisticated tools including tomography, Magnetic Resonance Imaging, and laser scanning fluorescence microscopy, have been developed to allow for the flies' hearts to be probed in detail (Choma, Izatt et al. 2006, Null, Liu et al. 2008, Bradu, Ma et al. 2009). The Bernstein lab has produced numerous papers while investigating the *Drosophila melanogaster* indirect flight muscle (IFM) system and its myosin heavy chain (*Mhc*) gene (Bernstein and Milligan 1997, Cammarato, Dambacher et al. 2008, Kronert, Dambacher et al. 2008, Kronert, Dambacher et al. 2008, Bloemink, Dambacher et al. 2009, Kronert, Melkani et al. 2010, Bloemink, Melkani et al. 2011, Kronert, Melkani et al. 2012).

Drosophila makes an excellent model organism to study muscle function and for recombinant myosin production for many reasons. First, relative to vertebrate models with multiple *Mhc* genes, the fly has only one muscle myosin heavy chain gene, with alternative RNA splicing, for production of all myosin heavy chain isoforms (Bernstein, Mogami et al. 1983, Rozek and Davidson 1983, George, Ober et al. 1989). Second, the ability to insert a recombinant gene into a specified chromosome location with the PhiC31 integrase-mediated transgenesis system (Bischof, Maeda et al. 2007). Third, that Drosophila males have no genetic recombination and that in females recombination is controlled with special, modified "balancer chromosomes". The balancer chromosomes

multiple nested inverted repeats (induced by radiation) stop recombination through disruption of the synapsis between homologous chromosomes during meiotic prophase (Greenspan 2004). The balancers have easily recognizable dominant phenotypic markers that allow for genetic crosses to be made with 100% reliability while following the invisible chromosome with the mutated or modified myosin gene. Fourth, the availability of the *Mhc*^{10} fly line, a myosin heavy chain null line for the indirect flight and jump muscles (Collier, Kronert et al. 1990). The combination of these features allows for the ability to design fly mating schemes (genetic crosses) between engineered fly lines with an IFM MHC-null fly line as a recipient to express engineered MHC proteins.

1.5. Myosin protein structure

Myosin is constructed of three domains; 1) the motor domain that binds actin and has ATPase activity, 2) the neck domain which binds light chains, and 3) the tail domain which serves to anchor and position the motor domain so it may interact with actin (Sellers 2000). Structurally, myosin heavy chain is a large asymmetric molecule: it has a globular head and a long α-helical tail.

The head is also known as the motor domain or cross-bridge. The motor domain is well conserved in myosins of various organisms and among myosins of various classes, it has a highly conserved core sequence in all myosin classes (Coluccio 2008). The head contains the ATP binding pocket and actin-binding region. Numerous X-ray crystal structures of the head have been solved. (Table

1.1) Structurally, the head is about 65 Å by 40 Å wide and 165 Å long. The various structures show a very similar protein fold with conformational changes due to differences in content of the ATP-binding pocket. They all contain a similar 7-stranded β-sheet, known as the transducer, which is surrounded by several α-helices. The actin-binding region is split by a deep cleft that opens and closes in response to ATP binding. The converter domain rotates through 60° in response to ATPase product release (Geeves and Holmes 2005). The α-helical converter is the anchor of the "lever arm", the region where the structural changes induced by ATP binding and product release are amplified (Coluccio 2008). The neck region is also known as the "lever arm"; it consists of a long α-helix, which has two IQ motifs (IQxxxRGxxxR). The IQ motifs are where the two light chains bind.

The MHC tail region, also known as the "rod", is an extremely long α-helix extending more than 1,000 residues. MHC self-assembly into dimers relies on an α-helical characteristic in the tail region. The MHC tail consists of a repetitive sequence which includes forty 28-amino-acid repeats of seven-residue units (Emerson and Bernstein 1987). The heptad repeat (a, b, c, d, e, f) has hydrophobic residues at positions (a) and (d) (McLachlan and Karn 1982). These residues form a seam between two α-helices of the coiled-coil which is further reinforced by salt bridges between charged residues at positions (e) and (g). The heptad repeats are further organized into 40 zones of non-identical 28 residue repeats that allows for the staggered arrangement in the thick filament

(McLachlan and Karn 1982). The outer surface of the coiled-coil has a high charge density with a periodic 98-residue charge distribution which promotes thick filament assembly (Emerson and Bernstein 1987). Structurally, the myosin tail domain is about 1,600 Å long and 20 Å wide that consists of two MHC tails wound together. The chemical properties of the myosin rod along with accessory proteins, such as flightin, help to assemble the thick filaments (Reedy, Bullard et al. 2000). Adult fruit flies thick filaments have a hollow core made of ~1% paramyosin and are approximately 3 μM long (Reedy and Beall 1993).

Drosophila melanogaster skeletal muscle myosin is a large (>500 kDa) heterohexamer. It is comprised of two myosin heavy chains (MHC), each with a globular head and a long α-helical rod, the shape is reminiscent of a golf club. Each heavy chain (224 kDa) has an essential light chain (ELC, also known as the myosin alkali light chain, Mlc1) (17.5 kDa) and regulatory light chain (RLC, also known as myosin light chain 2, Mlc2) (23.7 kDa) bound to the neck region (Marygold, Leyland et al. 2013). The light chains are calmodulin-like and provide buttressing and regulatory functions, see Figure 1.2.

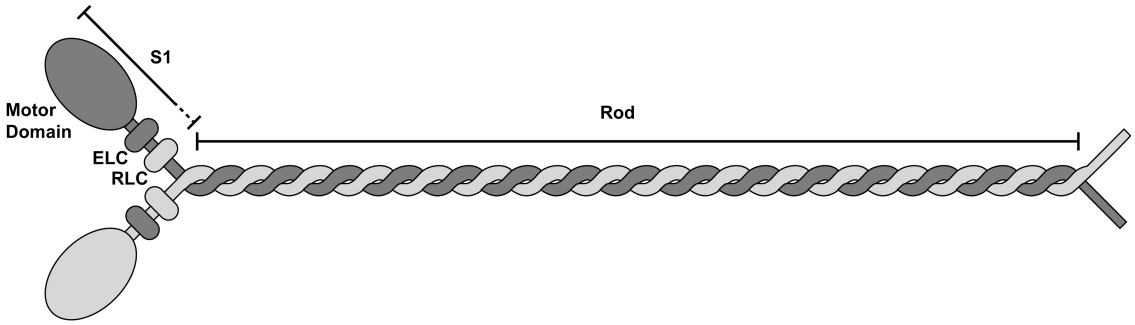

Figure 1.2: Myosin II schematic

Prior to assembly into thick filaments myosin molecules dimerize via their α-helical tail regions into the heterohexamer shown here.

Table 1.1: Table of myosin X-ray structures

Abbreviations: PDB ID: Protein Data Base identification number; M: Myosin class; S1: subfragment-1; LC: light chain; P: purified from primary tissue, EB: expressed in baculovirus; ED: expressed in *Dictyostelium*, EM: expressed in *Mus musculus*, Sf9: expressed in *Spodoptera frugiperda* cells
Ligand abbreviations: Adenosine diphosphate (ADP), Adenylyl-imidodiphosphate (AMP.PNP), Adenosine triphosphate (ATP), para-phenyl dimaleimide (*p*-PDM) o,p-dinitrophenyl aminoethyldiphosphate-beryllium trifluoride (DAE), o,p-dinitrophenyl aminopropyldiphosphate beryllium trifluoride (DAQ), o,p-dinitrophenyl aminopropyldiphosphate beryllium trifluoride (NMQ), m-nitrophenyl aminoethyldiphosphate beryllium trifluoride (MNQ), o-nitrophenyl aminoethyldiphosphate beryllium trifluoride (OPN), p-nitrophenyl aminoethyldiphosphate beryllium trifluoride (PNQ), pentabromopseudilin (PBP), 2,4-dichloro-6-(3,4,5-tribromo-1H-pyrrol- 2-yl)phenol (H70), (S)-blebbistatin (BIT), 2,3,4,6,8-pentachloro-9h-carbazol-1-ol (PCIP), (3aS)-3a-hydroxy-5-methyl-1-phenyl-1,2,3,3a-tetrahydro-4H-pyrrolo[2,3-b]quinolin-4-one (BL4), (3aS)-3a-hydroxy-7-methyl-1-phenyl-1,2,3,3a-tetrahydro-4H-pyrrolo[2,3-b]quinolin-4-one (BL6), (3aS)-3a-hydroxy-1-phenyl-1,2,3,3a-tetrahydro- 4H-pyrrolo[2,3-b]quinolin-4-one (BL7)

Description	PDB ID	Enzymatic State	Ligand	Amino Acids	Resolution (Å)	Citation
***Gallus gallus*, chicken, skeletal muscle M II, S1**						
chicken skeletal muscle, M II, S1, 2 LC, P	2MYS	post-rigor	SO_4^{2-}	800	2.8	(Rayment, Holden et al. 1993)
***Argopecten irradians*, bay scallop, striated muscle, M II, S1**						
bay scallop S1, M II, 2 LC, P	1B7T	near-rigor	ADP	835	2.5	(Houdusse, Kalabokis et al. 1999)
bay scallop S1, M II, 2 LC, P	1DFK	post-rigor	Apo (Ca^{2+})	830	4.2	(Houdusse, Szent-Gyorgyi et al. 2000)
bay scallop S1, M II, 2 LC, P	1DFL	pre-power stroke	$ADP.VO_4$	831	3.8	(Houdusse, Szent-Gyorgyi et al. 2000)
bay scallop S1, M II, 2 LC, P	1KK7	near-rigor	SO_4^{2-}	837	3.2	(Himmel, Gourinath et al. 2002)

Table 1.1: Table of myosin X-ray structures, continued

Description	PDB ID	Enzymatic State	Ligand	Amino Acids	Resolution (Å)	Citation
bay scallop S1, M II, 2 LC, P	1KK8	internally uncoupled state	ADP.BeF_x	837	2.3	(Himmel, Gourinath et al. 2002)
bay scallop S1, M II, 2 LC, P	1L2O	internally uncoupled state	ADP, *p*-PDM	835	2.8	(Himmel, Gourinath et al. 2002)
bay scallop S1, M II, 2 LC, P	1KQM	internally uncoupled state	AMP.PNP	835	3.0	(Himmel, Gourinath et al. 2002)
bay scallop S1, M II, 2 LC, P	1KWO	internally uncoupled state	ATP-γ-S, p-PDM	835	3.8	(Himmel, Gourinath et al. 2002)
bay scallop S1, M II, 2 LC, P	1QVI	pre-power stroke	ADP.VO_4	806	2.5	(Gourinath, Himmel et al. 2003)
bay scallop S1, M II, 2 LC, P	1SR6	post-rigor	SO_4^{2-}	801	2.8	(Risal, Gourinath et al. 2004)
bay scallop S1, M II, 2 LC, P	1S5G	rigor-like	ADP	840	3.1	(Risal, Gourinath et al. 2004)
***Placoplecten magellanicus*, sea scallop, M II, S1**						
slow "catch" muscle, M II, 2 LC, P	2OS8	rigor-like	Apo, Ca^{2+}, Mg	840	3.3	(Yang, Gourinath et al. 2007)
slow "catch" muscle, M II, 2 LC, P	2OTG	post-rigor	MgADP, Ca^{2+}	840	3.1	(Yang, Gourinath et al. 2007)
striated muscle, M II, 2 LC, P	2EC6	rigor-like	Apo, Ca^{2+}	838	3.3	(Yang, Gourinath et al. 2007)
***Doryteuthius pealeii*, longfin inshore squid, striated muscle, M II, S1**						
longfin squid S1, M II, Japanese squid 2 LC, P	3I5F (2OY6)	post-rigor	MgADP	839	3.1	(Yang, Gourinath et al. 2007)
longfin squid S1, M II, Japanese squid 2 LC, P	3I5G (2OVK)	rigor-like	MLI (Malonate ion)	839	2.6	(Yang, Gourinath et al. 2007)
longfin squid S1, M II, Japanese squid 2 LC, P	3I5H (2EKV)	rigor-like	Apo, Ca^{2+}	839	3.4	(Yang, Gourinath et al. 2007)
longfin squid S1, M II, Japanese squid 2 LC, P	3I5I (2EKW)	rigor-like	SO_4^{2-}, Ca^{2+}	839	3.3	(Yang, Gourinath et al. 2007)

Table 1.1: Table of myosin X-ray structures, continued

Description	PDB ID	Enzymatic State	Ligand	Amino Acids	Resolution (Å)	Citation
***Dictyostelium discoideum*, slime mold, M II, S1**						
M II, 0 LC (ED)	1MMD	post-rigor	ADP.BeF_x	733	2.0	(Fisher, Smith et al. 1995)
M II, 0 LC (ED)	1MND	pre-power stroke	ADP.AlF_4^-	762	2.6	(Fisher, Smith et al. 1995)
M II, 0 LC (ED)	1MNE	post-rigor	$H_2P_2O_7$ POP	762	2.7	(Smith and Rayment 1995)
M II, 0 LC (ED)	1VOM	pre-power stroke	ADP.VO_4	730	1.9	(Smith and Rayment 1996)
M II, 0 LC (ED)	1MMA	post-rigor	ADP	719	2.1	(Gulick, Bauer et al. 1997)
M II, 0 LC (ED)	1MMG	post-rigor	ATP.γS	741	2.1	(Gulick, Bauer et al. 1997)
M II, 0 LC (ED)	1MMN	post-rigor	AMP.PNP	737	2.1	(Gulick, Bauer et al. 1997)
M II, 0 LC (ED)	1LVK	post-rigor	mant-ADP.BeF_x	762	1.9	(Bauer, Kuhlman et al. 1997)
M II, 0 LC (ED)	1D0X	post-rigor	MNQ	761	2.0	(Gulick, Bauer et al. 2000)
M II, 0 LC (ED)	1D0Y	post-rigor	ONP	761	2.0	(Gulick, Bauer et al. 2000)
M II, 0 LC (ED)	1D0Z	post-rigor	PNQ	761	2.0	(Gulick, Bauer et al. 2000)
M II, 0 LC (ED)	1D1A	post-rigor	DAE	761	2.0	(Gulick, Bauer et al. 2000)
M II, 0 LC (ED)	1D1B	post-rigor	DAQ	761	2.0	(Gulick, Bauer et al. 2000)
M II, 0 LC (ED)	1D1C	post-rigor	NMQ	761	2.3	(Gulick, Bauer et al. 2000)
M II, 0 LC (ED)	1FMV	post-rigor	APO	761	2.1	(Bauer, Holden et al. 2000)
M II, 0 LC (ED)	1FMW	post-rigor	ATP	761	2.2	(Bauer, Holden et al. 2000)
M II, engineered lever arm (ED)	1G8X	"open" conformation	ADP	1010	2.8	(Kliche, Fujita-Becker et al. 2001)
M II, (with attached dynamin A GTPase domain) (ED)	1JWY	only the dynamin structure was analyzed	ADP and BCG (beta-D-glucose)	776	2.30	(Niemann, Knetsch et al. 2001)

Table 1.1: Table of myosin X-ray structures, continued

Description	PDB ID	Enzymatic State	Ligand	Amino Acids	Resolution (Å)	Citation
M II, (with attached dynamin A GTPase domain) (ED)	1JX2	only the dynamin structure was analyzed	ADP and BGC (beta-D-glucose)	776	2.30	(Niemann, Knetsch et al. 2001)
M II, (with attached rat dynamin GTPase domain) (ED)	1Q5G	rigor-like	apo	763	1.9	(Reubold, Eschenburg et al. 2003)
M II, 0 LC (ED)	1YV3	pre-power stroke	ADP.VO_4 BIT	762	2.0	(Allingham, Smith et al. 2005)
M II, 0 LC (EB) S456Y mutant	1W9I	post-rigor	ADP.BeF_3	754	1.8	(Morris, Coureux, Well, Houdesse, Sweeney) unpublished
M II, 0 LC (EB) S456Y mutant	1W9J	pre-power stroke	ADP.AlF_4	766	2.0	(Morris, Coureux, Well, Houdesse, Sweeney) unpublished
M II, 0 LC (EB) S456E mutant	1W9K	post-rigor	ADP.BeF_3	759	2.1	(Morris, Coureux, Well, Houdesse, Sweeney) unpublished
M II, 0 LC (EB) S456E mutant	1W9L	pre-power stroke	ADP.AlF_4	759	2.0	(Morris, Coureux, Well, Houdesse, Sweeney) unpublished
M II, 0 LC (ED)	3BZ7	pre-power stroke	ADP.VO_4 BL4	762	2.00	(Lucas-Lopez, Allingham et al. 2008)
M II, 0 LC (ED)	3BZ8	pre-power stroke	ADP.VO_4 BL6	762	2.20	(Lucas-Lopez, Allingham et al. 2008)
M II, 0 LC (ED)	3BZ9	pre-power stroke	ADP.VO_4 BL7	762	2.10	(Lucas-Lopez, Allingham et al. 2008)
M II, 0 LC (ED)	2JHR	pre-power stroke	ADP.AlF_4 (meta) PBP	788	2.80	(Fedorov, Bohl et al. 2009)
M II, 0 LC (ED)	2JJ9	pre-power stroke	ADP.AlF_4 (meta)	788	2.30	(Fedorov, Bohl et al. 2009)
M II, 0 LC (ED)	3MJX	pre-power stroke	ADP.AlF_4 BIT	788	2.20	(Fedorov, Bohl et al. 2009)
M II, 0 LC (ED)	3MYH	pre-power stroke closed sw II	ADP.AlF4 BIT	762	2.01	(Frye, Klenchin et al. 2010)

Table 1.1: Table of myosin X-ray structures, continued

Description	PDB ID	Enzymatic State	Ligand	Amino Acids	Resolution (Å)	Citation
M II, 0 LC (ED)	3MYK	pre-power stroke closed sw II	ANP BIT	762	1.84	(Frye, Klenchin et al. 2010)
M II, 0 LC (ED)	3MYL	open sw II	$H_2P_2O_7$, POP	762	2.00	(Frye, Klenchin et al. 2010)
M II, 0 LC (ED)	3MNQ	pre-power stroke	ADP.AlF_4 (meta) resveratrol	788	2.20	(Schneider, Manstein et al.) unpublished
M II, 0 LC (ED)	2X9H	pre-power stroke	ADP.AlF_4 (meta) (PCIP)	695	2.70	(Fedorov, Manstein et al.) unpublished
M II, 0 LC (ED)	2XO8	pre-power stroke	ADP.VO_4 H70	776	2.40	(Preller, Chinthalapudi et al. 2011)
M II, 0 LC (EB)	2XEL	pre-power stroke	ADP.VO_4 IA2	776	2.5	(Chinthalapudi, Taft et al. 2011)
M II, 0 LC (ED) G680A	2Y0R	pre-power stroke	none	758	2.85	(Preller, Bauer et al. 2011)
M II, 0 LC (ED) G680A	2Y8I	pre-power stroke	ADP	758	3.13	(Preller, Bauer et al. 2011)
M II, 0 LC (ED) G680V	2Y9E	pre-power stroke	none	758	3.402	(Preller, Bauer et al. 2011)
M II, 0 LC (ED)	4AE3	pre-power stroke	ADP.VO_4 (ortho) 27X	776	2.50	(Chinthalapudi, Heissler, Fenical, Manstein) unpublished
***Gallus gallus*, chicken, smooth muscle M II, S1**						
M II, 1 LC (EB)	1BR1	pre-power stroke	ADP.AlF_4	787	3.5	(Dominguez, Freyzon et al. 1998)
M II, 0 LC (EB)	1BR2	pre-power stroke	ADP.AlF_4	673	2.9	(Dominguez, Freyzon et al. 1998)
M II, 1 LC (EB)	1BR4	pre-power stroke	ADP.BeF_x	781	3.6	(Dominguez, Freyzon et al. 1998)
***Homo sapiens*, human, cardiac muscle, beta isoform, M VII**						
M II, 0 LC, (EM)	4DB1	AMP.PNP	AMP.PNP	783	2.60	(Klenchin, Rayment et al. 2012) unpublished
***Sus scrota*, pig, M VI**						
M VI, with *Drosophila* calmodulin (Sf9)	2BKH	post-rigor (end of power stroke)	Glycerol, Ca^{2+}	814	2.4	(Menetrey, Bahloul et al. 2005)

Table 1.1: Table of myosin X-ray structures, continued

Description	PDB ID	Enzymatic State	Ligand	Amino Acids	Resolution (Å)	Citation
M VI, with chicken calmodulin (Sf9)	2BKI	(end of power stroke)	SO_4^{2-}, Ca^{2+}	858	2.9	(Menetrey, Bahloul et al. 2005)
***Gallus gallus*, chicken, smooth muscle M V, S1**						
M V, 1 LC (EB)	1OE9	rigor-like closed-cleft state	SO_4^{2-}	792	2.1	(Coureux, Wells et al. 2003)
M V, 1 LC (EB)	1W7I	actin-bound myosin state	ADP	792	3.0	(Coureux, Sweeney et al. 2004)
M V, 1 LC (EB)	1W7J	post-rigor	$ADP.BeF_3$	792	2.0	(Coureux, Sweeney et al. 2004)
M V, 0 LC (EB)	1W8J	rigor-like	SO_4^{2-}	766	2.7	(Coureux, Sweeney et al. 2004)
***Dictyostelium discoideum*, slime mold, M I, S1**						
M I, *MyoE* (ED)	1LKX	pre-power stroke	$ADP.VO_4$	697	3.0	(Kollmar et al., 2002);

1.6. Myosin sub-fragment 1 crystal structures

In this section I will cover the knowledge base obtained from the study of myosin structures determined by X-ray crystallography (see Table 1.1).

Obtaining the first high-resolution structure of myosin (2MYS) in 1993 was a heroic effort by Ivan Rayment's lab at the University of Wisconsin. They overcame many crystallization problems during a ten year period: purification of myosin with two ELC isozymes (both were in the crystal, one had an additional 41 residues on the N terminus) from chicken pectoralis muscle, the 520 kDa size of the molecule, and the heterogeneity of the protein due to it being a product of proteolysis. The production of myosin amenable to crystallization required the chemical modification of the lysine residues by reductive methylation. Amazingly, for each purification trial, the Rayment lab, prepared and then set up approximately 700 mg of S1 for crystallization (Rayment, Rypniewski et al. 1993).

In 1995, Fisher and Rayment et al., solved 2 structures of the truncated head of myosin II from *Dictyostelium discoideum*, a type of slime mold or soil amoeba, with ATP analogs: beryllium fluoride with magnesium ADP (1MMD), and aluminum fluoride with magnesium ADP (1MND). These crystal structures revealed for the first time, with 2.0 Å data, which amino acids defined the active site (Fisher, Smith et al. 1995). It was determined that the gamma phosphate binding site is located in the middle of the large β-sheet that forms the major structural motif in the myosin head and lies at the C-terminal end of the central

β-strand. The 1MND structure with aluminum fluoride indicated that myosin undergoes a conformational change during hydrolysis that is not associated with the nucleotide-binding pocket but rather occurs in the C-terminal region of the motor domain. The Rayment lab continued with the 1MNE structure that contained pyrophosphate which verified that the conformational change of actomyosin caused by ATP binding is due to the beta and gamma phosphate groups binding (Smith and Rayment 1995).

In 1995, Smith and Rayment published the next structure, 1VOM, with the highest resolution yet, a 1.8 Å vanadate-trapped ADP complex of *Dictyostelium discoideum* S1 (S1dC). This structure confirmed that vanadate puts myosin in a configuration that is a model for the transition state and it demonstrated the water placement surrounding the gamma phosphate pocket. A water molecule is stabilized in the appropriate position for an in-line nucleophilic attack on the γ-phosphorous of ATP (Fisher, Smith et al. 1995).

The Rayment lab continued to investigate the nucleotide binding of *Dictyostelium discoideum* myosin S1 with three more ATP analogs; two nonhydrolyzable nucleotide analogs, AMP-PNP and $ATP_{\gamma}S$, and a structure with the product of nucleotide hydrolysis, ADP. The most striking result of these structures was the similarity of the structures nucleotide binding pocket root mean square (rms) differences even thought the analogs have physiologically contrasting affects (Dantzig, Walker et al. 1988, Schoenberg 1989, Resetar and Chalovich 1995). The values were reported as 0.17 Å between the AMP-PNP

and $ATP_{\gamma}S$ structures (AMP-PNP leaves myosin in a strongly bound state whereas $ATP_{\gamma}S$ dissociates myosin from actin and leaves it in a weakly bound state), 0.24 Å between the AMP-PNP and ADP structures (the myosin-ADP complex is presumed to be in a strongly bound state for the start of the power stroke), and 0.21 Å between $ATP_{\gamma}S$ and ADP (Geeves 1991, Gulick, Bauer et al. 1997). The conclusions were the similarity of the structures has implications for understanding the physiological effects of the analogs and the imposed limits on the structural states available to myosin (Gulick, Bauer et al. 1997). Interestingly, Rayment reported MgATP could be diffused into crystals of S1dC-$MgPP_i$ without immediate damage to the crystals (C.B. Bauer and I. Rayment unpublished results).

The 1LVY structure of *Dictyostelium discoideum* S1 (S1dC) was complexed with mant-ADP and beryllium fluoride. The fluorescence spectroscopic study of the kinetic mechanism of myosin with Mant (2'(3')-O-(N -methylanthraniloyl)) labeled nucleotides, mimicking ATP, has proven to be very useful (Hiratsuka 1983). Using acrylamide quenching of the fluorescence emission, mant-ATP was used to investigate the exposure of bound ATP/ADP in the nucleotide-binding pocket of S1dC. It was found that the fluorophore was relatively exposed and protruded through the nucleotide binding cleft, which allowed quenching by solvent contact (Bauer, Kuhlman et al. 1997).

In an effort to parse out the nucleotide base binding interactions of the nucleotide-binding groove, Gulick et al., determined the crystal structures of

Dictyostelium discoideum S1 complexed with six non-nucleotide analogs. The systematic study of these six nanologs allowed for the identification of the contributions of the triphosphate, ribose, and adenosine moieties of ATP to the binding affinity of a nucleotide or analog to the active site (Gulick, Bauer et al. 2000). The kinetic properties of these six analogs were studied extensively and with the combination of the structural data suggested that small changes in analog binding in the active site was sufficient to abolish muscle tension or movement although the analogs were hydrolyzed readily.

In 1999, Dominguez et al., reported the first crystal structures of an expressed chicken smooth muscle motor domain (MD) with bound MgADP.AlF_4^-, as well as an MD-essential light chain complex (MDE) with two different nucleotide analogs, MgADP.AlF_4^- (an ADP.Pi analog) and MgADP.BeF_x (an ATP analog) bound in the active site (Dominguez, Freyzon et al. 1998). Although the structures contained different nucleotide analogs, which could have caused significant conformational changes, the structures were found to be remarkably similar. The similarity of the structures combined with the fact that both analogs produce weak binding states raise the possibility that MgATP binding, and not hydrolysis, may cause the lever arm to move into the pre-power stroke state (Dominguez, Freyzon et al. 1998).

In 1999, Anne Houdusse et al., published the first scallop, ADP bound, striated muscle myosin crystal structure. The conformation was unlike any myosin structure previously published and was thought to represent myosin in

the state just after it bound ATP and released from actin. Myosin was complexed with ADP and was described as in a detached state with the SH1 helix melted, which corresponds to a weakly bound, long-lived ATP state. However, the authors stated that for this and all the previous structures, the precise relationship between the conformation of the models and their correspondence to a specific step in the enzymatic cycle had not been established (Houdusse, Kalabokis et al. 1999).

Houdusse et al., went on to describe two more structures of scallop striated muscle S1, 1DFK and 1DFL, however these were of low resolution from 4 Å data. The 1DFK 4.2 Å structure was described as a near-rigor nucleotide free state due to the correlation of the lever arm position to the three-dimensional reconstructions of S1-actin complexes (Rayment, Holden et al. 1993). The 1DFL 3.8 Å structure was described as a transition state with a primed lever arm which corresponds to a pre-power stroke conformation before phosphate release (Houdusse, Szent-Gyorgyi et al. 2000).

Bauer and Rayment continued to solve more structures of *Dictyostelium* S1. In 2000, they published the structures of the motor domain (MD) in a nucleotide free state (1FMV) and another complexed with MgATP (1FMW). The ATP was soaked into the lattice after crystal formation. It was noted for this ATP bound structure that very little hydrolysis took place in the crystal even though the myosin in solution was fully active (Bauer, Holden et al. 2000). The apo structure had the “open conformation” and this conformation remained even after ATP

binding because the conformation would not allow for ATP hydrolysis. After a structural analysis of the conformation and nucleotide binding arrangement the mechanochemical state was determined to be “pre-hydrolysis” for these and previous structures such as 2MYS (chicken S1), 1MMG (S1dC.MgATP.γS), 1MMN (S1dC.AMP.PNP) and 1MND (S1dC.ADP.BeF_x) (Bauer, Holden et al. 2000).

In 2001, Kliche, et al., performed an experiment to determine if a myosin S1 fusion construct could be used as a platform for crystallization and rapid structure determination. The structure of a genetically engineered myosin with α-actin repeats 1 and 2 (in place of the myosin lever arm) was expressed in *Dictyostelium discoideum*. The engineered protein included a 7xHis-tag on the C-terminus and a R238E mutation. The mutation of the positively charged Arginine residue to a negatively charged Glutamate residue disrupted a salt bridge between switch 1 and switch 2, which was essential for nucleotide hydrolysis and a “closed” myosin conformation. The salt bridge is conserved in both myosin and kinesin motors (Onishi, Ohki et al. 2002). The engineered protein structure was solved at 2.0 Å resolution, however the non-mutated construct did not produce diffraction quality crystals (Kliche, Fujita-Becker et al. 2001). Also mentioned in this paper was the fact that myosin, kinesin and the G-protein family of molecular motors have 3 highly conserved structural and sequential motifs. These motifs surrounding the nucleotide binding site include the P-loop (conserved sequence GxxxxGKS/T), which binds to the α- and β-

phosphates of the nucleotide, and switch I (NxxSSR) and switch II (DxxGxE), which sense the presence or absence of the γ-phosphate (Kliche, Fujita-Becker et al. 2001).

The 1JWY and 1JX2 dynamin protein structures were solved with a novel "myosin fusion approach". The 96 kDa dynamin (2-316) was engineered to express at the C-terminus of the myosin II motor domain (3-765) in *Dictyostelium discoideum*. The established *Dictyostelium discoideum* myosin purification protocol was used to purify the fusion construct. The N-terminus His-tag myosin (with fusion protein) was separated from the bulk cytosolic lysate by pelleting it with actin. The pellet was homogenized with ATP to dissociate the actin and myosin and then centrifuged to separate insoluble proteins and any remaining acto-myosin. The supernatant was applied to a Ni-NTA column, which was washed and eluted with imidazole. The purified fusion protein was flash frozen and stored at -80 °C until needed (Manstein and Hunt 1995, Manstein, Schuster et al. 1995). It was noted that myosin, used as a purification and crystallization "tag", led to enhanced expression and simplified crystallographic phase determination by molecular replacement (Niemann, Knetsch et al. 2001).

In 2002, Himmel, Cohen, et al., published five structures of scallop myosin S1. All five structures had an unwound SH1 helix, despite various ATP analogs and cross-linking with para-phenyl dimaleimide (*p*-PDM). The IKK7, 1KQM, 1L2O, 1KWO structures all had a "internally uncoupled" state characterized by an

unwound SH1 helix, an extended switch II loop (thereby not allowing hydrolysis), a constrained switch I conformation, and similar orientations of the lever arm (Himmel, Gourinath et al. 2002). In the apo near rigor state 1KK7 structure, there are twists about three residues of switch II relative to the other four structures. The structures 1L2O and 1KWO show for the first time the unexpected 3D structure of the SH2 reactive thiol (C693) cross-linked with the K705 residue; *p*-PDM has been utilized in many enzymatic studies but was thought to link the SH1 and SH2 residues.

In 2002, Kollmar, Kull, et al., published the first class-I myosin structure, 1LKX. The *Dictyostelium discoideum* myosin class IE is a monomeric unconventional (not of the myosin class-II) myosin; it was determined to have similar core regions of the motor domain when compared to class-II myosin structures. The recombinant myosin was engineered to have an 8xHis-tag on the C-terminus. The myosin was crystallized with MgADP.VO_4 in the active site, which produced a closed structure (Kollmar, Durrwang et al. 2002). Myosin has a “closed” state when ATP or an ATP analog is bound.

In 2003, Coureux, Sweeney, Houdusse, et al., published the first chicken myosin class-V structure, 1OE9. The engineered proteins (truncated chicken myosin V heavy chain and the essential light chain LC1-sa) were co-expressed using the baculovirus/SF9 cell system. This 2.0 Å structure was without a bound nucleotide. The lever arm was in a position consistent with the actomyosin rigor

complex. Myosin V is a two-headed processive motor protein; it walks head over head along the actin filament without detachment. The authors referred to the structural conformation as “closed-cleft” and in a “rigor-like” state. The crystal structure revealed the nature of the structural communication between the actin and nucleotide-binding sites and provided an explanation of how strong binding of myosin to actin weakens the affinity of myosin for nucleotide and vice versa (Coureux, Wells et al. 2003).

In 2003, Reubold, Manstein, et al., published the third myosin II and dynamin fusion structure (previous were 1JWY and 1JX2, of which the myosin structures were solved but not described). The dynamin structure was published separately as 2AKA. The myosin structure, 1Q5G, was described in detail with comparisons to several existing structures. A complex structural communication pathway, which links the nucleotide-binding region, the structures responsible for force amplification, and the actin-binding domain, was analyzed to illuminate a previously unobserved link. This link between the nucleotide-binding region and the actin-binding domain explained the reciprocal relationship between actin and nucleotide affinity (Reubold, Eschenburg et al. 2003).

In 2003, Gourinath, Himmel, Cohen, et al., published the 1QVI structure. The pre-power stroke state of a complete scallop myosin head, including the motor domain, the essential and regulatory light chains, and the transition state ATP analog MgADP.VO_4 was analyzed. It was determined that the motor

domain has four subdomains (upper and lower 50 kDa, N-terminal domain, and the converter domain), which undergo relatively small rearrangements coordinated by conformational changes in the single-stranded joints between them (switch II, relay, and SH1 helix) that produce the relatively large power stroke (Gourinath, Himmel et al. 2003).

In 2004, Risal, Cohen, et al., published two more scallop S1 structures in the near rigor state (1S5G and 1SR6). The 1S5G structure with ADP had a novel binding of the diphosphate moiety. The diphosphate moiety was positioned on the surface of the pocket rather than deep within, as previous structures had shown. The 1SR6 structure, without a nucleotide bound, led to the discovery of a conserved complex salt bridge between the upper 50 kDa subdomain and the n-terminal subdomain. It was determined that this salt bridge is present only in crystal structures with a strong coupling or reciprocal relationship between actin and nucleotide binding (Risal, Gourinath et al. 2004).

In 2004, Coureux, Sweeney, and Houdusse published three *Dictyostelium discoideum* myosin class-V motor domain structures. The structures included an apo structure that demonstrated a rigor-like conformation (1W8J), an ADP bound structure that had an actomyosin conformation (1W7I) and an ADP.BeF_x bound structure (1W7J). The comparison of these structures allowed for a detailed analysis of the communication pathways involved between the actin interface and the nucleotide-binding site. The authors named the seven-stranded β-sheet (and

the associated loops and linkers) the “transducer” for its role in the control of the sequential release of the hydrolysis products (P_i followed by ADP) from the nucleotide-binding pocket during force generation (Coureux, Sweeney et al. 2004). It was noted the 1W8J structure had four molecules in the asymmetric unit (AU), all with different crystal packing contacts, which were also different from the previously published 1OE9 structure’s contacts leading to the conclusion that the structures rigor-like states are not affected by crystal packing (Coureux, Sweeney et al. 2004).

In 2005, Allingham, Smith and Rayment, published the 1YV3 structure. It was the first myosin structure with an inhibitor bound to the motor domain of *Dictyostelium discoideum*. Only three compounds have been found that inhibit myosin. In this structure, Blebbistatin, which specifically stabilizes the metastable or “transition” state, was bound near the ADP vanadate (transition state analog of ATP) blocking the complete closure of the 50 kDa cleft (Coureux, Wells et al. 2003). Blebbistatin, a 1-phenyl-2-pyrrolidinone derivative, has been shown to inhibit nonmuscle myosin II and certain isoforms of muscle myosin II, but does not inhibit myosin from classes I, V and X9 (Straight, Cheung et al. 2003). The other two compounds, 2,3-butanedione monoxime (BDM) and N-benzyl-p-toluene sulfonamide (BTS), inhibit skeletal muscle myosin II (Higuchi and Takemori 1989, Cheung, Dantzig et al. 2002).

In 2005, Menetrey, Sweeney, Houdesse et al., published the first porcine

myosin class-VI structures (2BKH and 2BKI). Class-VI myosins travel in the reverse direction (toward the pointed or minus-end of actin filaments) than most other myosin classes and have binding sites for two calmodulin molecules. The structural analysis provided details of two unique endogenous inserts. The first insert near the nucleotide-binding pocket alters the rate of nucleotide association and dissociation, which allows for the processivity of two-headed myosins "walking" along an actin filament without releasing the filament (Altman, Sweeney et al. 2004). The second insert, part of the converter domain, along with a calmodulin bound to a novel site within the insert, undoubtedly accounted for the redirection of the "lever arm" (which included a second calmodulin bound to a IQ motif) (Menetrey, Bahloul et al. 2005).

In 2007, Yang, Cohen, et al., published several structures of myosin class II from sea scallop and squid. The sea scallop structures included: 2OVK (S1 with Ca^{2+} bound without nucleotide), 2OS8 (S1 with Ca^{2+} and Mg bound without nucleotide), and 2OTG (S1 with MgADP bound). The 3I5F structure, (supersedes 2OY6) was the MgADP bound motor domain of longfin inshore squid with Japanese flying squid essential and regulatory light chains (ELC and RLC). The authors qualitatively explored the energetics of the arrangements of the myosin head (motor domain), which consists of four major subdomains (upper 50 kDa, lower 50 kDa, N-terminal, and converter), that are connected by highly conserved, flexible, single-stranded joints, including switch II, the ‘‘relay,’’

the so called ‘‘SH1’’ helix (named so because the helix contains the “SH1” cysteine residue with the most reactive sulfur atom in myosin S1 (Coluccio 2008)), and the less flexible ‘‘strut’’. Interestingly, the purification included MgADP to stabilize the motor domain, which was subsequently removed with dialysis prior to crystallization, which allowed the rigor-like structures to be determined (Yang, Gourinath et al. 2007).

In 2008, Lucas-Lopez, Rayment, and Westwood, et al. published 3 structures of *Dictyostelium discoideum* myosin II S1. The structures contained analogs of Blebbistatin with the single methyl group placed at 3 available positions on the benzyl ring of the tricyclic core. The structures were virtually identical with the original Blebbistatin structure with rms values less than 0.2 Å (Lucas-Lopez, Allingham et al. 2008). This study was ultimately directed at the development of novel myosin inhibitors with improved affinity and different selectivity profiles from Blebbistatin itself for the experimental investigation of normal and aberrant cellular function, especially cytokinesis and cell migration.

In 2009, Fedorov and Manstein, et al., published the 2JHR and 2JJ9 *Dictyostelium discoideum* (*Dd*) myosin class II structures. The authors intensely investigated the modulation of myosin function by a small molecule inhibitor, pentabromopseudilin (PBP), which has strong therapeutic potential. The study included steady state kinetics, transient kinetics, crystallization, single-fiber mechanics, molecular-modeling, *in vitro* motility analysis and *in vivo* yeast

assays. PBP binding was found to allosterically inhibit *Dd* myosin-5*b* ATPase rate ten-fold by rearranging the interactions in the nucleotide-binding pocket (Fedorov, Bohl et al. 2009). The crystal structure 2JHR had unambiguous density for PBP. PBP was bound in a previously unknown allosteric site near the tip of the upper 50-kDa region, at a distance of 16 Å from the nucleotide binding site and 7.5 Å away from the blebbistatin binding pocket (Fedorov, Bohl et al. 2009). The 2JJ9 structure was a control experiment without bound inhibitor.

In 2010, Frye and Rayment, et al., investigated the importance of hydrogen bonding in the γ-phosphate binding pocket by Ser236, a highly conserved residue (*Dictyostelium discoideum* numbering). They constructed, expressed, and purified S1dC myosin II mutant S236A. Three crystal structures were determined. The "closed" myosin structure 3MYH was crystallized with MgADP.VO_4 and Blebbistatin (it also crystallized without the inhibitor but crystals were of higher quality with Blebbistatin). The second "closed" (referring to switch II and the relation to the nucleotide-binding site) myosin structure 3MYK was crystallized with AMP.PNP in the active site. The third "open" structure, 3MYL was crystallized with $MgPP_i$ in the nucleotide-binding site. The mutation did not cause any significant changes in the amino acid residues but only in the position of the water molecules in the active site as compared with other crystal structures (Frye, Klenchin et al. 2010). The S236A mutant myosin had hydrolytic activity and motility although it caused a 4-fold rate reduction of the nucleotide release step in the transient-state kinetics. These findings suggested the serine's

hydroxyl was not essential for functionality but rather that the mutant's hydrogen-bonding network in the NBS stabilized a closed active site.

In 2011, Preller and Manstein, et al., published several *Dictyostelium discoideum* myosin class-II motor domain structures with bound inhibitors. The structure 2XEL had pentachloropseudilin (PCIP) bound. PCIP acts as a reversible and allosteric inhibitor of ATPase and motor activity. PCIP bound to the same pocket as pentabromopseudilin did in the 2JHR structure, however, the conformation of the inhibitor and bonding interactions with myosin were different. The authors used a multi-faceted approach combining direct functional (HeLa cell assays and fluorescence ATPase assay), crystallographic, and *in silico* modeling to determine the inhibitory effect on several myosin classes (including myosin classes Ic (mammalian), II, V, but no inhibition on human classes VI and VIIa) (Chinthalapudi, Taft et al. 2011). *Dictyostelium discoideum* myosin-II was employed as a crystallographic model system to interpret the binding site of PCIP because co-crystallization trials with class-I myosins failed.

In the crystal structure 2XO8, which had another member of the marine alkaloid family of halogenated pseudilins, 2,4-dichloro-6-(3,4,5-tribromo-1H-pyrrole-2-yl)phenol (H70), complexed with the motor domain, Chinthalapudi and Manstein, et al., investigated modulation of function of specific myosin isoforms for drug discovery. A congeneric series of halogenated pseudilins were analyzed with molecular dynamics (based on crystal structure data), and structure-activated relationships were determined based on steady-state ATPase

measurements, which provided half maximal inhibitory concentrations (IC_{50}). It was concluded that small ligand "population-shift" allosteric regulation proceeded through a direct relay path via a network of hydrogen bonds. The direct relay system mechanism rearrangements of amino acid side chains (over a ~19Å distance) was responsible for the absence of the lytic water molecule, which usually is positioned properly for an in-line attack to the γ-phosphate mimic of the nucleotide analogue (for most structures solved in the pre-power stroke state as the structure without bound inhibitor had shown) (Preller, Chinthalapudi et al. 2011).

In 2011, Preller, Fedorov, Geeves, Manstein, et al., published the three structures of *Dictyostelium discoideum* myosin-2 S1 with the G680A and G680V mutations. The authors investigated G680, one of three conserved glycine residues in the SH1 region of myosin, in order to determine why cold-sensitive mutations in this region interfere with motor function (Patterson and Spudich 1995, Patterson and Spudich 1996). When the reactive thiols SH1 and SH2 (both are cysteines in other myosin isoforms but in *Dictyostelium discoideum* the SH2 position is a threonine) are chemically cross-linked there are dramatic changes in myosin ATPase and actin binding affinity (Dalbey, Weiel et al. 1983, Titus, Ashiba et al. 1989). They cited 15 papers in the introduction setting up their hypothesis that the mutations G680A and G680V interfere with motor function. The hypothesis was assessed by structural analysis, transient kinetic measurements and molecular dynamics. The results determined the Gly-680

mutation in the linker loop, between the SH1 and SH2 helices, uncoupled the region from the surrounding structural elements, mainly the relay helix and the transducer. These steric alterations stabilized the occupancy of the ADP-like state, with ADP tightly bound to the active site with increased enthalpic and reduced entropic contributions assisting the stronger binding (Preller, Bauer et al. 2011).

1.7. This dissertation: The use of *Drosophila melanogaster* as the expression system of choice for recombinant myosin for X-ray crystallography

In *Drosophila melanogaster*, recombinant myosin isoforms expressed in the indirect flight muscle can be functionally tested. In the living fly, flight tests can be performed which directly correlate to the molecular function of the myosin motor (Ramanath, Wang et al. 2011). From dissected fly indirect flight and jump muscle, the mechanical properties of muscle fibers can be determined (Swank 2012). From purified muscle protein, the combination of static crystallographic approaches and kinetic experiments together with computational homology modeling provide insights into the mechanism responsible for the chemomechanical myosin motor activity. The Bernstein lab and collaborators have established a large amount of kinetic, mechanical, and homology modeling structural data on *Drosophila* myosin and the differences due to various

proteoforms and mutants (Swank, Bartoo et al. 2001, Zhang and Bernstein 2001, Kronert, Dambacher et al. 2008, Bloemink, Melkani et al. 2011, Kronert, Melkani et al. 2012). The determination of high-resolution structures through X-ray crystallography was necessary in order to unambiguously resolve the conformation of these myosin isoforms. However, without an actual system to produce milligram quantities of purified protein, structural work could not be started. We set out do solve this problem.

Chapter 2

Materials and Methods

2.1. Introduction

I employed a myosin isolation protocol for microdissected fruit flies (Margossian and Lowey 1982), with further modifications (Swank, Bartoo et al. 2001). Myosin from microdissected honeybees was initially purified by modifying a bulk myosin isolation protocol (Anthony Cammarato personal communication), which had been modified from (Bárány, Gaetjens et al. 1964). The final protocol was further optimized based upon observations of myosin yield and purity.

2.2. Subjects

2.2.1. *Drosophila melanogaster*

The common fruit fly, *Drosophila melanogaster*, (english translation: black-bellied dew-lover) was employed as a model organism for this study. The "wild type" control fly line was "*yw"*, with yellow body and white eyes. Several fly lines with balancer chromosomes were employed for selective breeding schemes for transgenic protein expression. The dominant marker of the *TM2* balancer is Ubx^{130}, which expressed a bristle on each of the enlarged halteres. The dominant marker for the *TM3* balancer is Ser^{1}, which expressed serrate wings with multiple notches at the distal ends. The dominant markers for *TM6B* balancer are *Hu,* which expressed additional humeral bristles, and Tb^{1}, *which* expressed a short and stout body shape. The dominant marker for the MKRS

balancer is *Sb*^{1}, which expressed stubble bristles on the dorsal thorax (Chyb and Gompel 2013).

2.2.2. *Apis mellifera*

Common European honeybees were obtained live from a variety of sources: purchased from Bee Weaver Apiaries, whose strain DH4 was used for the *Apis mellifera* genome (Honeybee Genome Sequencing 2006); donated by Adkins Bee Service, San Diego, CA; and gifted by Dr. Gro Amdam, Arizona State University (research grade specimens from the "HP line"). Only female worker bees were selected for microdissection.

2.3. Microdissection of indirect flight muscles from insects

2.3.1. *Drosophila melanogaster*

The tools used for the dissection were: Vannas-style spring scissors (Fine Science Tools Cat. No. 15000-00 (flies) and 15006-09 (bees)), forceps (Dumont #5/45, Fine Science Tools Cat. No. 11251-35), a small (1") custom Plexiglas dissection dish and a low profile ice bucket. The dissection required custom wire probes to tease out the IFM. (Custom wire probe manufacturing procedure: Tungsten wires, of 0.005 inch diameter, were made pointed on one end with electrochemical etching in a saturated solution of $NaNO_3$. A direct current power supply was connected to a carbon rod, the negative terminal, that was immersed

in the nitrate solution and the other end of the circuit, the positive terminal, was connected to an alligator clip. The clip was connected to the shaft of a hypodermic needle into which the tungsten wire was inserted and crimped into place. Then it was dipped in the solution for electrolysis. The wire was then bent with the appropriate curve to scrape the IFM from the thorax cuticle (Swank 2012).

Larger flies, the females, were selected for dissection, anesthetized on a CO_2 gas emission stage and viewed with a compound dissection microscope. The flies were placed with their ventral side up. The tweezers were applied to the flies neck region to stabilize the insect. The forceps were used to brush back the legs and cut through the abdominal connection and the rear two pairs of legs and wings with one cut. The scissors were then used to stabilize the thorax while the head was then pulled forward slowly removing the front legs and alimentary canal with it. The scissors were placed into the neck hole and a cut was made though the centerline between the legs. The tweezers were used to roll the thorax 180° while still on the scissor blade. Another cut was made through the thorax down the dorsal centerline. The bisected thorax was placed in YMG solution until ~30 were dissected for the next step. The bisected thoraces were placed on their side and stabilized with a tweezers while carefully scraping out the IFMs with the custom wire probe. The dissected muscle was placed in an Eppendorf tube containing York Modified Glycerol without Triton X-100 (YMG-Tx: 20 mM potassium phosphate, pH 7.0, 2 mM $MgCl_2$, 1 mM EGTA, 8 mM DTT,

50% v/v glycerol) with a protease inhibitor cocktail (Complete Mini, Roche Applied Science, Indianapolis, IN) kept in an ice bucket (Peckham, Molloy et al. 1990, Swank, Bartoo et al. 2001).

2.3.2. *Apis mellifera*

The tools used for the microdissection were: a Leica stereo dissection scope with gooseneck halogen lighting, a CO_2 emitting anesthetizing stage, Vannas-style spring scissors (10 mm cutting edge, Fine Science Tools Cat. No. 15006-09) and forceps (Dumont #5/45, Fine Science Tools Cat. No. 11251-35), a custom Plexiglas dissection dish and an ice bucket. The honeybee dissection was carried out in the same fashion as the Drosophila dissection. However, the indirect flight muscles had to be cut from the cuticle because of the strong attachment. The muscle tissue was stored in relaxing storage buffer (100 mM NaCl, 3 mM $MgCl_2$, 0.2 mM EGTA, 5 mM PIPES, 5 mM NaH_2PO_4 , 1 mM NaN_3 , 0.5 mM PMSF, 5 mM ATP, 2 Roche complete mini protease inhibitor cocktail tablets (per 50 ml solution) (Cat. No. 11 836 153 001), and 50% glycerol), in the -20 °C freezer.

2.4. Purification of endogenous myosin from dissected indirect flight muscles of *Drosophila melanogaster*

After dissection of 100 flies as described above (~1-3 minute per fly dissection time), the IFMs were suspended in YMG (with Triton X-100), incubated for 30 min, centrifuged (8,500*g*), and washed in YMG-Tx sans glycerol. Myosin was extracted with three volumes (55 μl) of 1.0 M KCl, 0.15 M potassium phosphate, pH 6.8, 10 mM sodium pyrophosphate, 5 mM $MgCl_2$, 0.5 mM EGTA, and 8 mM DTT for 10 min and centrifuged (8,500*g* for 5 min at 4 °C). The extracted myosin was precipitated by decreasing KCl to 40 mM and incubating for 16 hours (overnight). Following a 15-min centrifugation in a Beckman TL-100.3 /rotor at 100,000*g*, the pellet was dissolved in an equal volume (18 μl) of Wash B (2.4 M KCl, 100 mM histidine, pH 6.8, 0.5 mM EGTA, 8 mM DTT) (Hynes, Block et al. 1987). Actomyosin was precipitated by dilution with water until the KCl concentration was decreased to 300 mM and centrifuged (60,000*g* for 30 min at 4 °C). The supernatant was removed and further diluted to 30 mM KCl and centrifuged (100,000*g* for 30 min at 4 °C). The final pellet was resuspended in 30 μl of myosin storage buffer (0.5 M KCl, 20 mM MOPS, pH 7.0, 2 mM $MgCl_2$, and 8 mM DTT) (Swank, Bartoo et al. 2001).

2.5. Purification of endogenous myosin from dissected indirect flight muscles of *Apis mellifera*

Previously dissected IFMs were kept at -20 °C in a relaxing storage solution. The protein solutions were maintained at 4 °C for the purification. The epi tubes with relaxing solution that contained the IFMs (50 honeybees total) were centrifuged (12,000*g* for 5 min at 4 °C). The supernatant was discarded. The pelleted IFMs were suspended in 10 ml homogenization buffer (12.5 % sucrose, 40 mM KCl, 10 mM imidazole-Cl pH 8.2, 2 mM $MgCl_2$, 0.2 mM EGTA (pH 7.0), 2 Roche complete mini protease inhibitor cocktail tablets (per 25 ml solution), 0.5 % Triton X, 1 mM DTT, final pH 7.60) and then transferred with a 1 ml pipette tip (with the end cut off) to a nylon in glass, 30 ml Dounce homogenizer. The IFMs were homogenized manually with several strokes of the pestle.

2.5.1. Spin 1: low salt homogenization solution 40 mM

The homogenate was transferred to Beckman 26.3 ml centrifuge tubes (Cat. No. 355618) and centrifuged with a Beckman Coulter L8-60K in a Ti 60 rotor (40,000*g* for 15 min at 4 °C). The yellow tinted supernatant was discarded. The pellet was resuspended with 7.70 ml of myosin extraction buffer (600 mM KCl, 10 mM imidazole-Cl, 5 mM $MgCl_2$, 0.2 mM EGTA, 1 mM DTT, 10 mM pyrophosphate, pH 7.6), incubated for 10 min, then sonicated with a Fisher

Scientific Sonic Dismembrator Model 100 with a micro-tip for 20 one second pulses at a setting of 5. Followed by a 30 min incubation for the myosin to solubilize.

2.5.2. Spin 2: high salt myosin extraction buffer 600 mM

The MEB myosin solution was centrifuged (100,000*g* for 35 min at 4 °C). The supernatant was divided and diluted 15-fold to 40 mM KCl with addition of 10 mM DTT (1.5 ml myosin solution diluted with 21.0 ml 10 mM DTT in each of 5 tubes). Solutions incubated on ice overnight in the cold room.

2.5.3. Spin 3: low salt 40 mM precipitation of myosin

The extracted myosin solution was centrifuged with a Beckman Coulter L8-60K in a Ti 60 rotor (100,000*g* for 35 min at 4 °C). The supernatant was discarded and each pellet was carefully resuspended with 1.0 ml of Wash B solution (1.2 M KCl, 0.5 mM EGTA, 100 mM L-Histidine, titrated to pH 6.8 with 250 μl 3 M KOH, 10 mM DTT). The pooled volume was 6.0 ml after the pellets were combined into one tube and the addition of a 1.0 ml rinse. The solution was decanted into a 50 ml beaker on a stir plate set at medium to fast speed in the 20 °C cold room. Incubation time was 2 hours for solubilization of the pellets. The solution was diluted 4-fold (addition of 18.0 ml 10 mM DTT) to a final salt concentration of 300 mM KCL.

2.5.4. Spin 4: 300 mM salt for precipitation of actomyosin

The myosin solution was centrifuged with a Beckman Coulter L8-60K in a Ti 60 rotor (60,000*g* for 30 min at 4 °C). Then 3.0 ml of the supernatant was pipetted into each of 8 tubes and diluted with 22.0 ml 10mM DTT with a transfer pipet. The supernatant was diluted with the 10 mM DTT to precipitate myosin by lowering the ionic strength. No incubation time followed.

2.5.5. Spin 5: low salt 30 mM to precipitate final myosin pellet

The solution was centrifuged with a Beckman Coulter L8-60K in a Ti 60 rotor (177,500*g* for 50 min at 4 °C). The supernatant was slowly decanted, and then 0.30 ml digestion buffer (120 mM NaCl, 20 mM NaP_i buffer, 1 mM EDTA, 4mM DTT, pH 6.2) was used to suspend 3-4 pellets (1-2 mm diameter) with a pipette. Then the tubes were rinsed with 0.20 ml digestion buffer. The solution was pooled into 2 homogenizer sample tubes, each with ~1.0 ml. The pellet was resuspended with a disposable sample tube pellet pestle. The solution was then transferred to two pre-cooled ultracentrifuge tubes for proteolysis (Beckman microfuge tube polyallomer Cat. No. 199226).

2.5.6. Proteolysis followed by size exclusion chromatography

The Beckman centrifuge tube (Cat. No. 357448) containing 1.0 ml of the full-length myosin sample was placed in the 20 °C water bath for 3-5 min to

equilibrate temperature. The α-chymotrypsin solution (10 mg/ml) (Worthington Cat. No. 56H8870-A) was mixed and then added (20.0 μl) to the temperature-equilibrated myosin. The final concentration of protease in the reaction solution was 0.2 mg/ml. The proteolysis incubation time was for 6 min. The proteolysis reaction was quenched with 7.65 μl of 200 mM phenylmethlysulfonyl fluoride (PMSF). The quenched solution was immediately placed on ice and then centrifuged with a Beckman TL-100 Ultracentrifuge in a TLA-100.3 rotor (198280*g* for 25 min at 4 °C). The subfragment 1 (S1) supernatant was pipetted into a 3 ml syringe for injection into the GE Healthcare Life Sciences ÄKTA FPLC sample loop for size exclusion chromatography. Liquid chromatography was carried out with a 16/60 column loaded with Superdex 200 resin. The column was equilibrated and run with filtered and degassed low salt buffer (30 mM KCl, 5 mM $MgCl_2$, 1 mM DTT, 20 mM MOPS pH 7.0). Two ml fractions were collected and those that contained the S1 peak were concentrated and analyzed by SDS-PAGE. The concentrated S1 was split into 16 μl aliquots for crystallization or storage at -80 °C.

2.6. Preparation of *E. coli* cloning and expression plasmids

2.6.1. 6-His labeled Embryonic Body Wall MHC (*6HisEmb*)

The construction strategy for the *pattB6HisEmb* plasmid is depicted in Figure 2.1. The 5' *Actin88F* promoter fragment (1406 bp) (Geyer and Fyrberg 1986) was produced by PCR from the plasmid pL116-4 (Cripps, Suggs et al.

1999) with the forward primer act88fXba1 5'-AAT ATC TAG AAT GCA CAA TAG GCA AAT TTA GTT AAG-3' and reverse primer act88fPvu1 5'-ACG CCG ATC GGT CTG TCC TGC CTT TAT ATC-3'. The PCR amplification conditions were denaturation at 95 °C$^{3:00}$, elongation, annealing, and extension at [95 °C$^{1:00}$ 50 °C$^{1:00}$ 72 °C$^{2:00}$]^{35}, final extension at 72 °C$^{5:00}$, incubation at 4 °C$^{\infty}$. A second fragment containing the 3' *Actin88F* promoter region, which also encodes the amino-terminal His-tag, tobacco etch virus (TEV) protease recognition site, and *Mhc* exon 2 5' region, was generated in three steps by standard PCR. First, the pL116-4 plasmid was amplified using the forward primer ActPvu1 5'-GAC AGA CCG ATC GGC GTG CCA T-3' and reverse primer ActHisTEV 5'-GAG GTT TTC GTG GTG GTG GTG GTG GTG CAT CTT GGC AGT TGT TTA TCT GG-3' to produce the 3' *Act88F* region, 6 His-tag, and TEV cut site (695 bp). Next, the p5'emb plasmid (Wells, Edwards et al. 1996) was amplified with the forward primer HisTEVMhc 5'-CAC CAC GAA AAC CTC TAC TTC CAA GGC CCG AAG CCA GTC GCA AAT CAG G-3' and reverse primer MhcPst1 5'- ACC CTG CAG ACC AAC GGA GAC G -3' to produce the His-tag (HHHHHH), TEV cut site (ENLYFQG), and Mhc 5' exon 2 region (222 bp) and then the two overlapping 695 and 222 bp fragments were joined by amplification with the forward primer ActPvuI and reverse primer MhcPst1 for a final 890 bp fragment. These 5' *Actin88F* and 3' fragments were digested with Pvu I and ligated together. They were then digested with Xba I and Pst I before ligation with the similarly digested p5'emb vector. Genomic DNA from the Apa I site in exon 12 through exon 19 to

the Kpn I site was next ligated with the similarly digested vector construct. Finally, the entire *Actin88F* promoter, His-tag, TEV site, EMB isoform, 3' *Mhc* genomic DNA construct (14,094 bp) was removed and ligated into the Xba I and Kpn I sites of the pattB vector (7411 bp) (Bischof, Maeda et al. 2007). The pattB6HisEmb plasmid sequence was confirmed by the California State University MicroChemical Core Facility prior to shipment for injection into embryos. The resulting myosin isoform is expected to contain the EMB S1 region joined to the IFM form of the myosin rod, which includes a subfragement-2 hinge region encoded by alternative exon 15a and a C-terminal tailpiece encoded by alternative exon 18 (George, Ober et al. 1989).

2.6.2. 6-His labeled Indirect Flight Muscle MHC (*6HisIFI*)

For the construction of pattB6HisIFI plasmid, the p9b11a plasmid was digested with Xba I and PspOM I and the resulting DNA fragment (6194 bp) containing the Mhc promoter and exons 1, 2, 3a, 3b, 5-8, 9b, 10, and 11a was gel purified (Figures 2.2A and 2.2B). The fragment was ligated into a pKS vector (2889 bp) digested with Xba I and PspOM I; the ligation was performed by Bill Kronert. The completed vector was named pKSIFI1 (9083 bp). The pKSIFI1 vector was digested with Xba I and Pst I (6496 bp) and the gel purified fragment pJTCA6H Xba I Pst I (2291 bp), which contained the Actin88f promoter, 6xHis-tag, TEV cut site and the 5' portion of *Mhc* exon 2 was ligated in. The vector was

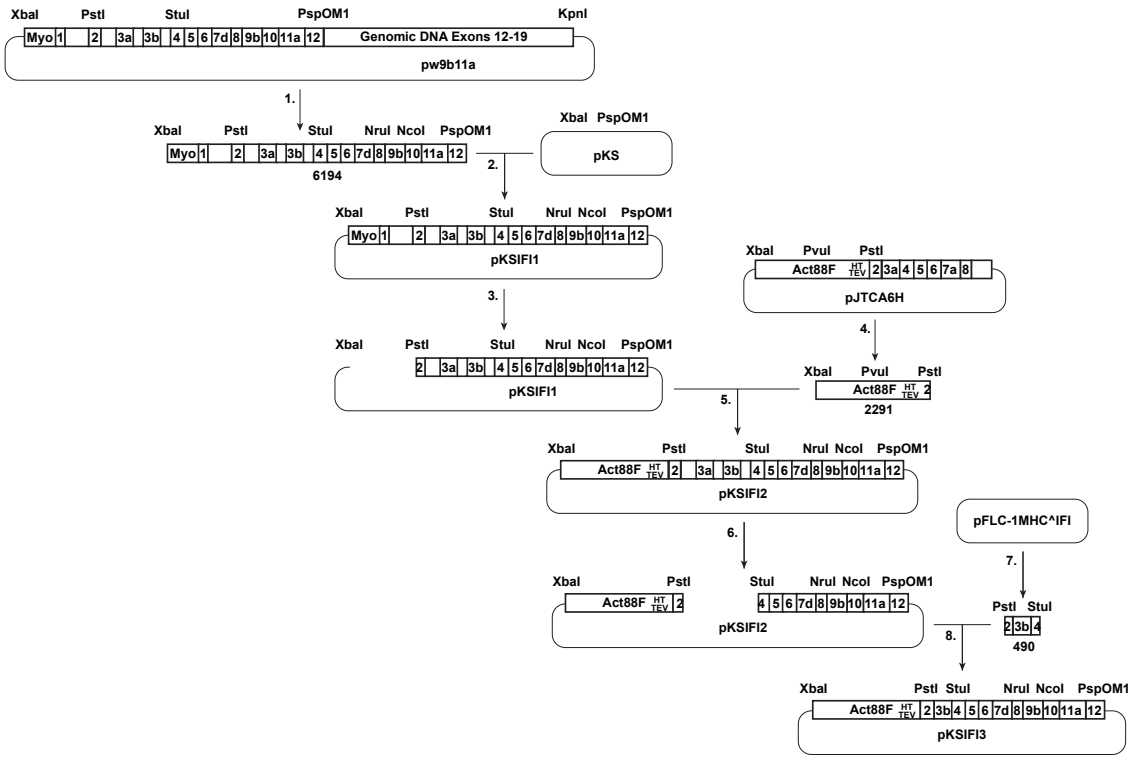

Figure 2.2A: Steps 1-8 of pattB6HisIFI construction. (His-tag indirect flight muscle isoform plasmid)

This His-tag indirect flight muscle isoform plasmid construction was done in sequential steps per the numbers. The entire coding region for exons 2-12 and the restriction sites used for ligation were sequenced for verification before the plasmid was sent to Bestgene, Inc. for injection into the fly embryos.

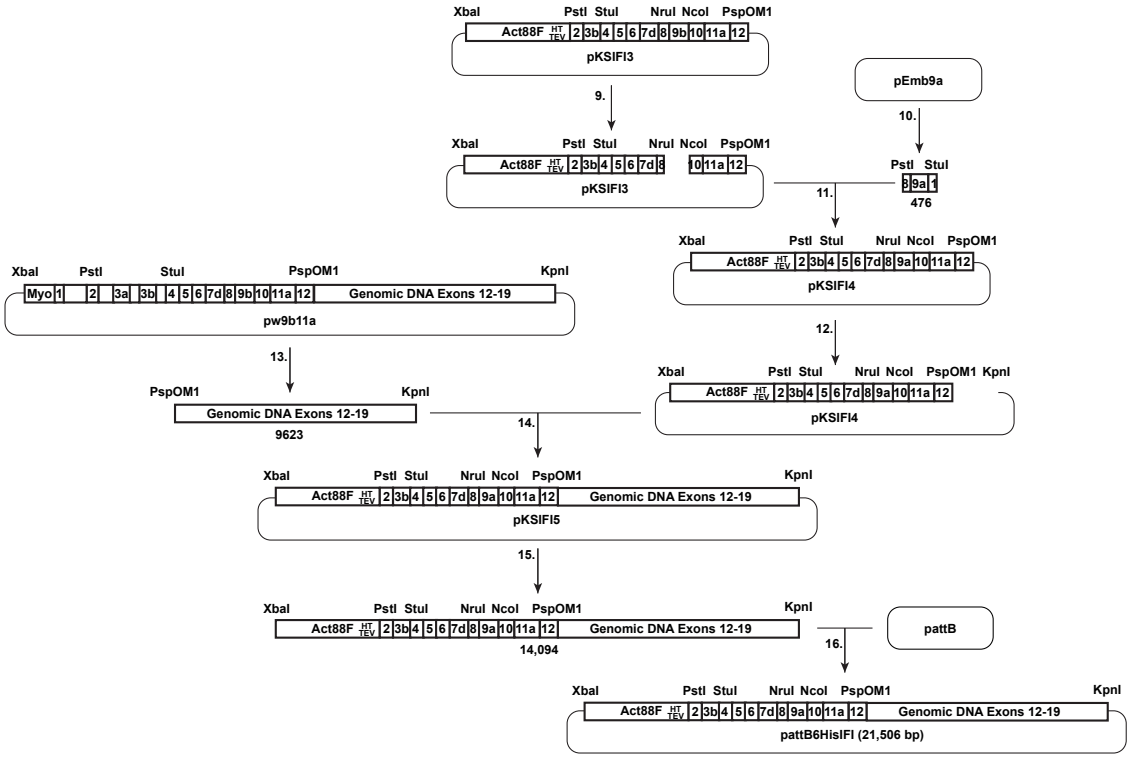

Figure 2.2B: Steps 9-16 of pattB6HisIFI construction. (His-tag indirect flight muscle isoform plasmid)

This His-tag indirect flight muscle isoform plasmid construction was done in sequential steps per the numbers. The entire coding region for exons 2-12 and the restriction sites used for ligation were sequenced for verification before the plasmid was sent to Bestgene, Inc. for injection into the fly embryos.

named pKSIFI2 (8787 bp). The region between exons 2 and 4, which included introns and exons 3a and 3b (1918 bp) was removed with Pst I and Stu I and replaced with exon 3b. The exon 3b fragment containing the 5' exon 2 Pst I region, exon 3b, and the 3' exon 4 Stu I region was produced with PCR and purified with the QIAquick PCR Purification kit (Cat. No. 28104) per manufacturer's instructions. The vector template DNA, pFLC-MHC^IFI, was obtained from Doug Swank's lab (RPI). The forward primer was James16 5'-GTT GGT CTG CAG GGT GGA GAG-3' and reverse primer was James17 5'-TTA CCG AAG GCC TCA AGC AC-3'. The pKSIFI2 vector was digested with Pst I and Stu I (6869 bp), run out on an agarose gel, extracted with the MoBio Ultraclean Gelspin kit (Cat. No. 12400-250), ligated together with the PCR product (490 bp) and named pKSIFI3 (7359 bp). The presence of the PCR exon 3b fragment in the vector was confirmed by ETON Bioscience sequencing with the lab primer 9 (exon 4-2) 5'-CAGAGATGGCGAAAATATGG-3'. The pKSIFI3 vector was digested with Nru I and Nco I (6883 bp) to removed exon 9b. Bill Kronert ligated a Nru I exon 9a Nco I (476 bp) fragment in. The respective vector was named pKSIFI4 (7359 bp). The pKSIFI4 vector was digested with PspOM I and Kpn I (7353 bp) to allow for insertion of exon 12-19 genomic DNA. The pw9b11a PspOM I Kpn I insert (9623 bp) was digested, gel purified and then ligated into the digested PKSIFI4 vector. This ligation completed the gene and the vector was named pKSIFI5 (16976 bp). The gene then had to be removed from pKS and ligated into the pattB (7418 bp) injection vector with Xba I and Kpn

I (7412 bp). The final vector ligation was completed by Bill Kronert in June 2011 and was named pJTC3 (aka pattb6HisIFI 21505 bp).

The final construct pJTC3 was purified using QIAfilter Plasmid Maxi Kit (Qiagen Inc., Valencia, CA) according to manufacturer's instructions. The ligation sites, *Actin88F* promoter, His-tag, TEV cut site, and cDNA for exons 2-12 were verified with DNA sequencing by Eton Biosciences (San Diego, CA) to ensure no cloning artifacts were introduced prior to shipment for injection into embryos. The resulting myosin IFI isoform is expected to contain the IFI S1 region joined to the IFI form of the myosin rod, which contains a subfragement-2 hinge region encoded by alternative exon 15a and a C-terminal tailpiece encoded by alternative exon 18 (George, Ober et al. 1989).

2.7. Transformation of *Drosophila* with the embryonic MHC isoform and indirect flight muscle isoform constructs

BestGene Inc. (Chino Hills, CA) injected the pattB6HisEmb plasmid into 200 *Drosophila* embryos of FlyC31 strain 24485 (carrying a mutation in the white eye color gene) with the estimated target cytosite 68E (chromosome 3). The PhiC31 integrase-mediated transgenesis system was selected for transformation due to the advantage of site-directed insertion of the transgene (Bischof, Maeda et al. 2007). Five culture vials were received containing transformant flies with very light orange (~tan) eyes as the phenotypic marker for the transgene

encoding the engineered myosin. The same procedure was completed for the pattB6HisIFI plasmid (pJTC3) with five culture vials received.

2.8. Culturing flies

The healthiest fly cultures were grown at 25 °C, which allowed for a 10 day generation time from egg to adult. Some stocks were kept at room temperature or 18 °C to slow growth for convenience. Fly food consisted of 30 g agar, 120 g sucrose, 75 g active dry yeast, 2.325 g calcium chloride dihydrate, 2.325 g ferrous sulfate heptahydrate, 12 g sodium potassium tartrate, 0.75 g sodium chloride, 0.75 g manganese chloride and 1.5 L water, which was autoclaved for 30 min (Carpenter 1950). The food was cooled to 50 °C in a water bath. Then 12 ml of 10% Nipagen was added. The food was poured into the appropriate culture vials and bottles. The fly food was capped with flugs (dense weave cellulose acetate stoppers) and cooled at room temperature overnight. The fly food was stored for up to 2 weeks at 20 °C. If the fly food became too wet with condensation, then Carolina Biological Blue food (Cat. No. 173200) was powdered in a coffee grinder and then dusted over the surface so the flies would not become entrapped in the sticky food.

2.9. Drosophila genetic crosses

2.9.1. Selection for a lab stock of homozygous EMB-expressing flies in *yw* background

The 5 vials of heterozygous transgenic lines received from Bestgene, Inc. (Chino Hills, CA), which had a slightly orange eye phenotype, were self-crossed (Figure 2.3 EMB lab stock). The slightly darker orange-eyed homozygous transgenic flies were selected and self-crossed which produced a true breeding homozygous transgenic line.

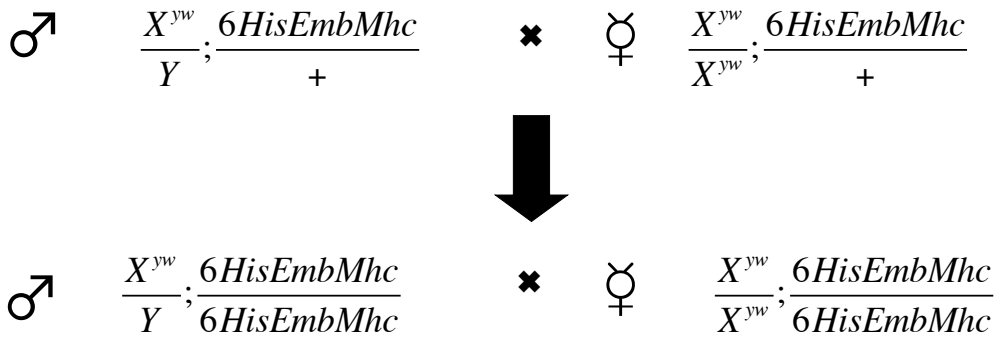

Figure 2.3: Fly cross to produce the homozygous 6HisEmb line

The homozygous 6HisEmb line was produced for the maintenance of the transgenic fly line in the lab stock collection.

2.9.2. Selection for a purification stock of homozygous EMB-expressing flies in *Mhc^{10}* background

The 5 heterozygous transgenic lines were also crossed to produce lines in the *Mhc^{10}* background (Figure 2.4). *Mhc^{10}* is a myosin heavy chain null line for the indirect flight and jump muscles (Collier, Kronert et al. 1990). The heterozygous transgenic flies were crossed with A12 flies (*w; CyO/Bl^{1}; TM2, Ubx130/ TM6B, Tb^{1}, Hu*); the progeny were screened for curly-winged, light orange-eyed flies. The selected flies were crossed to the *Mhc^{10}* line; the selected progeny were self crossed to produce a homozygous *Mhc^{10}* (lacking curly wings), heterozygous transgenic myosin line which was self-crossed to produce the final true breeding homozygous transgenic line (darker orange eyes) in the homozygous *Mhc^{10}* background.

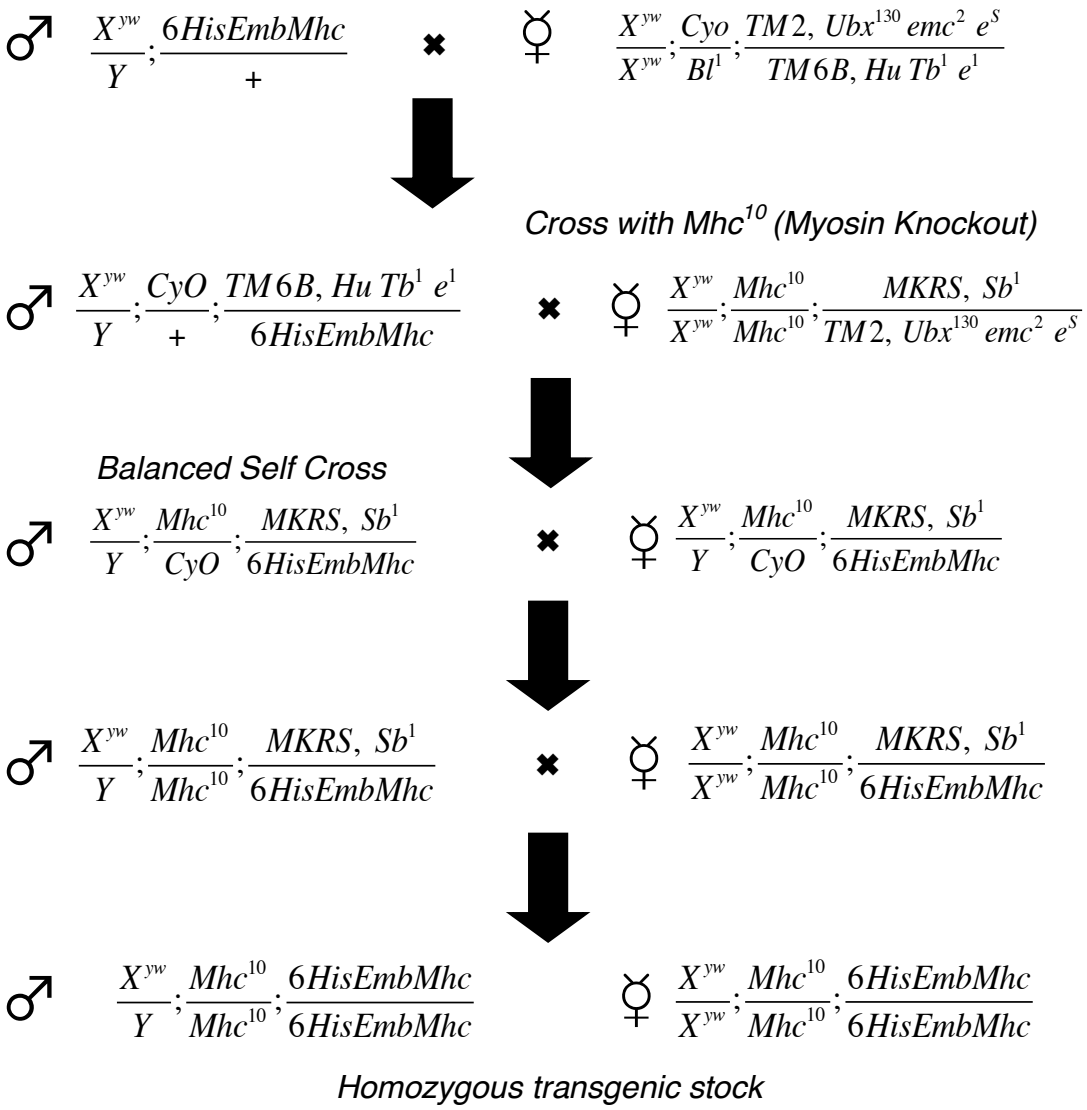

Figure 2.4: Fly cross of the 6HisEmb line into *Mhc[10]* background

This cross was made to produce a fly line that expressed the tagged myosin in an endogenous myosin knockout background (knockout in IFM and jump muscles only) for purification purposes.

2.9.3. Selection for a lab stock of homozygous IFI-expressing flies in *yw* background

The 5 heterozygous transformant lines received from Bestgene, Inc. (Chino Hills, CA), which had a slightly orange eye transgenic phenotype, were crossed to X^{yw}/X^{yw}, *TM3,* Ser^1 y^+*/MKRS,* Sb^1 flies (serrated wings and stubble bristles phenotype). The slightly darker orange-eyed heterozygous transgenic flies with serrated wings were selected and self-crossed. The non-serrate winged homozygous transgenic progeny with dark orange eyes were collected and self crossed to produce the homozygous transgenic lab stock line (Figure 2.5).

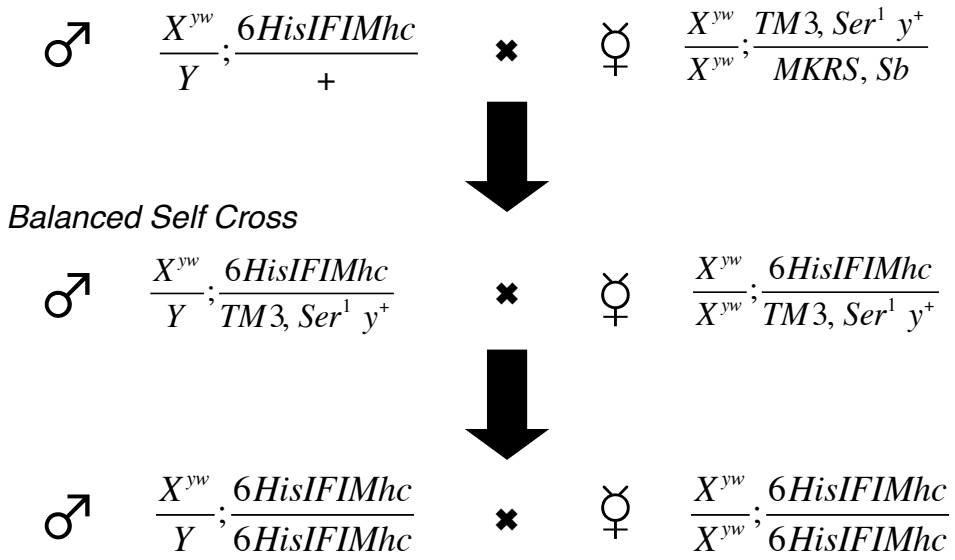

Figure 2.5: The 6HisIFI fly cross for the production of a homozygous transgenic line in yw homozygous background

This fly line was produced for the maintenance of the transgene in the lab stock collection.

2.9.4. Selection for homozygous IFI-expressing flies

Standard genetic crosses were made to generate a homozygous transgenic line in the *Mhc*^{10} background (Figure 2.6). *Mhc*^{10} is a myosin heavy chain null line for the indirect flight and jump muscles (Collier, Kronert et al. 1990). The heterozygous transgenic flies were crossed with A12 flies (*w; CyO/Bl*^{1}*; TM2, Ubx130/ TM6B, Tb*^{1}*, Hu*); the progeny were screened for curly-winged, light orange-eyed flies. The selected flies were crossed to the *Mhc*^{10} line; the selected progeny were self crossed to produce a homozygous *Mhc*^{10}, heterozygous transgenic myosin line which was self-crossed to produce the final true breeding homozygous transgenic line (darker orange eyes) in the homozygous *Mhc*^{10} background.

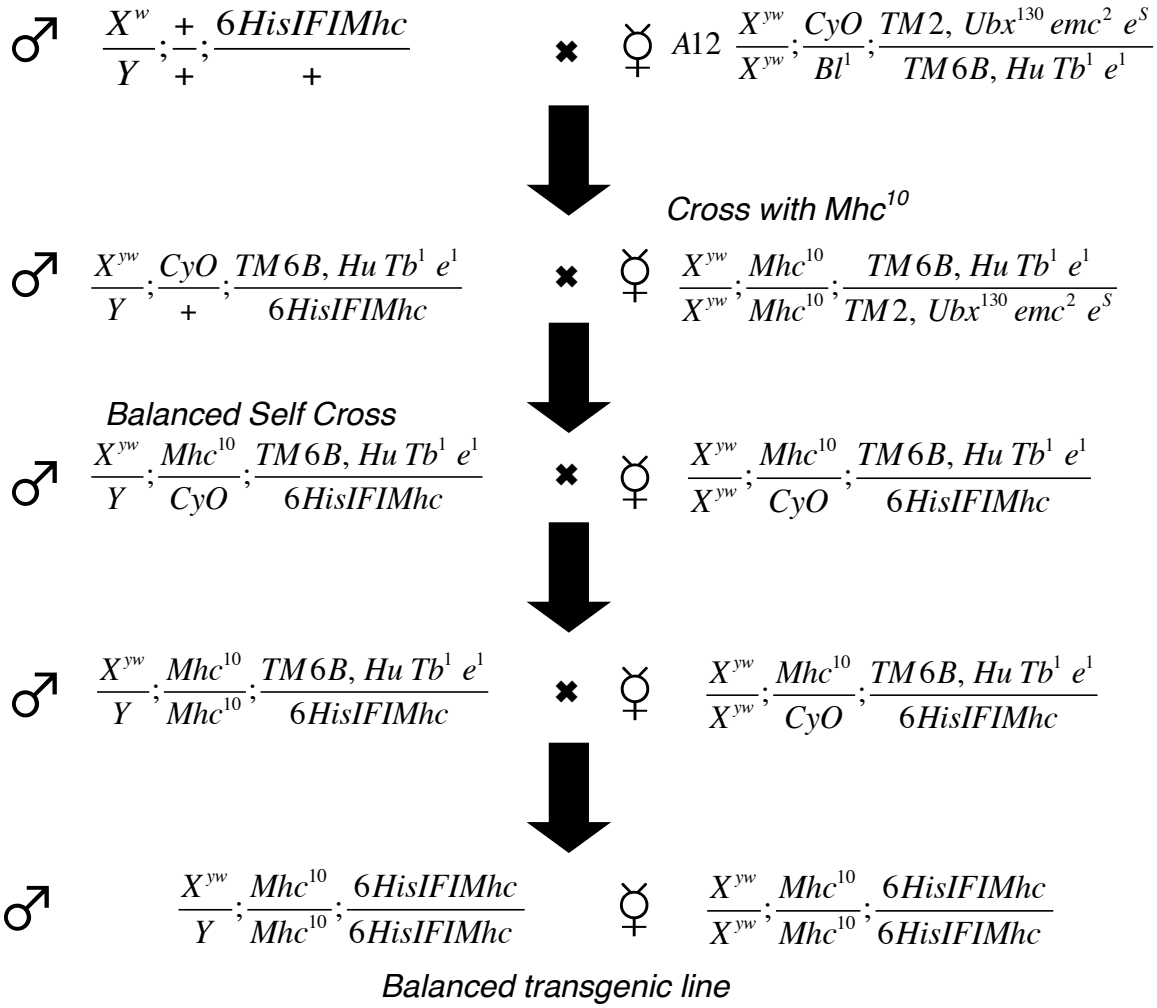

Figure 2.6: The 6HisIFl fly cross for production of a homozygous transgenic line in Mhc10 (myosin knockout in IFM and jump muscle) homozygous background

This line was produced for the transgenic expression of tagged myosin for purification purposes.

2.10. Transgenic myosin expression level quantification by protein electrophoresis and densitometry

2.10.1. Sample preparation:

The transgenic protein level was evaluated by densitometry of a sodium dodecyl sulfate-polyacrylamide gel electrophoresis (SDS-PAGE) gel. The protocol was modified from Swank et al. (Swank, Bartoo et al. 2001). The transgenic flies' protein expression was compared to *yw* flies as a positive control. Female flies that were less than 24 hours old were selected for upper thorax dissection. The flies were placed on their dorsal side on a dissection scope's CO_2 anesthetizing stage. The abdomen was removed with microdissection scissors along with the legs and wings. The head was pulled off with a microdissection forceps with careful effort made to pull out the gut. The hole left by the head was used as guide for where to set the end of a razor blade for a longitudinal cut to the haltere region for removal of the upper thorax. The upper thorax was immediately placed in an epi tube with 180 μl Laemmli sample buffer kept at 4° C. Six flies were dissected for each sample. The upper thoraces were homogenized with an epi tube homogenizer and then boiled for 5 min. The samples were centrifuged at 10,000*g* for 6 min. The supernatant was removed and mixed (150 μl) for SDS-PAGE analysis.

2.10.2. Protein electrophoresis

The samples were loaded into the 10% Bio-Rad Mini-Protean TGX Gel (Cat. No. 456-1036) wells with increasing amounts from 8-15 μl. SDS-PAGE was performed according to Laemmli (Laemmli), using a BioRad Protean Mini-protean IV electrophoresis system. The Bio-Rad Precision Plus Protein Standards Kaleidoscope (Cat. No. 161-0375) ranging from 10-250 kDa, were used as a benchmark. The electrophoresis was for 100 min at 100 volts. The gel was stained with 50 ml Coomassie Blue stain (one liter stock: 450 ml methanol, 450 ml water, 100 ml glacial acetic acid, 2.5 g Brilliant Blue C (Sigma-Aldrich Cat. No. B7920-50G)) for 15-20 min on the shaker platform. The gel was placed in 100 ml destaining solution (one liter stock: 450 ml methanol, 450 ml water, 10 ml glacial acetic acid) with solution exchange until clarified. The gel was then placed in 5% acetic acid to allow it to return to its to original size.

2.10.3. Densitometry

The gel was scanned in black and white jpeg format at 300 dpi with an Epson flatbed scanner. Adobe Photoshop software was used to size and adjust the image. The scanned image was quantitatively analyzed with Image J software. The ratio of the myosin band to actin band was calculated, averaged across lanes and expression was reported as a percentage in relation to the control (*yw* flies).

2.11. Verification of transgenic sequence transcription for the 6HisEMB and 6HisIFI fly lines: 6His-tag through exon 12 portion only

2.11.1. Step 1: RNA purification from Indirect Flight Muscle

Indirect flight muscle was isolated as in Swank (Swank, Bartoo et al. 2001). Fifty upper thoraces were dissected as in the above section with the exception of bisecting the thorax through the head hole with two lateral cuts of the scissors. The thoraces were homogenized in 600 μl solution 1 (6 M urea, 3 M LiCl, not autoclaved), with a pestle with 1.5 ml tube (Research Products International Corp. Cat. No. 199226). The sample was placed on ice overnight (minimum of 2 hours). The tube was centrifuged at 10,000*g* for 10 min at 4 °C. The pellet was resuspended with 300 μl solution 2 (10 mM Tris/HCl pH 7.5,10 mM EDTA, 1% SDS, autoclaved). Then 300 μl phenol was added, which formed an upper p layer that contained RNA. The tube was vortexed for 5 sec. Then 300 μl chloroform was added which formed a denser bottom organic layer. The tube was then vortexed for 5 sec. The sample was centrifuged at 10,000*g* for 5 min at room temperature. There was a cloudy interface which contained DNA in a phase separation. The top layer that contained the RNA was removed with a pipet and transferred to a new 1.5 ml Eppendorf tube. The addition of chloroform through the removal of the top layer was repeated, which removed the majority of residual phenol. The RNA was precipitated with the addition of 20 μL 5.0 M

NaCl, and then mixing, followed by the addition of 1 ml ethanol. The sample was then placed at -80 °C for 20 min. The tube was placed in ice for 3-5 min to raise the temperature prior to centrifugation at 12,000*g* at 4 °C. The supernatant was carefully removed and discarded. The sample was placed in the speed vac to dry it completely. The RNA was dissolved in 25 μl sterile water and stored at -20 °C.

2.11.2. Step 2: Reverse Transcription-Polymerase Chain Reaction (RT-PCR) for cDNA synthesis

The cDNA synthesis was performed using the Protoscript M-MuLV Taq RT-PCR Kit (New England BioLabs, Ipswich, MA, Cat. No. E6500S) according to the manufacturer's instructions. First strand cDNA synthesis reaction included: 0.2 μg of total RNA, 1 μl gene specific negative primer: Mhc Exon 13-3 (-) primer (5'-GCGGTCTTCTCAGCCAAAAGC-3'), and 8 μl water. The mixture was denatured at 70 °C for 5 min. Then 10 μl of the M-MuLV reaction mix (which contained dNTPs and an optimized buffer) and 2 μl of the M-MuLV enzyme mix (which included the M-MuLV Reverse Transcriptase and the murine RNase Inhibitor) was added and incubated for elongation at 42 °C for 1 hour. The enzyme was heat deactivated at 80 °C for 5 min. The reaction was then diluted with 30 μl water prior to storage at 20 °C.

2.11.3. Step 3: Polymerase Chain Reaction (PCR)

The cDNA areas of interest were amplified by PCR with the Roche Expand High Fidelity PCR System (Cat. No. 11 732 641 001). The PCR reaction mixtures were set up with 1 μl 25mM dNTP mixture, 3 μl DNA template, 2 μl each of forward and reverse primers, 0.75 μl DNA polymerase, 5 μl 10X buffer and 36.25 μl water. The Bio-Rad iCycler Thermal Cycler was programed to run at: 94 °C for 2 min, 25 cycles of 94 °C for 15 sec; 51-55 °C (primer specific) for 30 sec; 72 °C for 1 min, 72 °C for 7 min, and 4 °C for infinity. The primer pairs used were as follows:

James 22 6His (+) 5' ATG CAC CAC CAC CAC CAC C 3'

James 23 exon 4 (-) 5' TGG TCT GCA CAA CCT GAT CTT 3'

Lab primer 12 exon 5 (+) 5' GGC TGG TGC TCA TAT TGA GA 3'

James 21 exon 10 (-) 5' TCT TCT CCA ACC AAC CGG TGA 3'

Lab primer 39 exon 10 (+) 5' GTT CCC CAA GGC CTC CGA TCA 3'

James 24 exon 13 (-) 5' GCG GTC TTC TCA GCC AAA AGC 3'

The PCR products were purified with Qiagen's QIAquick PCR Purification Kit (Cat. No. 28104). The purified DNA was sent to Eton Bioscience Inc., San Diego for sequencing. The results were analyzed with Serial Cloner v2.1, NCBI Align Sequences Nucleotide BLAST and 4Peaks v1.7.2 software.

2.12. Protein extraction

The method developed for myosin extraction from transgenic *Drosophila* lines expressing His-tagged myosin isoforms are described here.

2.12.1. Bulk whole fly homogenization

1. Cultured twenty-five 8 oz culture bottles of transgenic flies (*yw, Mhc^{10}, 68E: Act88F6HisEmb*) and cleared the adults 24 hours before collection of newly eclosed offspring.

2. On the day of the extraction, the flies were anesthetized with CO_2. Collected newly eclosed adults (less than 24 hours old) and removed any pupae or larvae. Placed the flies in a 50 ml Falcon tube. Flies were flash frozen in liquid nitrogen and stored at -80 °C for convenience.

3. Weighed the flies 3.35 g is ~3500 flies at an average weight of 0.96 mg/fly.

4. Poured the flies into an ice cooled (4 °C) grinding chamber (Wheaton Potter-Elvehjem Tissue Grinders, 55 ml, Cat. No. 358054) with 45 ml homogenization buffer (12.5 % sucrose, 40 mM NaCl, 10 mM imidazole-Cl, 2 mM $MgCl_2$, 0.2 mM ethylene glycol tetraacetic acid (EGTA), 1 mM dithiothreitol (DTT), 0.5 % Triton X-100, and a Roche complete protease inhibitor cocktail tablet (Cat. No. 04 693 116 001)). Mounted the Teflon pestle in a Wheaton overhead stirrer (Cat. No. 903475), set the speed to 4 and inserted into the grinding chamber containing the flies. Under constant pressure, the grinding chamber was raised to pass the flies

by the pestle at least once. Caution was taken to keep constant pressure to prevent the pestle from spinning at an increased rate and denaturing the proteins due to heating.

2.12.2. Clarification of the supernatant

1. Transferred the dark grey homogenate to two 26.3 ml ultracentrifuge tubes (Beckman #355618). Balanced and centrifuged in a Beckman Type 60 Ti rotor (18,178*g* for 15 min at 4 °C) with the Beckman Coulter L8-60M centrifuge.

2. Discarded the supernatant by decanting into a beaker. The pellet consisted of two layers formed along the tube's length, the inner one of whitish tissue and the outer black exoskeleton. Resuspended each pellet with a transfer pipet and 22 ml homogenization solution. Transferred the solution into the glass 55 ml grinding chamber and homogenized using the glass pestle 2-4 times manually.

3. Poured the homogenate into clean ultracentrifuge tubes. Rinsed the homogenizer with 5 ml homogenization solution and added to the tubes. Centrifuged the tubes in a Beckman Type 60 Ti rotor (18,178*g* for 15 min at 4 °C). Discarded the supernatant.

4. Repeated step 6 with 50 ml wash buffer (homogenization buffer without protease inhibitor, 12.5 % sucrose, 40 mM NaCl, 10 mM imidazole-Cl, 2 mM $MgCl_2$, 0.2 mM EGTA, 1 mM DTT, 0.5 % Triton X-100).

5. Balanced the tubes and centrifuged in a Beckman Type 60 Ti rotor (39,214*g* for 15 min at 4 °C). Discarded the supernatant.

2.12.3. High salt solubilization of myosin

1. Resuspended each pellet in 22 ml myosin extraction buffer/Nickel column binding buffer (500 mM NaCl, 20 mM sodium phosphate buffer, 30 mM imidazole-Cl, pH 7.4) by repeated pipetting with a transfer pipet. Transferred the solution to the grinding chamber. Homogenized with the glass pestle manually and decanted into the centrifuge tubes. The solution was black with fine particulates.

2. Sonicated the solution in the 26.3 ml tubes on ice with 20 quick pulses at 50% duty cycle, setting of 5, with a micro tip (Fisher Scientific Sonic Dismembrator Model 100).

3. Incubated the tubes on ice for 3 min and sonicated for another 20 quick pulses in order to break up the tissue and possibly solubilize the thick filaments.

4. Incubated the tubes on ice for 30 min to allow for a more complete dissolution of the thick filaments.

5. Centrifuged the tubes in a Beckman Type 60 Ti rotor (177,520*g* for 35 min at 4 °C). The pellet contained the exoskeleton and some unextracted myosin along with the remainder of the cellular components.

2.12.4. Low salt precipitation of myosin

1. Divided the supernatant equally (8.3 ml each) into six 70 ml ultracentrifuge tubes (Beckman Cat. No. 355622). Filled the tubes to capacity with 4 mM DTT. Left the tubes in an ice bucket overnight at 4 °C.

2. Centrifuged the tubes with the diluted myosin solution in a Beckman Type 45 Ti rotor (158,420*g* for 35 min at 4 °C). Discarded the supernatant, shook out the remaining solution and placed the tubes upside down on a paper towel to dry for a few min.

2.12.5. Solubilization of the myosin pellets

1. Removed/resuspended the enriched myosin pellets (~1 cm diameter) with 3 ml of pellet resuspension buffer (1.5 M NaCl, 30 mM imidazole-Cl, 20 mM sodium phosphate buffer, pH 7.4) and was careful to collect all of the sticky pellet material with the pipet tip.

2. Transferred the solution to a chilled 50 ml beaker with a stir bar and covered with Parafilm. Washed/rinsed/collected the remaining pellet from the tubes with a 1 ml pipet and 3.0 ml pellet resuspension buffer.

3. Placed the beaker on a stir plate set at ~90 rpm for 45 min, and mixed the settled pellet with a 1 ml pipet periodically. Added 20 ml binding buffer to lower the ionic strength and dilute the protein. The optimal salt concentration for the Ni column is 500 mM. After an additional 45 min incubation, decanted and pipetted the remainder of the solution into a 60 ml syringe. Resuspension of the myosin pellets was difficult and takes patience, sometimes requiring a few hours; this time was used to prepare the Ni-affinity column.

4. Filtered the protein solution with a 0.45 μm syringe filter (Fisher Scientific Cat. No. 09-719D). The filter clogged and needed to be replaced several times.

2.12.6. Myosin purification by Ni-affinity chromatography

1. Prepared chromatography solutions for column run. The buffers were mixed and filtered with either the Corning 500 ml Vacuum Filter/Storage Bottle System with 0.22 μm membrane (Cat. No. 430769) or the Millipore Steriflip 50 ml disposable vacuum filtration system with 0.22 µm Millipore Express PLUS Membrane (Cat. No. SCGP00525), depending on the volume needed.

2. Prepared a GE Healthcare HisTrap HP 5 ml column (Cat. No. 17-5248-02) attached to a Luer-Lok syringe. The flow rate was held at approximately 5 ml/min (100 drops/min).

3. Washed the column with 25 ml filtered water (used a 30 ml syringe).

4. Equilibrated the column with 30 ml binding buffer (500 mM NaCl, 20 mM sodium phosphate buffer, pH 7.4, 30 mM imidazole-Cl). Positioned the column in a clamp on a stand with a 500 ml beaker placed underneath for collection of waste.

5. Loaded the column with the filtered enriched myosin solution.

6. Washed the column with 60 ml binding buffer.

7. Eluted the column with a single step elution buffer (500 mM NaCl, 20 mM sodium phosphate buffer, pH 7.4, 250 mM imidazole-Cl). Collected the eluate in two Amicon Ultra-15 concentrators (Cat. No. UFC905024).

8. Centrifuged the concentrators in a Sorvall Legend RT centrifuge (3000*g* for up to 30 min at 4 °C) to reduce the volume to 2.5-3.0 ml.

9. Determined concentration of the purified myosin solution

spectrophotometrically with quantification of absorbance at 280 nm (absorbance coefficient of 0.53 cm^{-1} for 1 $mg \cdot ml^{-1}$) (Margossian and Lowey 1982, Swank, Bartoo et al. 2001).

2.13. Limited proteolysis: subfragment-1 preparation and purification

2.13.1. Solution exchange and contaminant removal

1. Divided the concentrated purified myosin solution equally into six polycarbonate ultracentrifuge tubes (13 x 51 mm, 3.5 ml, Beckman Cat. No. 349622), then diluted with 3.0 ml 4 mM DTT (final NaCl concentration ~70 mM).
2. Incubated for one hour on ice for myosin precipitation. This also removed soluble contaminants that non-specifically bound to the Ni-affinity column.
3. Centrifuged the solution in a Beckman TL-100 ultracentrifuge, in a pre-cooled TLA-100.3 rotor (106,120*g* for 35 min at 4 °C). Discarded supernatants and resuspended each ~2 mm wide pellet with 250 μl digestion buffer (120 mM NaCl, 20 mM sodium phosphate pH 7.0, 1 mM EDTA, 4 mM DTT). Myosin pellets did not readily dissolve at 120 mM salt. Used the pipet tip to collect and remove the sticky pellet and pipetted the remainder of the pellet and solution into two pre-cooled ultracentrifuge tubes (Beckman microfuge tube polyallomer, Cat. No. 357448).
4. Carefully homogenized the whitish-colored clear pellets with an epi tube

pestle (Research Products International Corp., Cat. No. 199226). The solution was milky colored and translucent.

2.13.2. Time-limited proteolysis

1. Placed the two tubes in a 20 °C water bath for 3 min to equilibrate temperature.

2. Performed proteolysis based upon previously published methods (Miller, Nyitrai et al. 2003, Silva, Sparrow et al. 2003, Bloemink, Melkani et al. 2011). Prepared a 10 *μ*g/*μ*l α-chymotrypsin solution by gently mixing water with the lyophilized powder (Worthington Biochemical Corp., Cat. No. LS001475). Added 15 *μ*l chymotrypsin solution to the temperature-equilibrated myosin solution. Final chymotrypsin concentration was approximately 0.20 mg/ml.

3. After 6 min, quenched the proteolysis reaction by addition of 5 *μ*l of 200 mM phenylmethanesulfonyl fluoride (PMSF) in ethanol. Mixed in the PMSF/ethanol solution gradually so as not to precipitate the protein. Final PMSF concentration was approximately 1.5 mM. Immediately placed the tubes on ice and then into the TLA 100.3 rotor.

4. Centrifuged the solution to precipitate the insoluble myosin rod and any remaining undigested full-length myosin at (196,280*g* for 25 min at 4 °C).

5. Carefully pipetted the enriched S1 supernatant into an Eppendorf tube and placed on ice.

2.14. Purification by high-performance liquid chromatography

1. Performed size exclusion chromatography. The protein was eluted isocratically from a 16/60 column with Superdex 200 with an Amersham Biosciences AKTA system (flow rate of 1 ml/min, collected 2 ml fractions). Covered the protein-rich fractions, as determined by 280 absorbance, with parafilm and placed on ice overnight for convenience.

2. Performed SDS-PAGE analysis of protein peak fractions.

3. Concentrated the S1 fractions (6-8 ml total volume) with two 0.5 ml Millipore Biomax 5K NMWL centrifugal filter devices (Cat. No. UFV5BCC00). Six to ten centrifugations were performed at (10,700*g* for 15 min) in the Beckman Microfuge to reduce the volume to 200 μl.

4. Determined the concentration of the S1 solution spectrophotometrically by quantification of the absorption at 280 nm with the absorbance coefficient of 0.75 cm^{-1} for 1 $mg \cdot ml^{-1}$ (Margossian and Lowey 1982, Miller, Nyitrai et al. 2003).

5. Samples were taken at various steps throughout the extraction, proteolysis and purification process. The samples were evaluated with SDS-PAGE as described in the densitometry section of this dissertation.

6. The peak S1 protein fractions (usually fraction numbers 33-36, each containing 2 ml) from size exclusion chromatography were pooled and concentrated with Millipore Amicon Ultra centrifugal filter units with the Ultracel 50K membrane (Cat. No. ufc905024). The concentrators were centrifuged (3000*g* for 45-60 min) to reduce the final volume to 125-175 μl (preferred final

concentration was 5-8 mg/ml). The protein solution was divided into 16 μl aliquots and flash frozen in liquid nitrogen before storage at -80 °C.

2.15. Myosin preparation from microscopic dissection of the indirect flight muscles

In addition to the His-tagged myosin purification procedure as described above, preparation of myosin from microdissected IFMs was performed (180-200 EMB or His-tagged EMB transgenic flies). The methods for dissection and myosin purification were essentially as described previously (Swank, Bartoo et al. 2001, Kronert, Dambacher et al. 2008, Kronert, Melkani et al. 2010). The concentration of the purified myosin was determined spectrophotometrically by measuring the absorption at 280 nm. Purified myosin was used within 2hoursfor ATPase assays.

2.16. Determination of steady-state ATPase activity

ATPase activities of myosin from dissected muscles or Ni-affinity column chromatography were determined using [γ-^{32}P] ATP as previously described in detail (Swank, Bartoo et al. 2001, Kronert, Dambacher et al. 2008, Kronert, Melkani et al. 2010). After the nickel column, the eluate was concentrated, then diluted with 4 mM DTT and centrifuged in a Beckman TL-100 ultracentrifuge as described in section 2.13.1. This step removed soluble contaminants. Myosin

pellets were dissolved to a concentration of 2 μg/μl in myosin storage buffer (20 mM MOPS pH 7.0, 500 mM KCl, 20 mM DTT, 2 mM $MgCl_2$). For CaATPase assessment, 1 μl of the freshly prepared myosin solution was added to 125 μl CaATPase buffer (10 mM imidazole pH 6.0, 0.1 M KCl, 10 mM $CaCl_2$). CaATPase activity of myosin was initiated at 25 °C by addition of [γ-^{32}P] ATP. After a 15 min incubation the reaction was quenched with addition of 100 μl of 1.8 M $HClO_4$. Extraction and scintillation counting were done essentially as described previously (Swank, Bartoo et al. 2001). Basal MgATPase assessment was carried out in a similar fashion, except using 50 μl of MgATPase buffer (10 mM imidazole pH 6.0, 20 mM KCl, 2 mM $MgCl_2$, 0.1 mM $CaCl_2$, 1 mM [γ-^{32}P] ATP). Actin-stimulated MgATPase assays were performed in MgATPase buffer in the presence of increasing concentrations of chicken F-actin (0.1 to 2 μM). For assays in MgATPase buffer, the reaction was quenched after 25 min with 50 μl of 1.8 N $HClO_4$. Basal Mg^{2+}-ATPase activities obtained in the absence of actin were subtracted from actin-activated data points. Mean values from at least three different experiments were used to determine average ATPase values of each myosin. Maximal actin-activated ATPase (V_{max}) was obtained by fitting all data points from several preparations (minimum of three data points) of EMB and His-tagged EMB myosin with the Michaelis-Menten equation using Sigma Plot software. Values were averaged to give the mean ± standard deviation. Statistical comparisons of ATPase data were carried out using Student's *t* tests.

2.17. Crystallization

EMB S1 crystals were initially grown by the hanging drop, vapor diffusion method. Crystallization conditions were found using Hampton Research crystal screens (Cat. No. HR2-110 and HR2-112). One microliter of concentrated S1 was mixed with 1 μl mother liquor on a glass coverslip, which was then inverted and sealed over the reservoir containing 1 ml mother liquor. Microcrystals were grown by incubation at room temperature with mother liquor containing 0.1 M HEPES pH 7.5, 20% w/v polyethylene glycol 10,000. Larger rod-shaped crystals formed when using mother liquor containing 0.1 M HEPES pH 7.5, 17.5% w/v polyethylene glycol 8,000.

Crystallization was miniaturized with a robotic liquid handler, the TTP Labtech mosquito Crystal, which provided precise and repeatable nanoliter pipetting (Jenkins and Cook 2004). Purified EMB S1 from the final 1F *6HisEMB* line was used to carry out an extensive crystallization screens in the presence and absence of added ATP or AMP-PNP. For example, the 5/1/12 S1 3.4 mg/ml preparation (120 mM NaCl, 25 mM HEPES pH 7.0, 1 mM EGTA, 4mM DTT, final pH 7.18) was previously flash frozen and stored in -80 °C prior to crystallization. The crystallization screens were carried out using 200 nl crystallization droplets (100 nl protein solution and 100 nl crystallization condition) equilibrated in a sitting-drop geometry over 100 μl reservoirs which contained 60 μl of mother liquor (MRC 2 Well Crystallization Plates, Swissci, Hampton Research Cat. No. HR3-083). This approach allowed the efficient screening of over 2300 unique

crystallization conditions. Single crystals were collected with Hampton Research crystal loops (Cat. No. HR4-338) and Mitogen MicroMounts (Cat. No. M2 L18SP-A2). The crystals were submerged in cryoprotectant solution containing the crystallization condition with 23% w/v glycerol (typically for <20 seconds).

2.18. Data collection

Crystal diffraction data were collected at Argonne National Laboratory's Advanced Photon Source (D.O.E. 2013). The NE-CAT 24-ID-C synchrotron X-ray variable-energy beamline was set at 12658 eV. The hutch was equipped with a MD-2 Microdiffractometer which provided an exceptionally well collimated beam set at a 30 μm diameter. We utilized the Advanced Light Source (ALS)-type robotic sample auto-mount system to mount the crystals. The user end station was fully equipped with state of the art instrumentation and camera systems capable of visualizing crystals down to 1 micron in diameter. Data collection was performed with a new Pilatus 6M-F detector that operated in a single photon counting mode with a super fast minimal "dead time" of 5 ms (DECTRIS Ltd., Switzerland). The high speed and noise-less single photon signal allowed for diffraction data to be collected in a continuous mode without the opening and closing of the shutter for each frame.

2.19. Data processing

The data processing was automated while at Argonne National Laboratory's NE CAT 24-ID-C. The unpublished software suite was RAPD (https://rapd.nec.aps.anl.gov/rapd/). The data integration portion of the program incorporated XDS and CCP4 (Collaborative Computational Project 1994, Kabsch 2010).

2.20. "Phase problem" solution

The initial molecular replacement model of EMB S1 was determined by the automated molecular replacement software, BALBES (Long, Vagin et al. 2008). The server-based software was uploaded with the mtz file and the amino acid sequences for EMB S1 and the ELC. The resulting model had one portion of the motor domain correctly placed in electron density and five incorrectly placed amino acid chains, which were subsequently deleted.

2.21. Model building, refinement and validation

The electron density map exhibited N-terminal electron density to fill. The next step was the addition of an N-terminal 6-77 residue model from 1QVI (Gourinath, Himmel et al. 2003). The 71 residues were added in COOT taking into account a +3 shift and a gap in each sequence (Emsley and Cowtan 2004). The non-identical residues were mutated to alanine. This "chain A" model file

was uploaded into the CCP4 MOLREP program to find another independent "chain B" in the asymmetric unit (Collaborative Computational Project 1994, Vagin and Teplyakov 2010). The resulting model was run through rigidbody and restrained refinements in CCP4 REFMAC5 while limited to 3.6 Angstrom resolution (Murshudov, Skubak et al. 2011).

A homology model for the ELC was created with SWISS-MODEL (Arnold, Bordoli et al. 2006). The 1QVI PDB (scallop myosin) was uploaded in the automated modeling mode GUI and the coordinates sequence was converted to the *Drosophila* IFI-specific isoform ELC amino acid sequence (Falkenthal, Graham et al. 1987). The resultant *Drosophila* ELC homology model was produced. The sequence numbering was verified with the gaps in each sequence taken into account. The ELC homology model was aligned onto "chain A" with COOT software by superposing the 1QVI structure over the EMB structure and then superposing the EMB ELC over the 1QVI ELC. The chains were renamed to reflect EMB MHC as "chain A" and the corresponding EMB ELC as "chain B"; the other EMB MHC in the asymmetric unit was renamed as "chain C" (the second ELC was not modeled at this point.) The coordinates for the EMB with a single ELC were saved and a rigidbody refinement was performed with CCP4 REFMAC5. The resulting model was run through Phenix AutoBuild in order to improve the models fit into electron density (Terwilliger, Grosse-Kunstleve et al. 2008, Adams, Afonine et al. 2010). Further model building was carried out with COOT and KiNG (Chen, Davis et al. 2009). Further refinement

and model validation was performed in Phenix and Molprobity (Adams, Afonine et al. 2010, Chen, Arendall et al. 2010).

2.22. Acknowledgment to the Argonne National Laboratory

This work is based upon research conducted at the Advanced Photon Source on the Northeastern Collaborative Access Team beamlines, which are supported by a grant from the National Institute of General Medical Sciences (P41 GM103403) from the National Institutes of Health. Use of the Advanced Photon Source, an Office of Science User Facility operated for the U.S. Department of Energy (DOE) Office of Science by Argonne National Laboratory, was supported by the U.S. DOE under Contract No. DE-AC02-06CH11357

Chapter 3

Microdissection and Purification of Endogenous Myosin

3.1. Introduction

3.1.1. Background for myosin experimentation

Biochemists have always been interested in the basic question of how muscles generate movement. The contraction of muscle takes place by the mutual sliding of two sets of interdigitating filaments: thick (containing the myosin) and thin (containing actin) organized in sarcomeres each 2-3 μm long which give muscle its striated appearance in electron micrographs (Figure 3.1). The relative sliding of thick and thin filaments is brought about by the interaction of myosin and actin, known as the "cross-bridge". Hugh Huxley and A.F. Huxley independently found the structure and it was named the cross-bridge because they could see the formation of a “bridge” in between the filaments in an electron micrograph (Huxley and Niedergerke 1954, Huxley and Hanson 1954, Huxley 1957). Andrew Huxley later concluded that it was part of the myosin molecule that sticks out from the myosin filament and interacts cyclically with the thin filaments, transporting them by a kind of rowing action; Hugh Huxley termed this the swinging crossbridge theory of muscle contraction (Huxley 1969, Huxley and Simmons 1971).

Myosin is a highly conserved enzyme, a ubiquitous eukaryotic motor protein, which interacts with actin (Weiss and Leinwand 1996). Myosin converts chemical energy in the form of ATP to mechanical energy, thereby generating force and movement. The most impressive variety of such movement is muscle

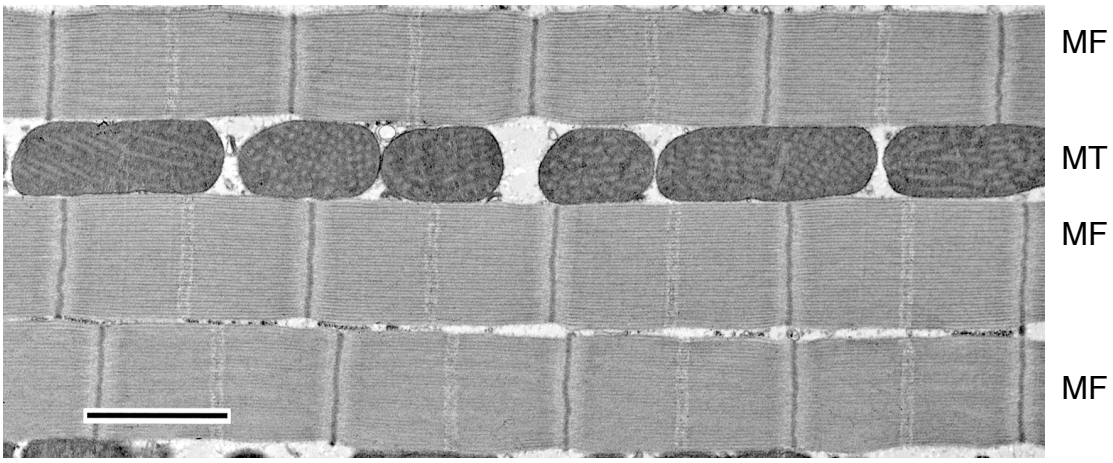

Figure 3.1: Transmission electron micrograph of *Drosophila* IFM

Drosophila dorsal longitudinal muscles are about a millimeter long (Swank 2012). Individual muscle cells are comprised of many myofibrils (shown here). The myofibrils have a striated appearance due to the basic units of contraction, the sarcomere.
Sarcomeres are 2-3 μm long. The sarcomere is composed of massive arrays of macromolecules. Myofibril (MF), mitochondria (MT), Bar = 2 μm
Photo courtesy of J. Suggs

contraction, which has provided the model for understanding actin-myosin interactions and the motor activity of myosin molecules. Interactions of actin and myosin are also responsible for a variety of movements of nonmuscle cells, including cell division, phagocytosis, pseudopod extension in amoebas, and filopodia extension in neurons. Therefore, myosins interactions with actin play a central role in cell biology.

Wilhelm Kühne discovered myosin almost 150 years ago (this “myosin” was later found out to be actomyosin) (Kühne 1864). Lohmann, at the Max Planck Institute for Biophysical Chemistry discovered adenosine triphosphate (ATP); he suggested that it was the energy source for muscle contraction in 1934 (Lohmann 1929, Szent-Gyorgyi 2004). In 1935, HH Weber developed a new technique for the *in vitro* study of contraction; he squirted “myosin” dissolved in high salt, into water, where it formed threads that became strongly birefringent upon drying (Weber 1935). Lyubimova and Engelhardt supported their hypothesis, that myosin has ATPase activity, thereby creating the term mechanochemistry. They found the contractile protein myosin that carries out the work also liberates the energy necessary for the work (Engelhardt and Liubimova 1939). ATP was also shown to dissociate actin from myosin (Guba 1943). Albert Szent-Györgyi was able to show that glycerol-treated muscle fibers, which contain only actin and myosin, shortened when ATP was added. This fiber shortening by ATP was further supported by using HH Weber’s artificial threads of actomyosin (Engelhardt 1941). Gergely was the first to initiate tryptic

proteolysis of myosin to reveal which regions of the molecule were responsible for the ATPase activity (Gergely 1950). Szent-Györgyi concluded that the ATPase region was solubilized and then named it heavy meromyosin (HMM) because it sedimented first. The slow component to sediment was named light meromyosin (LMM) (Szent-Gyorgyi 1953). Further exposure of HMM to trypsin for an extended time converted it to a single major component sedimenting more slowly, called subfragment 1 (S1), but also yielded a more heterogeneous component known as subfragment 2 (S2) (Mueller and Perry 1962) (Figure 3.2). In 1967, electron microscope studies established that a myosin molecule ended in two globules (cross-bridge, or myosin “heads”, now referred to as the motor domain) (Slayter and Lowey 1967). In 1971, Lymn and Taylor, originated their cross-bridge cycle theory, based on purified myosin and actin *in vitro*, which started the modern era of muscle contraction study. The cross-bridge theory finally described how ATP could both dissociate myosin from actin and cause muscle contraction (Lymn and Taylor 1971).

Myosins have been classified into more than 20 classes based on their phylogeny (Coluccio 2008) and classified into 36 classes based on the amino acid sequence homology of the motor domain (Odronitz and Kollmar 2007). The conventional myosin, class II, is characterized by the presence of a rod-like *α*-helical tail that winds with another tail to form two-headed dimers which further assemble into bipolar anti-parallel filaments (Cheney, Riley et al. 1993). The

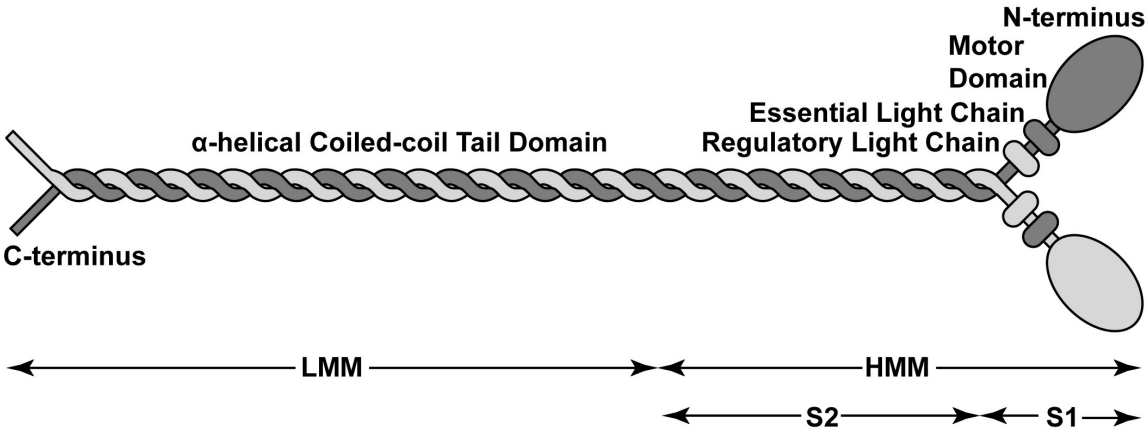

Figure 3.2: Myosin schematic showing proteolysis sites and fragments

Myosin II can be broken into fragments with time limited proteolysis. Partial digestion of skeletal muscle myosin II with *α*-chymotrypsin typically cleaves the molecule just below the regulatory light chain (light gray oval) binding domain, producing the S1 head and the rod domain. Biochemical and crystallization of S1 obviates difficulties with the full-length protein where the rod domain causes aggregation and precipitation in low ionic strength solutions. Digestion of vertebrate myosin II with trypsin cleaves the molecule into the HMM and LMM fragments.
LMM, light meromyosin, S1, subfragment-1, HMM, heavy meromyosin
Myosin schematic prepared by Tom Huxford.

quaternary structure of myosin consists of two heavy chain subunits (MHC), two essential light chain subunits (ELC, alkali MLC or MLC-1) and two regulatory light chain subunits (RLC or MLC-2) (Emerson and Bernstein 1987). A soluble proteolytic fragment of myosin, subfragment 1 (S1), (made of a single globular head and one or both of the light chains) contains the ATPase activity. The subfragment 2 (S2) comprises the N-terminal one-third of the rod and contains a hinge-like region that facilitates movement of the neck and head during a power stroke (Weiss, Schiaffino et al. 1999). LMM, the C-terminal two-thirds of the rod, is responsible for self-assembly and forms the backbone of the thick filament (Emerson and Bernstein 1987). The essential and regulatory light chains are not required for the motor domain (MD) to have ATPase activity (Margossian and Lowey 1973). ATPase activity is described as the hydrolysis of ATP that provides the chemical energy for the mechanical work done by myosin in which ATP is hydrolyzed to ADP (adenosine diphosphate) and phosphate (P_i).

3.1.2. *Drosophila melanogaster* indirect flight muscles (IFMs)

Insects have extremely fast muscle contractions which are required for the wing beat frequency needed to sustain flight for such a small animal (Vogel and de Ferrari 2001). Insect flight requires a highly specialized fibrillar, asynchronous muscle type (Pak 1986, Peckham, Molloy et al. 1990). *Drosophila melanogaster* have a wing beat frequency of 220 Hz. Each wing beat cycle requires a contraction of the *indirect* flight muscles (IFMs), the power muscle of insect flight,

which is directly attached to the exoskeleton, not the wings. The deformation of the exoskeleton by the IFMs causes the wings to move up and down. Two opposing sets of muscle cells make up the IFMs; there are 12 dorsal longitudinal muscle (DLM) fibers that contract to lower the wings and 14 dorsal ventral muscle fibers (DVM) that contract to raise the wings (Swank 2012).

The IFMs are asynchronous muscles (nerve action potentials are not synchronous with the IFM contractions); the nerve impulse occurs at a much lower frequency than the wing beat frequency (Levine and Wyman 1973). Furthermore, asynchronous muscles are stretch activated; the muscles are only partially activated by calcium ions and full activation is produced when the fibers are stretched to the order of 3% above their rest length (Peckham, Molloy et al. 1990). The IFMs are designated as fibrillar muscle type; the nuclei and mitochondria are scattered throughout the cytoplasm and six thin filaments surround each thick filament in a double hexagonal array (Bernstein, O'Donnell et al. 1993). The IFM fill the inner portion of the thorax and are controlled by the nervous system, however, once flight has been initiated, the muscles then have stretch activated contraction and shortening deactivated relaxation during flight while maintaining a relatively high calcium concentration (Josephson, Malamud et al. 2000).

Many insects, including *Drosophila*, are unusual with regard to their having a single muscle myosin heavy chain (*Mhc*) gene, which drives expression in all muscles of the fly (Emerson and Bernstein 1987). This is in contrast to having a

family of muscle myosin genes, as is the case with most other organisms in the Metazoan lineage with each gene coding for a muscle myosin isoform with a specialized niche (Odronitz and Kollmar 2008). In the human genome, 39 genes that encode for myosin have been identified and 15 have been confirmed to encoded conventional myosin II (Berg, Powell et al. 2001), with 8 of these encoding muscle myosin II (2 cardiac and 6 skeletal) (Weiss, Schiaffino et al. 1999). The *Drosophila Mhc* gene has 19 exons; 13 of these are constitutive exons, five are chosen from two or more alternatively spliced versions (exons 3, 7, 9, 11 and 15), and the penultimate exon (exon 18) is included or excluded from the mRNA (George, Ober et al. 1989, Zhang and Bernstein 2001). In the motor domain, four regions are encoded by *Drosophila Mhc* alternative exons: 3(a,b), 7(a,b,c,d), 9(a,b,c) and 11(a,b,c,d,e) (Bernstein and Milligan 1997). There are 120 combinations of alternative exons in the motor domain with at least 12 verified to exist (George, Ober et al. 1989, Hastings and Emerson 1991, Wells, Edwards et al. 1996, Swank 2012). Likewise, *Apis mellifera*, the honeybee has an alternative exon *Mhc* gene structure that encodes for a possible 384 isoforms with 96 of those combinations in the motor domain, see Figure 3.3 (Odronitz and Kollmar 2008).

Historically, access to myosin proteins has required extraction and purification from primary tissues. Some examples include extraction from frozen human muscle samples (Cuda, Fananapazir et al. 1997), extraction from fresh

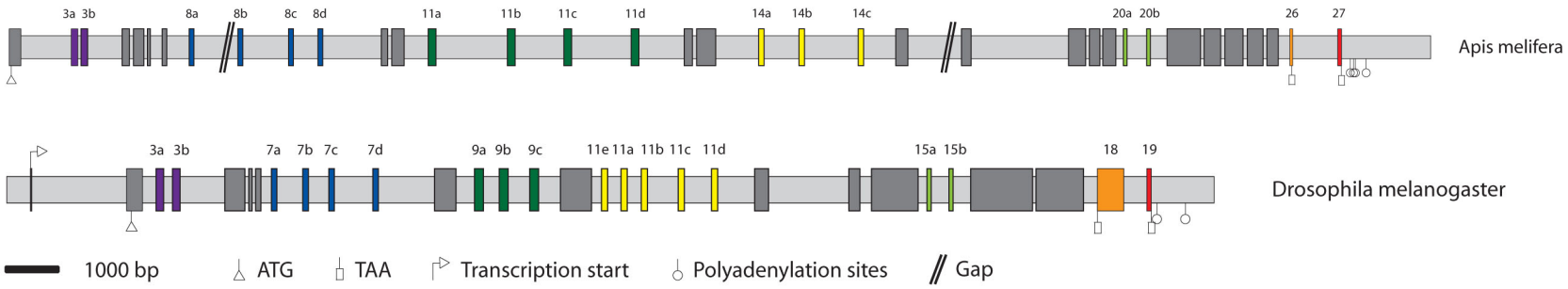

Figure 3.3: Apis mellifera and Drosophila melanogaster Mhc gene structure

The *Apis mellifera Mhc* gene contains 27 exons. Six exons are alternatively spliced and the others are constitutive in all transcripts. Five of these exons contain two or more alternates whereas the penultimate exon, exon 26, is either included or excluded from mRNA transcripts.
The *Drosophila melanogaster Mhc* gene contains 19 exons. Six exons are alternatively spliced and the others are constitutive in all transcripts. Five of these exons contain two or more alternates whereas the penultimate exon, exon 18, is either included or excluded from mRNA transcripts (Odronitz and Kollmar 2008).
Reproduced with permission from Odronitz and Kollmar, Comparative genomic analysis of the arthropod muscle myosin heavy chain genes allow ancestral gene reconstruction and reveals a new type of 'partially' processed pseudogene, BMC Molecular Biology.

chicken pectoralis muscle (Rayment, Rypniewski et al. 1993), extraction from freshly caught and filleted cod (Kristinsson 2001), extraction from fresh porcine semitendinosus muscles (Bowker, Swartz et al. 2004), His-tag myosin purification from mouse (Lowey, Lesko et al. 2008) and extraction from Drosophila indirect flight muscle (Swank, Bartoo et al. 2001). The many advantages of *Drosophila* make it a very appealing choice for investigating muscle development, muscle physiology and muscle protein structure and function. The genetics and morphological characteristics of the indirect flight muscle of *Drosophila melanogaster* make it an ideal system for evaluating the influence of protein mutations on muscle and cross-bridge stiffness, oscillatory power, and deriving cross-bridge rate constants (Swank 2012).

The Bernstein lab has investigated two isoforms of myosin II with completely different sets of alternative exons encoding the motor domain. The indirect flight muscle isoform (IFI) has exons 3b, 7d, 9a and 11e; the embryonic body wall isoform has exons 3a, 7a, 9 and 11c. The IFI is the wild type endogenous myosin found in the indirect flight muscles of the thorax that power flight. The EMB isoform is found in the larval stage transverse body wall muscles that power crawling (Bernstein and Milligan 1997). The differences between EMB and IFI, and their alternatively expressed exons, have been extensively studied with a battery of techniques including biochemical assays, biophysical testing of mechanical differences of the myofibers, microscopy viewing of the ultrastructure, locomotory testing on the living flies, and homology modeling

(Swank, Bartoo et al. 2001, Swank, Knowles et al. 2003, Miller, Bloemink et al. 2007, Yang, Ramanath et al. 2008, Bloemink, Dambacher et al. 2009). The isoforms were found to have significantly different properties of muscle function including ATPase rate, *in vitro* actin filament sliding motility velocity, power output and flight ability (see Table 3.1).

3.1.3. Myosin extraction from microdissected *Drosophila melanogaster*, fruit fly, and *Apis mellifera*, honeybee

The use of *Drosophila melanogaster* as an in vivo expression system for myosin proteins has been developed and as a result many different isoforms have been successfully expressed and purified on a small scale for biochemical studies by the Bernstein group. The *Drosophila* myosin heavy chain gene has been extensively studied and has produced a wealth of genetic information on mutants, as well as several of the 480 possible isoforms created through alternative exon splicing. These studies highlighted key residues and domains for myosin function (Swank, Bartoo et al. 2001, Miller, Bloemink et al. 2007, Odronitz and Kollmar 2008, Yang, Ramanath et al. 2008, Bloemink, Dambacher et al. 2009). In addition, ultrastructural and mechanical assays have been carried out for years. A substantial problem persists, however, as the high resolution structural studies of these isoforms have been limited by the use of homology modeling based upon scallop or chicken crystal structures with only 60% sequence homology at best (Miller, Bloemink et al. 2007). Therefore, an atomic

Table 3.1: EMB and IFI integrative analysis data

Myosin isoform	IFI	EMB
ATPase Activities (Littlefield, Swank et al. 2003)		
Basal Mg^{2+} ATPase rate (s^{-1} $head^{-1}$)	0.2 ± 0.04	0.07 ± 0.01[a]
Basal Ca^{2+} ATPase rate (s^{-1} $head^{-1}$)	7.6 ± 0.3 (6)	3 ± 0.3 (7)[a]
Maximal ATPase rate, Vmax (s^{-1} $head^{-1}$)	0.9 ± 0.04 (5)	0.7 ± 0.05 (5)[b]
K_M (μM)	0.7 ± 0.1	0.8 ± 0.2
Motility Characteristics (Swank, Bartoo et al. 2001)		
Actin filament sliding velocity ($\mu m/s^{-1}$)	6.4 ± 0.7 (4)	0.7 ± 0.1 (4)[c]
Step size	3.91 ± 2.36	4.38 ± 2.27
Off rate	3.2×10^6	1.9×10^6
Muscle mechanics (Swank, Knowles et al. 2002)		
Maximum Power output ($Watts/m^3$)	110 ± 12.0	25 ± 5.0[a]
Force pCa 4.5 (mN/mm^2)	1.2 ± 0.2	3.4 ± 0.7[a]
Locomotion parameters (Swank, Knowles et al. 2002)		
Wing beat frequency	181 ± 1.8 §	NA
Flight Index (0-6)	3.8 ± 0.2	0
Jump distance	4.9 ± 0.2 ‡	2.2 ± 0.1[a]

Values are mean ± standard deviation. Parentheses indicate number of myosin preparations used.
[a] IFI vs. EMB statistical significance determined by Student's *t*-test ($P < 0.05$); [b] IFI vs. EMB statistical significance determined by *Z*-test ($P < 0.05$); [c] IFI vs. EMB statistical significance determined by Student's *t*-test ($P < 0.005$); § Less than wild-type at 22 °C (200 Hz), caused by the Mhc^{10} background; ‡ The native jump muscle isoform is expressed, not IFI.

resolution model of *Drosophila* myosin would be of great interest, as it would allow for further insight into the mechanism by which myosin drives the function of muscles. The objective of my research is to elucidate the functional mechanism of a highly specialized skeletal muscle myosin II (subsequently referred to as myosin) by obtaining an atomic resolution molecular model. Specifically, I am interested in crystallizing the myosin head motor domain (Subfragment 1 or S1) from insect indirect flight muscle (IFM). This particular muscle is capable of exceptionally rapid contraction to generate a wing beat frequency of approximately 200 Hz in *Drosophil*a. The initial step of my research entails the acquisition of milligram amounts of myosin S1 required for crystallization trials.

The extraction of myosin from *Apis mellifera* was investigated because of the insufficient amount of myosin that was purified through microdissection techniques from wild type *Drosophila melanogaster*. Because crystallization screening and optimization trials require milligram amounts of myosin S1, the larger *Apis mellifera* (honeybee) was selected. *Apis mellifera* is a suitable alternative model system owing to its similarities with *Drosophila*. Both insects share IFM specialization; a single myosin heavy chain gene for myosin with alternative exon splicing that can produce multiple isoforms, and a sequenced genome (Consortium 2006, Odronitz and Kollmar 2008). Worker bees from the same genetically constrained standard stocks were obtained and dissected for a particular preparation; Dr. Gro Amdam, ASU, gifted these bees. The X-ray

crystallography determination of an *Apis mellifera* myosin would provide the first insight into an insect myosin and pave the way for solving the structure of *Drosophila* myosin isoforms and mutants.

3.2. Materials and Methods

(refer to chapter 2, section 2.12.)

3.3. Results

3.3.1. Microdissection of indirect flight muscle from fruit flies

Several hundred flies were anesthetized with carbon dioxide for practicing dissection. To remove the muscles from *D. melanogaster*, the flies were first anaesthetized with CO_2, and sorted by sex. Females were chosen for dissection due to their slightly larger size. The flies were placed on their dorsal side with their head to the left. The forceps were held in the left hand and were used to stabilize the fly with placement between the head and the thorax. The scissors were held in the right hand and were used to brush the legs away from the head to the right while positioning to cut through the joint between the thorax and abdomen. This first cut removed the abdomen along with the wings and the most posterior pair of legs. The scissors were then placed next to the forceps in between the head and thorax and pulled to the right slowly for separation of the

head with the digestive tract attached (less possibility of protease contamination). The thorax was bisected by insertion of one blade of the scissors in the hole where the head was attached and positioning the other blade at the bilateral line between the legs where the cut was then made. The thorax was then carefully rotated 180 degrees on the distal blade of the scissors for the second cut through the dorsal midline. The bisected thoraces were immediate placed into a small Plexiglas dish which contained YMG solution at 4 °C. After 50 flies were dissected to the bisected thoraces stage, the indirect flight muscles were removed. The bisected thorax was placed on its lateral side and the muscle tissue was carefully teased out of the exoskeleton shell with an electrolytically sharpened tungsten wire. After several practice sessions, 50 flies were dissected in ~3 hours. The preparation of myosin from the small amount of tissue failed to produce enough purified myosin to carry out proteolysis.

3.3.2. Microdissection of indirect flight muscle from honeybees

Live honeybees were obtained from several sources. The bees were anesthetized with CO_2. The IFMs dissected out easily compared to the fly microdissections. The IFMs were removed from freshly killed bees; however, the IFMs from whole thoraces stored in relaxing buffer were soft and not amenable to removal by microdissection. I visually observed that muscle mass dissected from one bee equaled the muscle mass dissected from approximately 100 fruit flies.

3.3.3. Purification of honeybee, *Apis mellifera,* myosin S1 fragments

Longitudinal indirect flight muscles were manually extracted from the dissected thoraces, which were then homogenized to extract muscle fibers. These fibers were subsequently washed, sonicated and centrifuged to obtain myofibrils. The myosin was extracted based on its solubility profile in high ionic strength solutions, which helped to exclude unwanted proteins via precipitation. The purification scheme required a series of centrifugations in either high salt (myosin soluble) or low salt (myosin insoluble) conditions. Myosin solubilized in high salt extraction buffer (>250 mM). Solubilized myosin was then polymerized into myosin filaments by low salt treatment and collected via centrifugation. Limited proteolysis yielded S1, which contain the motor domain, as well as the myosin rods. The myosin rods precipitated in low salt buffer and were separated by centrifugation. The collected myosin was digested with chymotrypsin, diluted to low ionic strength where the myosin rod became insoluble, and then centrifuged to pellet the rod and undigested myosin in order to obtain S1 in the supernatant. Size exclusion chromatography was carried out to prepare a highly purified S1 and to remove the chymotrypsin. The final S1 solution was then assessed for purity by SDS-PAGE (Figure 3.4). S1 was purified from the homogenizations of whole honeybee thoraces or from microdissected indirect flight muscles. Whether fresh or kept in relaxing buffer at 4 °C, either honeybee thoraces or IFMs provided similar results. The highest S1 yield attained after size exclusion purification was 274 μg (1.57 mg/ml) from 50 dissected IFMs (Table 2).

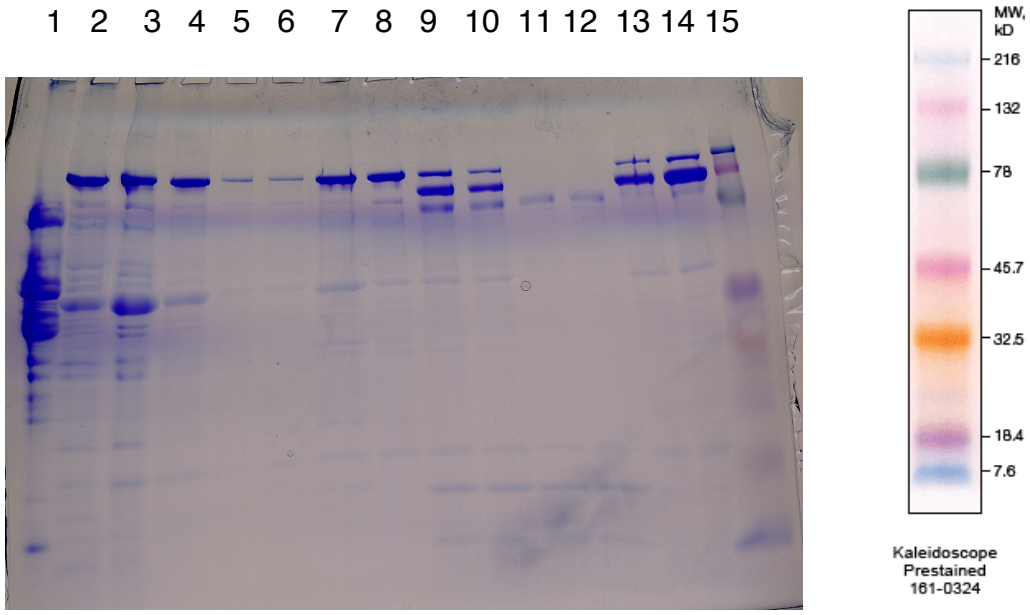

Figure 3.4A: Coomassie blue stained SDS-PAGE gel of *Apis mellifera* myosin purification

8-16% Tris HCl Bio-Rad Ready Gel 110V/90 min 8/14/2009
Well # samples are 1:1 with Laemmli buffer 15 µl loaded (unless noted)

1. Relaxing solution which contained *Apis mellifera* IFMs at -20 °C
2. Homogenate of 50 dissected IFMs
3. after sonication (in MEB)
4. supernatant MEB spin 2
5. wash B 6.0 ml plus 18 ml dilution
6. supernatant spin 4 300mM salt
7. bit of pellet spin 4 in 30 µl Laemmli buffer
8. final *Apis mellifera* myosin
9. quenched proteolysis tube #1
10. quenched proteolysis tube #2
11. Supernatant 25 min spin after proteolysis tube #1
12. Supernatant 25 min spin after proteolysis tube #2
13. tube #1 pellet in 200µl 1X Laemmli, 4 µl loaded
14. tube #2 pellet in 200µl 1X Laemmli, 4 µl loaded
15. 5 µl Kaliedoscope protein ladder (see right panel)

Refer to materials and methods section 2.5 for details.

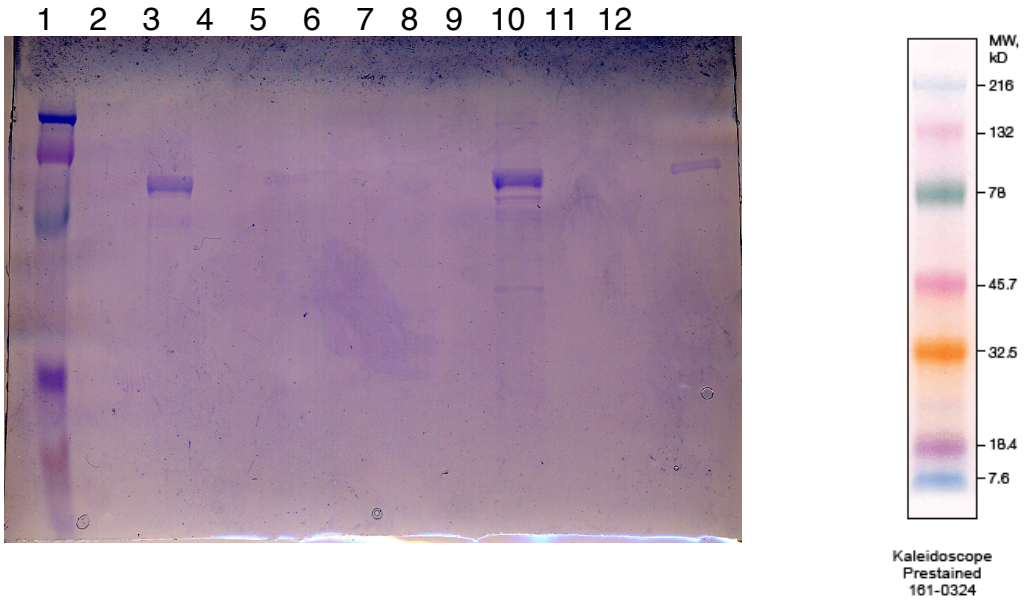

Figure 3.4B: Coomassie blue stained SDS-PAGE gel of *Apis mellifera* myosin purification steps

10% Tris HCl Bio-Rad Ready Gel 110V/90 min 8/14/2009
Well #
1. 5 µl Kaliedoscope protein ladder (see right panel)
2. Laemmli buffer only; empty lane
3. 1 µl *Apis mellifera* S1 after size exclusion and concentration
4. Laemmli buffer only; empty lane
5. *Apis mellifera* 1/10 dilution of lane 3
6. Laemmli buffer only; empty lane
7. *Apis mellifera* 1/100 dilution of lane 3
8. Laemmli buffer only; empty lane
9. *Apis mellifera* S1 15µl before size exclusion/ 15 µl dye, 13 µl loaded
10. flow through size exclusion column (sepharose Superdex 200) 13 µl loaded
11. 1:1 sample of chymotrypsin 13 µl loaded (cannot see, ran off gel)
12. size exclusion (sepharose Superdex 200) column wash 13 µl loaded

Refer to materials and methods section 2.5 for details.

Table 3.2: Summary of *Apis mellifera* (honeybee) myosin yields

Apis Mellifera Myosin Purification Yields			
Date	Bees Dissected	MHC Yield	S1 Yield
12/08/09	30 IFM		870* μg
10/21/09	30 IFM	3.7 mg	90* μg
10/13/09	20 IFM		428* μg
10/06/09	44 IFM		725* μg
08/26/09	28 IFM	1.6 mg	
08/12/09	50 IFM		211 μg SEC
06/10/09	50 IFM		274 μg SEC
01/28/09	10 IFM	2.7 mg	
06/05/08	37 whole thoraces	1.7 mg	

Values were calculated from determined concentrations of the purified myosin and S1 solutions. The concentrations were determined spectrophotometrically by quantifying the absorbance at 280 nm using an absorbance coefficient of 0.53 cm^{-1} for 1 $mg \cdot ml^{-1}$ for full length myosin and 0.75 cm^{-1} for 1 $mg \cdot ml^{-1}$ for S1 (Margossian and Lowey 1982, Swank, Bartoo et al. 2001)
*Note that the S1 yield for purifications without size exclusion chromatography (SEC) included chymotrypsin in the solution.

3.4. Discussion

3.4.1. *Drosophila melanogaster* microdissection and myosin purification

The Bernstein laboratory research has involved microdissection of fruit flies and purification of myosin for nearly 20 years (Kronert, O'Donnell et al. 1995, Cripps, Suggs et al. 1999). The published quantity of myosin purified from the IFM microdissection technique and purification protocol yielded 2.3-3.3 μg/fly depending on the fly phenotype (Swank, Bartoo et al. 2001). The yield I was able to attain was approximately 1 μg/fly. The paucity of material allowed for gel samples with nothing left over. The insufficiency of material obtained from dissection meant that 5,000-10,000 flies would have to be dissected in order to obtain 5-10 mg purified myosin. The purification was successful but the amount of purified myosin was dismally insufficient for crystallization trials. Whole fly homogenization purification methods would produce a heterogeneous mixture of myosin isoforms therefore this method was not a viable option. However, I followed through with Dr. Girish Melkani, a Bernstein lab post doc, with method optimization for proteolysis and purification of S1

This quantity of *Drosophila* myosin was insufficient to follow through with proteolysis and size exclusion chromatography for crystallization trials.

3.4.2. *Apis mellifera* myosin purification through microdissection

We had limited success working with bees. The IFMs were much easier to dissect out, relative to the *Drosophila*. However, the researcher must take care with handling bees to keep the number of stings low. I was stung at a 3% rate when dissecting the first 100 bees, after that the rate dropped to 1-2%. It was found that a freshly removed abdomen in the discard pile easily envenomated the researcher when brushed with a finger. To control the escape of bees from the shipping box, a small opening was made in the cardboard that allowed only one bee to exit the container which held several hundred bees, however some bees evaded capture and escaped. A melee of activity to capture or kill the escaped bee was performed successfully to ensure no other researchers were stung.

The development of a method for myosin purification from *Apis mellifera* IFMs with proteolysis to produce S1 was a novel undertaking. The procedure was based on established *Drosophila* myosin purification protocols, and scaling up to bulk purification (greater than one gram of starting material) was developed with Dr. Anthony Cammarato and from many lab discussions (Hynes, Block et al. 1987). The purpose of the experiments was to optimize myosin purification and proteolysis to recover milligram quantities of S1 for crystallization trials. However, the honeybee IFMs may contain multiple isoforms of myosin, which was never confirmed since the scale up did not work well. The problems with increasing the starting amount of muscle mass were likely due to not being able to homogenize the tissue well enough to solubilize the myosin. Alternatively, the

protein concentration may have been saturated during the high salt extraction (sample volume was limited by the volume of one set of centrifuge tubes, 8 x 26.3 ml).

Thus far, I have found that the preparation of pure concentrated *Apis mellifera* S1 protein from indirect flight muscle is possible, which was critical for crystallization trails to determine the structural model. However, the amount of myosin purified from honeybees was still not sufficient for crystallization trials (Table 3.2). Therefore, the honeybee myosin purification was terminated.

3.4.3. Conclusions regarding purification from primary tissue

The purpose of the microdissection technique was to purify enough myosin S1 to set up crystallization trials in order to obtain diffraction quality crystals for high-resolution structure analysis. However, this was a risky plan for several reasons. The potential for problems with heterogeneity both with respect to the potential multiple isoforms in the purified myosin as well as possible genetic and therefore protein differences between colonies of bees. When considering the history of macromolecular structure analysis through X-ray crystallography and the production of high-resolution molecular models of proteins since the 1950s, there are no guarantees for any of the current techniques in the crystallization of any particular protein (Rupp 2003). Furthermore, modern approaches of macromolecular crystallization to gain

diffraction quality crystals, is successful in perhaps 40% of cases (McPherson 1995).

On the bright side, myosin purification from primary tissue has produced several myosin structures in the Protein Data Bank (Rayment, Rypniewski et al. 1993, Houdusse, Kalabokis et al. 1999, Berman, Battistuz et al. 2002, Yang, Gourinath et al. 2007). Microdissection of insect muscle and myosin purifications have been a proven method for the study of muscle performance and biochemical assays (Swank, Bartoo et al. 2001, Swank, Knowles et al. 2002, Littlefield, Swank et al. 2003, Swank 2012).

From this study, we conclude that high-resolution biochemical characterization of insect myosin would require the development of a novel method for recombinant expression and purification. Myosin purification from primary tissue had seemed the best route for producing purified protein, however dissection on a preparative scale was impractical.

Chapter 4

Transgenic expression and purification of myosin isoforms using the *Drosophila melanogaster* indirect flight muscle system

Contents lists available at SciVerse ScienceDirect

Methods

journal homepage: www.elsevier.com/locate/ymeth

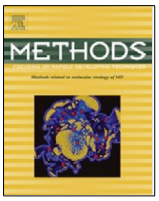

Transgenic expression and purification of myosin isoforms using the *Drosophila melanogaster* indirect flight muscle system

James T. Caldwell[1], Girish C. Melkani[2], Tom Huxford[1], Sanford I. Bernstein[2,*]

[1]Department of Chemistry & Biochemistry and

[2]Department of Biology

San Diego State University

5500 Campanile Drive

San Diego, CA 92182-4614

*Corresponding author. E-mail address: sbernst@sciences.sdsu.edu; Department of Biology, San Diego State University, 5500 Campanile Drive, San Diego, CA 92182-4614. Telephone: (619) 594-5629. FAX: (619) 594-5676.

Abbreviations: EMB, embryonic body wall muscle isoform of myosin heavy chain; *Mhc*, myosin heavy chain; S1, proteolytic subfragment-1 of myosin; TEV, tobacco etch virus.

4.1. Abstract

Biophysical and structural studies on muscle myosin rely upon milligram quantities of extremely pure material. However, many biologically interesting myosin isoforms are expressed at levels that are too low for direct purification from primary tissues. Efforts aimed at recombinant expression of functional striated muscle myosin isoforms in bacterial or insect cell culture have largely met with failure, although high level expression in muscle cell culture has recently been achieved at significant expense. We report a novel method for the use of strains of the fruit fly *Drosophila melanogaster* genetically engineered to produce histidine-tagged recombinant muscle myosin isoforms. This method takes advantage of the single muscle myosin heavy chain gene within the *Drosophila* genome, the high level of expression of accessible myosin in the thoracic indirect flight muscles, the ability to knock out endogenous expression of myosin in this tissue and the relatively low cost of fruit fly colony production and maintenance. We illustrate this method by expressing and purifying a recombinant histidine-tagged variant of embryonic body wall skeletal muscle myosin II from an engineered fly strain. The recombinant protein shows the expected ATPase activity and is of sufficient purity and homogeneity for crystallization. This system may prove useful for the expression and isolation of mutant myosins associated with skeletal muscle diseases and cardiomyopathies for their biochemical and structural characterization.

4.2. Introduction

Myosins comprise a large superfamily of molecular motor proteins that fulfill a variety of cellular functions (2008). Due to the vital role they play in functioning muscle and/or the high expression levels of some members of this class, the class II myosins are the most well characterized members of this superfamily and have been the focus of both biophysical and biochemical studies for decades (Tyska and Warshaw 2002). X-ray crystallography has been instrumental in elucidating the functional intermediates and reaction mechanisms of class II myosins from various organisms including: *Gallus gallus* (chicken) skeletal muscle myosin II (Rayment, Rypniewski et al. 1993) and smooth muscle myosin II (Dominguez, Freyzon et al. 1998), a modified version of *Dictyostelium discoideum* (slime mold) myosin II (Smith and Rayment 1996), and *Argopecten irradians* (scallop) muscle myosin II (Gourinath, Himmel et al. 2003). The chicken and scallop muscle myosin X-ray crystal structures were determined with myosin proteins purified directly from primary muscle tissue and the *Dictyostelium* protein was purified directly from a genetically modified version of the organism in culture (Fisher, Smith et al. 1995). Chicken smooth muscle myosin II was expressed in baculovirus-infected insect tissue culture cells (Trybus 1994).

One of the factors that limits our ability to carry out mechanistic studies on striated muscle myosin isoforms is the difficulty in preparation of purified functional myosins in quantities sufficient for biophysical and structural studies using recombinant expression systems. Some examples of striated muscle

myosin proteins that would be interesting to study are *Drosophila* indirect flight muscle myosin (Swank, Bartoo et al. 2001), mouse cardiac myosin (Lompre, Mercadier et al. 1981), and human beta cardiac myosin mutants responsible for hypertrophic or dilated cardiomyopathy (Tardiff 2005). Attempts to express these in *E. coli* or other bacterial recombinant protein expression systems have met with failure, as have efforts to use insect cells infected with recombinant baculoviruses. A recent study from the Leinwand laboratory (Resnicow, Deacon et al. 2010), based upon methods developed in the Winkelmann laboratory (Chow, Srikakulam et al. 2002, Wang, Moncman et al. 2003), reports the use of murine C_2C_{12} myoblasts to produce adequate amounts of functional recombinant human skeletal muscle myosin II isoforms. However, generation of appreciable amounts of purified material by this approach is expensive.

The fruit fly *Drosophila melanogaster* represents a novel and inexpensive system in which to study muscle myosin function (Swank, Wells et al. 2000). Unlike many organisms that contain multiple muscle myosin heavy chain genes, all the myosin heavy chain isoforms that are required throughout the fly life cycle are generated by alternative splicing of exons encoded by a single *Drosophila Mhc* gene (Bernstein, Mogami et al. 1983, Rozek and Davidson 1983). This gives rise to at least 15 different myosin heavy chain isoforms out of a possible 480 combinations (Zhang and Bernstein 2001, Odronitz and Kollmar 2008).

Muscle myosin is expressed at different times during the fruit fly life cycle (Taylor 2006). In adult flies, significant amounts of myosin are expressed in the

indirect fight muscles of the thorax. Use of transgenic flies expressing a specific myosin isoform in myosin-null indirect flight muscles allows the isolation of transgenically expressed myosins from dissected muscles (Swank, Bartoo et al. 2001). Our dissection of dorsal longitudinal indirect flight muscles from individual flies routinely yields purified myosin at roughly one microgram per fly. Standard methods to solubilize and proteolytically process the myosin to produce the functional head domain (subfragment-1, S1) is feasible and provides adequate materials for some kinetic studies (Miller, Nyitrai et al. 2003). However, production of milligram quantities of S1 required for crystallography is not practical by this approach, in that isolation of 1 mg of S1 would require 1.9 g (about 2,000) flies to be dissected.

In support of efforts aimed at producing large quantities of diverse muscle myosin proteins for structural and mechanistic studies, we have developed a method that employs *Drosophila melanogaster* as an *in vivo* expression system for tagged myosin proteins. Proof of concept was provided by Lowey et al. (Lowey, Lesko et al. 2008), who expressed and purified histidine-tagged myosin heavy chain in a mouse model for the study of familial hypertrophic cardiomyopathy. Our approach takes advantage of the single *Drosophila Mhc* gene and the ability to express transgenically encoded myosin heavy chain in the indirect flight muscles of a mutant lacking endogenous myosin in this muscle. Here we use the *Actin88F* promoter to drive high level expression of a histidine-tagged recombinant version of a *Drosophila* embryonic body wall myosin isoform

(EMB). The protein can be purified by affinity chromatography on extracts from whole flies and the S1 motor domain can then be isolated by proteolysis and size exclusion chromatography. Myosin prepared by this method retains its function, as evidenced by *in vitro* ATPase assays. The S1 fragment is of sufficient purity and homogeneity to support its crystallization. Herein we outline the methods employed to produce and isolate this functional myosin isoform, which should be applicable to other *Drosophila* muscle myosin isoforms and possibly to striated muscle myosins from other species.

4.3. Materials and Methods

4.3.1. Construction of pattB6HisEmb plasmid

The 5' *Actin88F* promoter fragment (1406 bp) (Geyer and Fyrberg 1986) was produced by PCR from the plasmid pL116-4 (Cripps, Suggs et al. 1999) with the forward primer act88fXba1 5'-AAT ATC TAG AAT GCA CAA TAG GCA AAT TTA GTT AAG-3' and reverse primer act88fPvu1 5'-ACG CCG ATC GGT CTG TCC TGC CTT TAT ATC-3'. A second fragment containing the 3' *Actin88F* promoter region, which also encodes the amino-terminal His-tag, tobacco etch virus (TEV) protease recognition site, and *Mhc* exon 2 5' region, was generated in three steps by standard PCR. First, the pL116-4 plasmid was amplified using the forward primer ActPvu1 5'-GAC AGA CCG ATC GGC GTG CCA T-3' and reverse primer ActHisTEV 5'-GAG GTT TTC GTG GTG GTG GTG GTG GTG

CAT CTT GGC AGT TGT TTA TCT GG-3' to produce the 3' *Act88F* region, 6XHis-tag, and TEV cut site (695 bp). Next, the p5'emb plasmid (Wells, Edwards et al. 1996) was amplified with the forward primer HisTEVMhc 5'-CAC CAC GAA AAC CTC TAC TTC CAA GGC CCG AAG CCA GTC GCA AAT CAG G-3' and reverse primer MhcPst1 5'- ACC CTG CAG ACC AAC GGA GAC G -3' to produce the His-tag, TEV cut site, and Mhc 5' exon 2 region (222 bp) and then the two overlapping 695 and 222 bp fragments were joined by amplification with the forward primer ActPvuI and reverse primer MhcPst1 for a final 890 bp fragment. These 5' *Actin88F* and 3' fragments were digested with Pvu I and ligated together. They were then digested with Xba I and Pst I before ligation with the similarly digested p5'emb vector. Genomic DNA from the Apa I site in exon 12 through exon 19 to the Kpn I site was next ligated with the similarly digested vector construct. Finally, the entire *Actin88F* promoter, His-tag, TEV site, EMB isoform, 3' *Mhc* genomic DNA construct (14,094 bp) was removed and ligated into the Xba I and Kpn I sites of the pattB vector (7411 bp) (Bischof, Maeda et al. 2007). The pattB6HisEmb plasmid sequence was confirmed by the California State University MicroChemical Core Facility prior to shipment for injection into embryos. The resulting myosin isoform is expected to contain the EMB S1 region joined to the indirect flight muscle form of the myosin rod, which contains a subfragement-2 hinge region encoded by alternative exon 15a and a C-terminal tailpiece encoded by alternative exon 18 (George, Ober et al. 1989). The pattB6HisEmb plasmid and its sequence are available from the authors.

4.3.2. Transformation of Drosophila with the embryonic Mhc isoform construct

BestGene Inc. (Chino Hills, CA) injected the pattB6HisEmb plasmid into 200 *Drosophila* embryos of FlyC31 strain 24485 (carrying a mutation in the white eye color gene) with the estimated cytosite 68E (chromosome 3). The PhiC31 integrase-mediated transgenesis system was selected for transformation due to the advantage of site-directed insertion of the transgene (Bischof, Maeda et al. 2007). Five culture vials were received containing transformant flies with light orange eyes as the phenotypic marker for the transgene encoding the engineered myosin.

4.3.3. Culturing flies

The healthiest fly cultures were grown at 25 °C, which allowed for a 10 day generation time from egg to adult. Some stocks were kept at room temperature or 18 °C to slow growth for convenience. Fly food consisted of 30 g agar, 120 g sucrose, 75 g active dry yeast, 2.325 g calcium chloride dihydrate, 2.325 g ferrous sulfate heptahydrate, 12 g sodium potassium tartrate, 0.75 g sodium chloride, 0.75 g manganese chloride and 1.5 L water, which was autoclaved for 30 min (Carpenter 1950). The food was then cooled to 50 °C before 12 mL of 10% Nipagen was added and then poured into the appropriate culture vials and bottles.

4.3.4. Selection for homozygous EMB-expressing flies

Standard genetic crosses were made to generate a homozygous transgenic line in the *Mhc*^{10} background. *Mhc*^{10} is a myosin heavy chain null line for the indirect flight and jump muscles (Collier, Kronert et al. 1990). The heterozygous transgenic flies were crossed with A12 flies (*w; CyO/Bl*^{1}*; TM2,Ubx*^{130}*/ TM6B,Tb,Antp*^{Hu}); the progeny were screened for curly-winged, light orange-eyed flies. The selected flies were crossed to the *Mhc*^{10} line; the selected progeny were self crossed to produce a homozygous *Mhc*^{10}, heterozygous transgenic myosin line which was self-crossed to produce the final true breeding homozygous transgenic line (darker orange eyes) in the homozygous *Mhc*^{10} background. The line we utilized expressed myosin at 76.4% of wild-type levels (relative to actin levels) in upper thoraces, as determined by densitometry (Suggs, Cammarato et al. 2007). The homozygous EMB-expressing flies are flightless in either the *Mhc*^{10} or *yw* background. This is expected, since EMB myosin alone does not support flight and it is dominant negative for flight (Wells, Edwards et al. 1996).

4.3.5. Protein extraction

Myosin extraction has been done since the 1940s (Szent-Györgyi 1945, Gilmour 1948). The charged amino acid repeats in the myosin rod influence the solubility behavior of the myosin and consequently the ionic strength needed to form or dissolve myosin filaments. Low ionic strength allows for filament

formation and precipitation of myosin, whereas high ionic strength favors myosin solubility. The methods developed for myosin extraction from transgenic *Drosophila* lines expressing His-tagged myosin are described here.

4.3.5.1. Bulk whole fly homogenization

1. Raise twenty-five 8 oz culture bottles of transgenic flies (*yw, Mhc^{10}, 68E: Act88F6HisEmb*) and clear the adults 24 h before collection of newly eclosed offspring.

2. On the day of the extraction, anesthetize the flies with CO_2, collect newly eclosed adults (less than 24 h old) and remove any pupae or larvae. Place the flies in a 50 mL Falcon tube. Flies may be flash frozen in liquid nitrogen and stored at -80°C for convenience.

3. Weigh the flies, 3.35 g is ~3500 flies at an average weight of 0.96 mg/fly.

4. Pour the flies into an ice cooled (4 °C) grinding chamber (Wheaton Potter-Elvehjem Tissue Grinders, 55 mL, Cat. No. 358054) with 45 mL homogenization buffer (12.5 % sucrose, 40 mM NaCl, 10 mM imidazole-Cl, 2 mM $MgCl_2$, 0.2 mM ethylene glycol tetraacetic acid (EGTA), 1 mM dithiothreitol (DTT), 0.5 % Triton X-100, and a Roche complete protease inhibitor cocktail tablet (Cat. No. 04 693 116 001)). Mount the Teflon pestle in a Wheaton overhead stirrer (Cat. No. 903475), set the speed to 4 and insert into the grinding chamber containing the flies. Using constant pressure, raise the grinding chamber to pass the flies by the pestle at least once. Be careful to keep constant pressure to prevent the

pestle from spinning at an increased rate and denaturing the proteins due to heating.

4.3.5.2. Clarification of the supernatant

1. Transfer the dark grey homogenate to two 26.3 mL ultracentrifuge tubes (Beckman #355618). Balance and centrifuge in a Beckman Type 60 Ti rotor at 16,000 rpm (18,178 x *g*) for 15 min at 4 °C in the Beckman Coulter L8-60M centrifuge.

2. Discard the supernatant by decanting into a beaker. The pellet consists of two layers formed along the tube's length, the inner one of whitish tissue and the outer black exoskeleton. Resupend each pellet with a transfer pipet and 22 mL homogenization solution. Transfer solution into the glass 55 mL grinding chamber and homogenize using the glass pestle 2-4 times manually.

3. Pour the homogenate into clean ultracentrifuge tubes. Rinse the homogenizer with 5 mL homogenization solution and add to the tubes. Centrifuge the tubes in a Beckman Type 60 Ti rotor at 16,000 rpm (18,178 x *g*) for 15 min at 4 °C. Discard the supernatant.

4. Repeat step 6 with 50 mL wash buffer (homogenization buffer without protease inhibitor, 12.5 % sucrose, 40 mM NaCl, 10 mM imidazole-Cl, 2 mM $MgCl_2$, 0.2 mM EGTA, 1 mM DTT, 0.5 % Triton X-100).

5. Balance the tubes and centrifuge in a Beckman Type 60 Ti rotor at 23,500 rpm (39,214 x *g*) for 15 min at 4 °C. Discard the supernatant.

4.3.5.3. High salt solubilization of myosin

1. Resuspend each pellet in 22 mL myosin extraction buffer/Nickel column binding buffer (500 mM NaCl, 20 mM sodium phosphate buffer, 30 mM imidazole-Cl, pH 7.4) by repeated pipetting with a transfer pipet. Transfer the solution to the grinding chamber. Homogenize with the glass pestle manually and decant into the centrifuge tubes. The solution will be black with fine particulates.

2. Sonicate the solution in the 26.3 mL tubes on ice with 20 quick pulses at 50% duty cycle, setting of 5, using a micro tip (Fisher Scientific Sonic Dismembrator Model 100).

3. Wait three min and sonicate for another 20 quick pulses in order to break up the tissue and possibly solubilize the thick filaments.

4. Incubate tubes on ice for 30 min to allow for a more complete dissolution of the thick filaments.

5. Centrifuge the tubes in a Beckman Type 60 Ti rotor at 50,000 rpm (177,520 x *g*) for 35 min at 4 °C. The pellet contains the exoskeleton and some unextracted myosin along with the remainder of the cellular components.

4.3.5.4. Low salt precipitation of myosin

1. Divide the supernatant equally (8.3 mL each) into six 70 mL ultracentrifuge tubes (Beckman Cat. No. 355622). Fill the tubes to capacity with 4 mM DTT. Leave the tubes in an ice bucket overnight at 4 °C.

2. Centrifuge the tubes with the diluted myosin solution in a Beckman Type 45 Ti rotor at 45,000 rpm (158,420 x *g*) for 35 min at 4 °C. Discard the supernatant, shake out the remaining solution and place the tubes upside down on a paper towel to dry for a few min.

4.3.5.5. Solubilization of the myosin pellets

1. Remove/resuspend the enriched myosin pellets (~1 cm diameter) with 3 mL of pellet resuspension buffer (1.5 M NaCl, 30 mM imidazole-Cl, 20 mM sodium phosphate buffer, pH 7.4) being careful to collect all of the sticky pellet material with the pipet tip.

2. Transfer the solution to a chilled 50 mL beaker with a stir bar and cover with Parafilm. Wash/rinse/collect the remaining pellet from the tubes with a 1 mL pipet and 3.0 mL pellet resuspension buffer.

3. Place the beaker on a stir plate set at ~90 rpm for 45 min, and mix the settled pellet with a 1 mL pipet periodically. Add 20 mL binding buffer to lower the ionic strength and dilute the protein. The optimal salt concentration for the Ni column is 500 mM. After an additional 45 min, decant and pipet the remainder of the solution into a 60 mL syringe. Resuspension of the myosin pellets is difficult and takes patience, sometimes requiring a few hours; this time can be used to ready the column.

4. Filter the protein solution with a 0.45 μm syringe filter (Fisher Scientific Cat. No. 09-719D). The filter may clog and need to be replaced once or twice.

4.3.5.6. Myosin purification by Ni-affinity chromatography

The general principle of Ni-affinity chromatography is that His-tagged recombinant proteins bind specifically while allowing other proteins to flow through, permitting elution of highly purified His-tagged proteins (Crowe, Masone et al. 1996).

1. Prepare solutions for column run. The buffers should be mixed and filtered with either the Corning 500 mL Vacuum Filter/Storage Bottle System with 0.22 µm membrane (Cat. No. 430769) or the Millipore Steriflip 50 mL Disposable Vacuum Filtration system with 0.22 µm Millipore Express PLUS Membrane (Cat. No. SCGP00525), depending on the volume needed.

2. Prepare a GE Healthcare HisTrap HP 5 mL column (Cat. No. 17-5248-02) using Luer Lock syringes and attempt a 5 mL/min flow rate by counting the drops to a timer (100 drops/min).

3. Wash the column with 25 mL filtered water using a 30 mL syringe.

4. Equilibrate the column with 30 mL binding buffer (500 mM NaCl, 20 mM sodium phosphate buffer, pH 7.4, 30 mM imidazole-Cl). Position the column in a clamp on a stand with a 500 mL beaker placed underneath for collection of waste.

5. Load the column with the filtered enriched myosin solution.

6. Wash the column with 60 mL binding buffer.

7. Elute the column with a single step elution buffer (500 mM NaCl, 20 mM sodium phosphate buffer, pH 7.4, 250 mM imidazole-Cl). Collect the eluate in

two Amicon Ultra-15 concentrators (Cat. No. UFC905024).

8. Centrifuge the concentrators in a Sorvall Legend RT centrifuge at 3000 x *g* for up to 30 min at 4 °C, in order to reduce the volume to 2.5-3.0 mL.

9. Determine concentration of the purified myosin solution spectrophotometrically by quantifying the absorbance at 280 nm using an absorbance coefficient of 0.53 cm^{-1} for 1 $mg \cdot ml^{-1}$ (Margossian and Lowey 1982, Swank, Bartoo et al. 2001).

4.3.6. Limited proteolysis: subfragment-1 preparation and purification

4.3.6.1. Solution exchange and contaminant removal

1. Divide the concentrated purified myosin solution equally into six polycarbonate ultracentrifuge tubes (13 x 51 mm, 3.5 mL, Beckman Cat. No. 349622), then dilute with 3.0 mL 4 mM DTT (final NaCl concentration ~70 mM).

2. Incubate for one h on ice for myosin precipitation. This also removes soluble contaminants that bound to the Ni-affinity column.

3. Centrifuge the solution in a Beckman TL-100 ultracentrifuge, in a pre-cooled TLA-100.3 rotor at 50,000 rpm (106,120 x *g*) for 35 min at 4 °C. Discard supernatants and resuspend each ~2 mm wide pellet with 250 μL digestion buffer (120 mM NaCl, 20 mM sodium phosphate pH 7.0, 1 mM EDTA, 4 mM DTT). Myosin pellets do not readily dissolve at 120 mM salt. Use the pipet tip to collect and remove the sticky pellet and pipet the remainder of the pellet and solution into two pre-cooled ultracentrifuge tubes (Beckman microfuge tube polyallomer,

Cat. No. 357448).

4. Carefully homogenize the whitish-colored clear pellets with an Eppendorf tube pestle (Research Products International Corp., Cat. No. 199226). The solution is milky colored and translucent.

4.3.6.2. Time-limited proteolysis

1. Place the two tubes in a 20 °C water bath for 3 min to equilibrate.

2. Perform proteolysis based upon previously published methods (Miller, Nyitrai et al. 2003, Silva, Sparrow et al. 2003, Bloemink, Melkani et al. 2011). Prepare a 10 µg/μL α-chymotrypsin solution by gently mixing water with the lyophilized powder (Worthington Biochemical Corp., Cat. No. LS001475). Add 15 μL chymotrypsin solution to the temperature-equilibrated myosin solution. Final chymotrypsin concentration is approximately 0.20 mg/mL.

3. After 6 min, quench the reaction by adding 5 μL of 200 mM phenylmethanesulfonyl fluoride (PMSF) in ethanol. Mix in the PMSF/ethanol solution carefully so as not to precipitate the protein. Final PMSF concentration is approximately 1.5 mM. Immediately place the tubes on ice and then into the TLA 100.3 rotor.

4. Centrifuge the solution to precipitate the insoluble myosin rod and any remaining undigested full-length myosin at 68,000 rpm (196,280 x *g*) for 25 min at 4 °C.

5. Carefully pipet the enriched S1 supernatant into an Eppendorf tube and place

on ice.

4.3.6.3. Purification by high-performance liquid chromatography

1. Perform size exclusion chromatography with isocratic elution of protein using an Amersham Biosciences AKTA with a 16/60 column with Superdex 200, a flow rate of 1 mL/min, collecting 2 mL fractions. Cover the protein-rich fractions, as determined by 280 absorbance (see chromatogram, Figure 4.2C), with parafilm and place on ice overnight for convenience.

2. Perform SDS-PAGE analysis of protein peak fractions.

3. Concentrate the S1 fractions (6-8 mL total volume) using two 0.5 mL Millipore Biomax 5K NMWL centrifugal filter devices (Cat. No. UFV5BCC00). Six to ten 15 min centrifugations at 12,000 rpm (10,701 x *g*) in the Beckman Microfuge are needed to reduce the volume down to 200 μL.

4. Determine the concentration of the S1 solution spectrophotometrically by quantifying the absorption at 280 nm using an absorbance coefficient of 0.75 cm^{-1} for 1 $mg \cdot mL^{-1}$ (Margossian and Lowey 1982, Miller, Nyitrai et al. 2003).

4.3.7. Guidance and avoiding potential pitfalls

The time period required for injection of DNA into embryos to the receipt of transgenic lines from BestGene, Inc. is approximately six weeks. Once the flies are received, crosses to generate homozygous lines in an Mhc^{10} background,

assessment of expression levels, and culturing of gram quantities of flies takes approximately four months. The myosin isolation protocol takes two days.

When resuspending the myosin pellet, which can be very viscous and sticky, careful pipetting and mixing with the pipet tip is required. The pellet can stick to anything it touches. This can lead to significant loss of material. Section 2.5.5, step 1 and section 2.7.1, step 3 requires that the myosin pellets be transferred within a pipet tip. To accomplish this, pipet the appropriate solution against the edge of the pellet to free it from the side of the tube. Then gently draw the pellet into the tip or hold it at the tip with the vacuum pressure created by the pipet. Then perform the transfer. Low-binding pipet tips, either treated polymer or siliconized glass, may prevent the pellet from sticking to the inside of the tip. If glass pipets are used, tips should be heat treated to produce rounded edges.

4.3.8. Myosin preparation from microscopic dissection of the indirect flight muscle

In addition to the His-tagged myosin purification procedure as described above, preparation of myosin from dorsolongitudinal indirect flight muscle was done from 180-200 EMB or His-Tagged EMB transgenic flies. Briefly, dorsolongitudinal indirect flight muscles were removed by microscopic dissection and purification of myosin was carried out at 4 °C using methods essentially as described previously (Swank, Bartoo et al. 2001, Kronert, Dambacher et al. 2008,

Kronert, Melkani et al. 2010). Concentration of the purified myosin was determined spectrophotometrically by measuring the absorption at 280 nm. Purified myosin was used within 2 h for ATPase assays.

4.3.9. Determination of steady-state ATPase activity

ATPase activities of myosin from dissected muscles or Ni-affinity column chromatography were determined using [γ-^{32}P] ATP as previously described in detail (Swank, Bartoo et al. 2001, Kronert, Dambacher et al. 2008, Kronert, Melkani et al. 2010). After the nickel column, eluate was concentrated, diluted with 4 mM DTT and centrifuged in a Beckman TL-100 ultracentrifuge as described in section 2.7. This step removes soluble contaminants. Myosin pellets were dissolved to a concentration of 2 μg/μL in myosin storage buffer (20 mM MOPS pH 7.0, 500 mM KCl, 20 mM DTT, 2 mM $MgCl_2$). For CaATPase assessment, 1 μL of the freshly prepared myosin solution was added to 125 μL CaATPase buffer (10 mM imidazole pH 6.0, 0.1 M KCl, 10 mM $CaCl_2$). CaATPase activity of myosin was initiated at 25 °C by addition of [γ-^{32}P] ATP. After a 15 min incubation the reaction was quenched by adding 100 μL of 1.8 M $HClO_4$. Extraction and scintillation counting were done essentially as described previously (Swank, Bartoo et al. 2001). Basal MgATPase assessment was carried out in a similar fashion, except using 50 μL of MgATPase buffer (10 mM imidazole pH 6.0, 20 mM KCl, 2 mM $MgCl_2$, 0.1 mM $CaCl_2$, 1 mM [γ-^{32}P] ATP). Actin-stimulated MgATPase assays were performed in MgATPase buffer in the

presence of increasing concentrations of chicken F-actin (0.1 to 2 μM). For assays in MgATPase buffer, the reaction was quenched after 25 min with 50 μL of 1.8 N $HClO_4$. Basal Mg^{2+}-ATPase activities obtained in the absence of actin were subtracted from actin-activated data points. Mean values from at least three different experiments were used to determine average ATPase values of each myosin. Maximal actin-activated ATPase (V_{max}) was obtained by fitting all data points from several preparations (minimum of three data points) of EMB and His-tagged EMB myosin with the Michaelis-Menten equation using Sigma Plot software. Values were averaged to give the mean ± SD. Statistical comparisons of ATPase data were carried out using Student's *t* tests.

4.3.10. Crystallization

Peak S1 protein fractions from size exclusion chromatography were pooled and concentrated to 7.28 mg/mL. S1 crystals were grown by the hanging drop, vapor diffusion method. Crystallization conditions were found using Hampton Research crystal screens (Cat. No. HR2-110 and HR2-112). One microliter of concentrated S1 was mixed with 1 μL mother liquor on a glass coverslip, which was then inverted and sealed over the reservoir containing 1 mL mother liquor. Microcrystals were grown by incubation at room temperature with mother liquor containing 0.1 M HEPES pH 7.5, 20% w/v polyethylene glycol 10,000. Larger rod-shaped crystals formed when using mother liquor containing 0.1 M HEPES pH 7.5, 17.5% w/v polyethylene glycol 8,000.

4.4. Results

4.4.1. Design and construction of indirect flight muscle protein expression system

In order to provide a cost effective and robust method for high level expression of class II myosin motor proteins (Figure 4.1A), we designed a *Drosophila melanogaster* expression system in which the endogenous indirect flight muscle myosin heavy chain isoform is replaced by an engineered transgenic isoform. This involves expressing the transgene in the Mhc^{10} strain, which lacks myosin heavy chain in its flight and jump muscles (Collier, Kronert et al. 1990). Placement of the target gene under transcriptional control of the *Actin88F* promoter (Geyer and Fyrberg 1986) insures that the myosin of the indirect flight muscle in the fly is composed entirely of the target myosin protein. Our system also allows for the addition of epitopes, such as a hexahistine tag (His-tag), to aid in detection and purification of the recombinant protein from whole organism homogenates (Figure 4.1B).

The fly line we generated is designed to express a skeletal muscle myosin II embryonic body wall muscle isoform (EMB) S1 domain (Figure 4.1C) attached to the indirect flight muscle rod region. The pattB6HisEmb plasmid that we constructed to express the modified EMB isoform (Figure 4.1B) was built into the PhiC31 injection vector pattB, which allows targeted and efficient germ line transposition (Bischof, Maeda et al. 2007). The insert contains the *Actin88F*

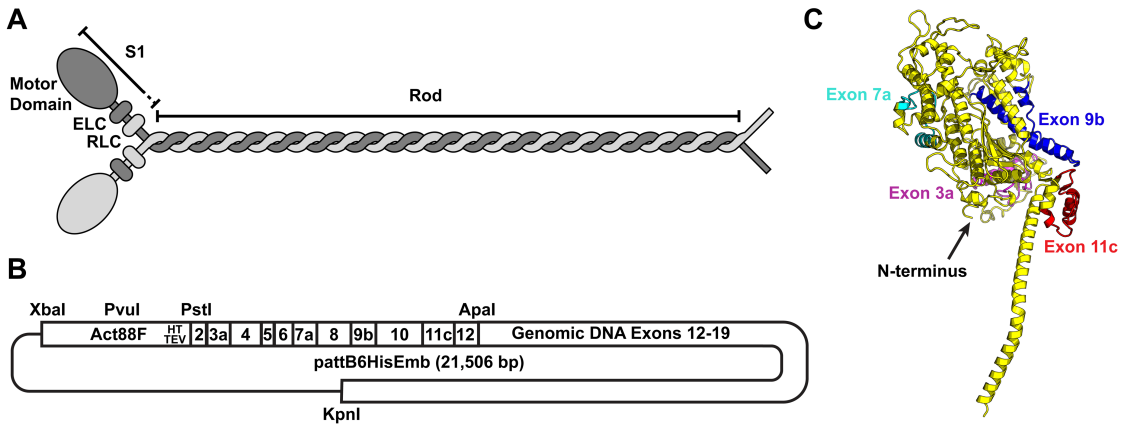

Figure 4.1: Myosin protein, transgene and encoded isoform

A) Schematic diagram of a functional class II myosin protein dimer. The two identical myosin heavy chain subunits are depicted in different shades of grey. The amino-terminal "Motor Domain", which contains the actin-binding sites and ATPase activity, is labeled as are the carboxy-terminal coiled-coil "Rod" regions. The proteolytically stable subfragment-1 region is labeled as "S1". One copy each of the essential and regulatory light chains, labeled ELC and RLC, respectively, are associated with each myosin heavy chain creating an overall functional hexamer. B) Graphic map for the PhiC31 pattB injection plasmid that was used to create the His-tagged EMB recombinant expressing transgenic fly line. Expression of the His-tagged EMB recombinant myosin isoform is driven by the *Actin88F* promoter primarily in the indirect flight muscle (Hiromi and Hotta 1985, Barthmaier and Fyrberg 1995, Nongthomba, Pasalodos-Sanchez et al. 2001). In addition to the N-terminal His-tag (HT), the transgene encodes a TEV protease recognition site. A cDNA encoding the S1 region of EMB (with alternative exons highlighted in color) is followed by genomic DNA containing exons and introns (coding for the indirect flight muscle version of the myosin rod) and the 3' termination sites of *Mhc.* C) Ribbon diagram representation of a homology model of the *D. melanogaster* EMB motor domain based upon the X-ray crystal structure from scallop (PDB ID:1QVI). Alternative exons specific to fly EMB (3a, 7a, 9b, and 11c) are colored and labeled. The amino-terminal end to which the His-tag is attached is also highlighted. The homology model was produced by loading the EMB sequence into SWISS-MODEL (Arnold, Bordoli et al. 2006) and running the SwissModel Automatic Modeling Mode followed by figure rendering using PyMOL software (The PyMOL Molecular Graphics System 2011).

promoter followed by coding regions for a His-tag and a recognition site for the TEV protease. This permits Ni-based chromatographic isolation as well as clipping of the His-tag from the encoded myosin. Myosin heavy chain cDNA containing exons 2-12 of EMB and genomic DNA for the exons 12-19 region encode the expressed myosin isoform. While the cDNA encodes the EMB S1 head, the genomic DNA is expected to encode transcripts that produce the indirect flight muscle version of the rod. This has isoform-specific domains at the subfragment-2 hinge and in the C-terminal tailpiece (George, Ober et al. 1989), which may provide higher stability to the myofibrils in the transgenic organisms (Cripps, Suggs et al. 1999, Swank, Bartoo et al. 2001, Suggs, Cammarato et al. 2007). The 3' non-coding region of the genomic DNA contains necessary transcription termination and polyadenlylation sites. The pattB6HisEmb plasmid was injected into *D. melanogaster* attP 68E *yw* embryos to produce transgenic lines with the PhiC31 targeted insertion. Selection based on eye color allowed for production of flies that are homozygous for the modified EMB gene.

The function of the EMB isoform has been studied by comparison to the indirect flight muscle isoform and various chimeric isoforms with regard to biophysical, enzymological, mechanical and ultrastructural properties (Wells, Edwards et al. 1996, Swank, Bartoo et al. 2001, Littlefield, Swank et al. 2003, Miller, Nyitrai et al. 2003, Swank, Knowles et al. 2003, Swank, Kronert et al. 2004, Miller, Zhang et al. 2005, Swank, Braddock et al. 2006, Miller, Bloemink et

al. 2007, Kronert, Dambacher et al. 2008, Littlefield, Ward et al. 2008, Yang, Ramanath et al. 2008, Bloemink, Dambacher et al. 2009). Hence isolation of large quantities of EMB S1 for further studies, particularly for production of high-resolution crystal structures, should provide deep insights into myosin structure-function relationships.

4.4.2. Purification of His-tagged EMB

Myosin can be purified from whole flies by microdissection and removal of the dorsolongitudinal indirect flight muscles and homogenization in high salt myosin extraction buffer (Swank, Bartoo et al. 2001). Solubilized myosin heterohexamers (two heavy chains and two each of the essential and regulatory light chains) can then be polymerized into myosin filaments at low salt and collected via centrifugation. Treatment with limiting amounts of protease yields S1 fragments that contain the myosin motor domain, as well as myosin rods (Figure 4.1A) (Miller, Nyitrai et al. 2003). The rods reassemble into high molecular weight filaments in low salt buffer and can be separated from S1 by centrifugation.

By virtue of its His-tag, isolation of engineered myosin that is expressed in the indirect flight muscle system does not require microdissection of individual muscle fibers from flies. Placement of the His-tag at the amino-terminus (Figure 4.1C) avoids its interference with myosin assembly and its catalytic mechanism. Lowey et al. (Lowey, Lesko et al. 2008) showed this to be the case for mouse

cardiac myosin. Whole flies can be harvested in gram amounts and myosin can be isolated following homogenization and various precipitation steps (Figure 4.2A). An initial homogenization of flies yields a protein mixture (Figure 4.2B, lane 2) from which the myosin can be enriched (Figure 4.2B, lane 7). His-tagged myosin can then be purified by Ni-affinity chromatography (Figure 4.2B, lane 10); typically ~10 mg of protein is produced. Similar treatment of wild-type *yw* control flies yields little or no myosin after affinity chromatography (Figure 4.3, top). The presence of the His-tag is confirmed by anti-His Western blots (Figure 4.3, bottom), and no detectable His-tagged protein is isolated from control flies (Figure 4.3, bottom). Low-salt precipitation of His-tagged proteins removes soluble contaminants, notably a protein of ~ 75 kDa (compare Figure 4.2B, lanes 10 and 11). Digestion of myosin isolated by Ni-affinity chromatography using α-chymotrypsin permitted preparation of the EMB S1 fragment and the rod (Figure 4.2B, lane 12).

Note that the α-chymotrypsin treatment clipped the His-tag, likely at sites in the TEV protease recognition site (data not shown). Removal of myosin rod and undigested myosin by centrifugation under low salt conditions (Figure 4.2B, lane 14) improves the purity of S1 (Figure 4.2B, lane 13). Size exclusion chromatography (Figure 4.2C) yields an EMB S1 fragment (Figure 4.2B, lane 15) that is sufficiently pure to be crystallized (Figures 4.2C, inset).

Our procedure allows us to isolate milligram amounts of full-length transgenic myosin. S1 fragment can be readily produced from this myosin and

Figure 4.2: Expression and purification of His-tagged EMB recombinant myosin in the indirect flight muscle system

A) Flowchart of the sequence of steps in purification. Horizontal arrows that shift down or up represent centrifugation steps in which the protein remains in either the pellet or the supernatant, respectively. B) Coomassie Blue stained 10% SDS PAGE analysis of samples taken during the course of purification. The initial homogenate (lane 2) is pelleted. Pelleted material is homogenized and sonicated in high salt buffer (lane 5) and centrifuged. The supernatant (lane 6) is filtered (lane 7) prior to loading on a Ni column. The concentrated eluate (lane 10) is highly enriched in myosin heavy and light chains, typically yielding ~10 mg of protein. This is further purified by low salt precipitation prior to proteolysis (lane 11). Proteolysis with α-chymotrypsin yields myosin rod and S1 (lane 12). Much of the remaining full-length myosin and rod can be removed by centrifugation (lanes 13 vs. 14). C) Chromatogram from size exclusion chromatography on mixture of products of proteolyzed His-tagged EMB (lane 13 in panel B). The major peak represents an S1 sample (lane 15, panel B) of sufficient purity for crystallization (inset; bar, 0.2 mm).

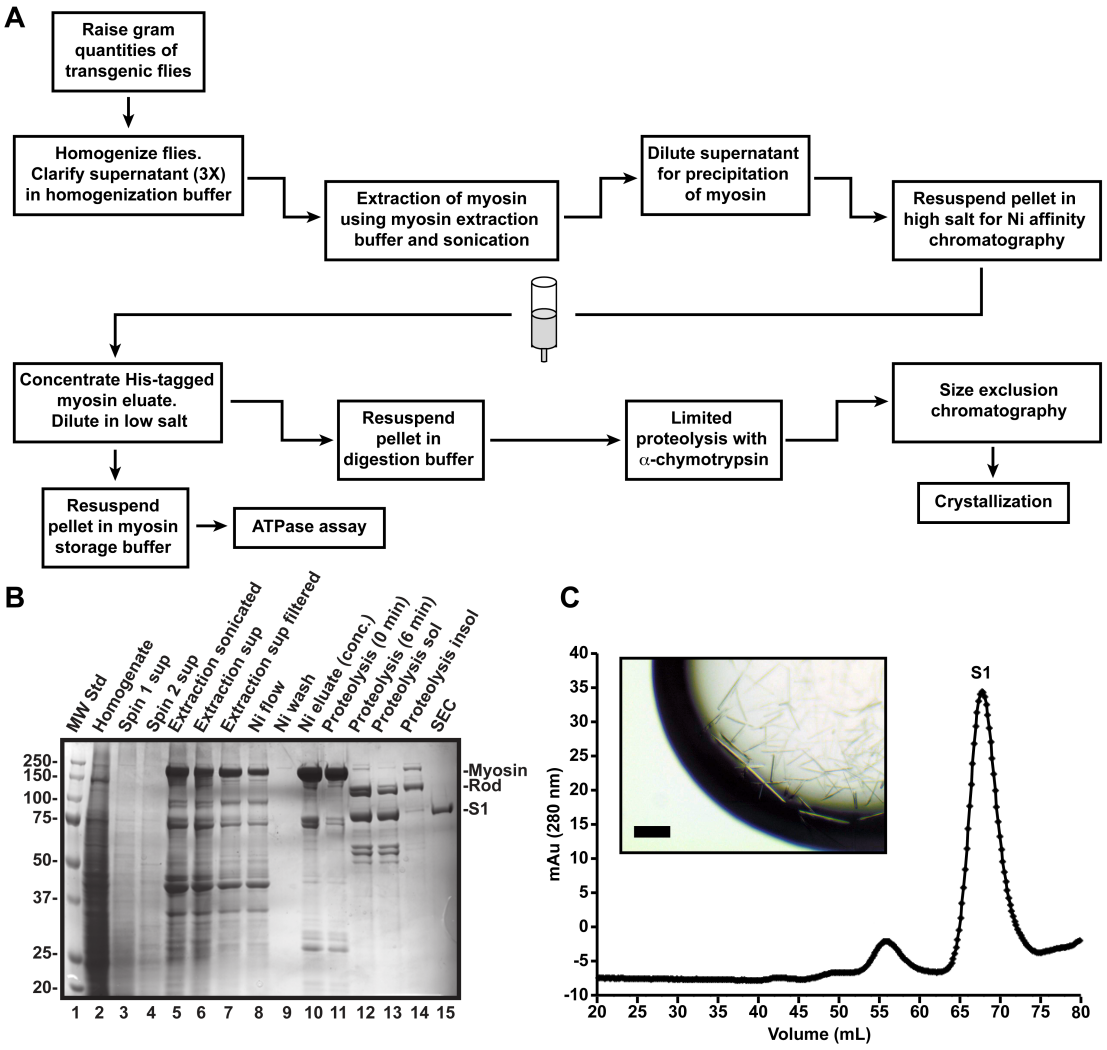
A
Raise gram quantities of transgenic flies
Homogenize flies. Clarify supernatant (3X) in homogenization buffer
Extraction of myosin using myosin extraction buffer and sonication
Dilute supernatant for precipitation of myosin
Resuspend pellet in high salt for Ni affinity chromatography
Concentrate His-tagged myosin eluate. Dilute in low salt
Resuspend pellet in digestion buffer
Limited proteolysis with α-chymotrypsin
Size exclusion chromatography
Crystallization
Resuspend pellet in myosin storage buffer
ATPase assay
B
MW Std
Homogenate
Spin 1 sup
Spin 2 sup
Extraction sonicated
Extraction sup
Extraction sup filtered
Ni flow
Ni wash
Ni eluate (conc.)
Proteolysis (0 min)
Proteolysis (6 min)
Proteolysis sol
Proteolysis insol
SEC
250-
150-
100-
75-
50-
37-
25-
20-
-Myosin
-Rod
-S1
1 2 3 4 5 6 7 8 9 10 11 12 13 14 15
C
S1
mAu (280 nm)
40 35 30 25 20 15 10 5 0 -5 -10
20 25 30 35 40 45 50 55 60 65 70 75 80
Volume (mL)

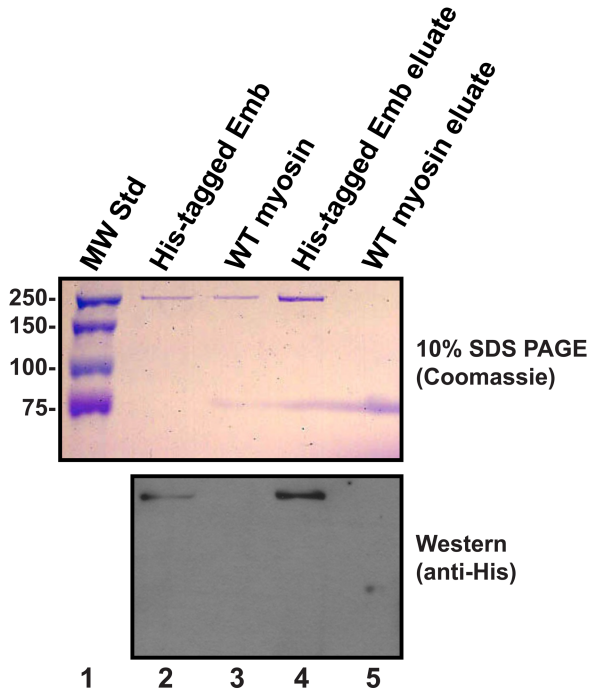

Figure 4.3: Identification of His-tagged EMB recombinant myosin

A Coomassie-Blue stained 10% SDS PAGE analysis of separate preparations of myosin produced by microdissection of the dorsal longitudinal indirect flight muscles from the transgenic fly line expressing His-tagged EMB (lane 2; upper panel) and a control (*yw*) wild-type fly line (lane 3; upper panel). Lanes 4 and 5 (upper panel) reveal the protein that eluted from Ni-affinity chromatography on the His-tagged EMB and wild-type lines, respectively. Note that no myosin was isolated by this approach from wild-type flies. The lower panel is a Western blot of samples in the same order that has been probed with anti-His antibody (Qiagen). Note that the His-tag is only present in myosin isolated from the transgenic lines expressing the recombinant EMB isoform.

isolated by size exclusion chromatography. In the purification shown in Figure 4.2B, we obtained 171 μg of S1. We note that S1 produced from flash-frozen flies can be crystallized, as can frozen S1. Hence collection of sufficient quantities of S1 for X-ray diffraction studies of crystals should be feasible using our system.

4.4.3. Basal and actin-activated ATPase activities

We measured the CaATPase, basal MgATPase, and actin-stimulated MgATPase activities of untagged EMB and His-tagged EMB recombinant transgenic myosins (Figure 4.4). As the ATPase activity and site of actin binding are in the S1 head, it is expected that the presence of the indirect flight muscle domains in the rod will not affect these properties. Indeed, we observe that His-tagged EMB recombinant myosin showed ATPase activity essentially identical to EMB myosin, which had previously been expressed without a His-tag (Swank, Bartoo et al. 2001, Swank, Knowles et al. 2003). This is true when the His-tagged EMB myosin is isolated from dissected indirect flight muscles or by Ni-affinity chromatography. CaATPase and basal MgATPase activities of EMB myosin are not statistically different from His-tagged EMB myosin (4.83 ± 0.83 vs. 4.58 ± 0.93 and 0.083 ± 0.029 vs. 0.091 ± 0.033 sec^{-1}, respectively). The measured actin-stimulated V_{max} for EMB is also not significantly different ($p > 0.05$) from His-tagged EMB (0.77 ± 0.05 vs. 0.73 ± 0.08 sec^{-1}). These results

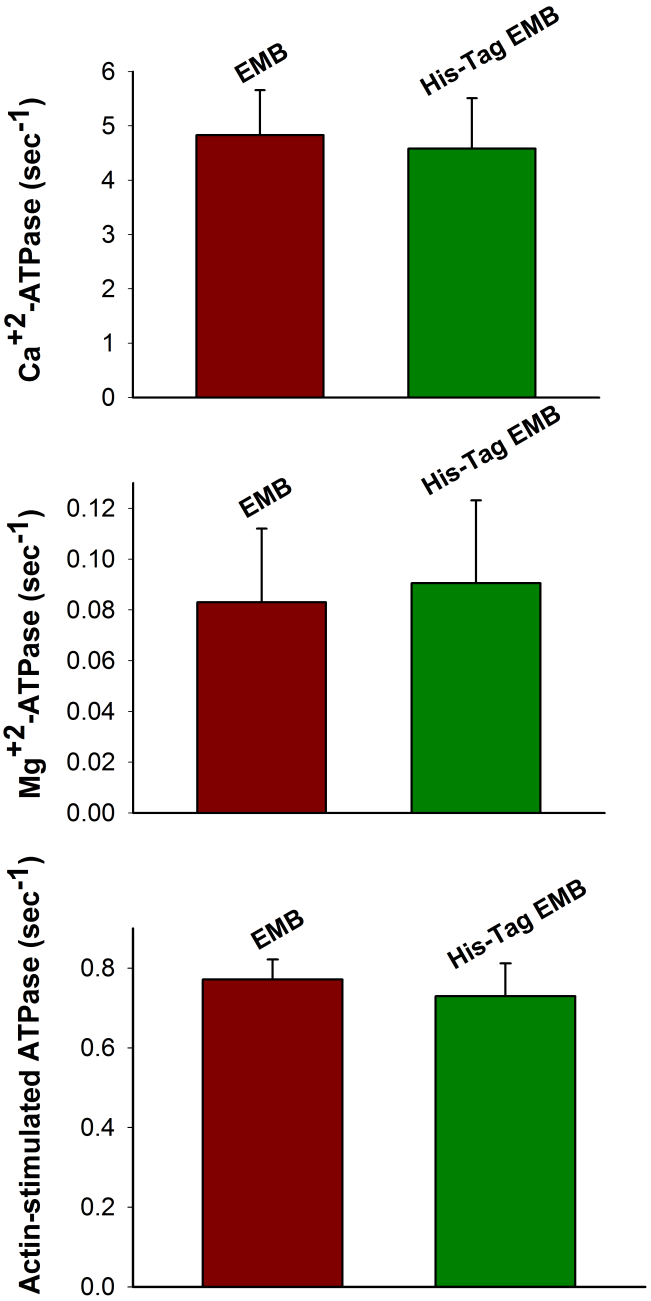

Figure 4.4: ATPase activity of full-length embryonic myosin isoforms

Histograms of Ca^{+2}, basal Mg^{+2}, and actin-stimulated MgATPase activities are shown from four experiments for EMB (maroon) and His-tagged EMB recombinant myosin (green).

confirm that His-tagged EMB recombinant transgenic myosin possesses enzymatic activity like that of EMB transgenic myosin lacking the His-tag.

4.5. Discussion

We have described a novel method for expression and purification of functional class II striated muscle myosin motor proteins using whole fruit flies and have illustrated its utility by generating highly pure preparations of the recombinant EMB isoform in quantities sufficient for crystallization. This approach has several advantages over the classical microdissection and extraction techniques. First, the need for time consuming and tedious microdissection is eliminated. Second, the amount of full-length His-tagged myosin that can be purified from gram quantities of fruit flies exceeds the amount that is typically purified through the microdissection technique. Third, the fact that His-tagged myosin can be extracted from frozen whole flies eliminates the need for synchronizing the eclosion of several thousand flies prior to the start of the protocol. Fourth, the Ni-affinity column can effectively interact with an amino-terminal His-tag on myosin, thereby eliminating the endogenous myosin during the affinity purification step. Finally, concentrated preparations of S1 derived from this method can be aliquotted, flash frozen, thawed, and crystallized.

It should be noted that the endogenous indirect flight muscle versions of the essential and regulatory myosin light chains are expected to be present in the myosin isolated in our system. The regulatory light chain appears to have a

single encoded isoform (Parker, Falkenthal et al. 1985), but there is an indirect flight muscle specific isoform of the essential light chain (Falkenthal, Graham et al. 1987). Presence of the indirect flight muscle essential light chain could affect enzymatic and mechanical properties of an isoform that is normally produced in a different tissue. Furthermore, the presence of the *Drosophila* light chains needs to be kept in mind should efforts be made to express myosin heavy chains from other organisms using the *Drosophila* system. Of course, RNAi or genetic approaches can be used to prevent fly light chain expression and additional transgenes encoding light chains from another organism can be introduced.

Currently, the method we developed is being employed to produce milligram quantities of His-tagged indirect flight muscle myosin for structural and biophysical studies and comparison to the EMB isoform. In the future, various other isoforms and mutant versions of the protein can be generated that should yield additional insights into structure-function relationships in the myosin molecule.

4.6. Acknowledgements

The authors thank A. Melkani for fly microdissections and J. Suggs, W. Kronert, and C.F. Lee for fly husbandry and molecular biology support. This research is supported by NIH/NIGMS Grant R01 GM032443 to SIB.

Biochemistry research at SDSU is supported in part by the California Metabolic Fund.

Chapter 4, in full, is a reprint of the material as it appears in Methods: Focusing on Rapidly Developing Techniques, Volume 56, Issue 1, January 2012, pages 25-32. Caldwell, JT., Melkani, G.C., Huxford, T., Bernstein, S.I. The dissertation author was the primary investigator and author of this paper.

Chapter 5

EMB X-ray Structure

5.1. Introduction

Myosin is a motor protein that is ubiquitous in eukaryotic organisms. Odronitz and Kollmar carried out a comparative genomic analysis of 2,269 myosins found in 328 organisms which resulted in the formation of 35 myosin classes (Odronitz and Kollmar 2007). Myosin links the energy released upon hydrolysis of ATP with movement. The force generated by myosin is dependent on binding with filamentous actin. Myosin II is the motor protein that powers contraction in skeletal, cardiac, and smooth muscle. The nonmuscle form of myosin II is found in nearly all eukaryotic cells and is the motor that drives cytokinesis and plays a role in cellular locomotion (Bresnick 1999).

In the insect world, myosin plays roles during each developmental stage. The fruit fly *Drosophila melanogaster* relies upon one gene for each of its muscle myosin II isoforms (Bernstein, Mogami et al. 1983). It accomplishes this by regulated splicing of alternative exons into the mRNA transcript (George, Ober et al. 1989). The *Drosophila melanogaster* transverse body wall embryonic isoform (EMB) of myosin II was first identified from a late embryonic cDNA library, which contained 4 embryonic isoforms (Wells, Edwards et al. 1996). At least 11 more isoforms are found in the adult, including the indirect flight muscle isoform (IFI), which differs in all 5 alternative exons as compared to the EMB isoform (Bernstein and Milligan 1997, Zhang and Bernstein 2001). The EMB isoform is encoded by exons 3a, 7a, 9b, 11c, and 15b while IFI is encoded by exons 3b, 7d,

9a, 11e, and 15a. There is much evidence that suggests *Drosophila* stage- and tissue-specific myosin isoforms containing exon-encoded variability have isoform-specific properties. For example, the *in vitro* actin sliding velocity of EMB is 9 times slower than IFI (6.4 $\mu m \cdot s^{-1}$ at 22 °C) (Swank, Bartoo et al. 2001). It is hypothesized that the functional diversity of the *Drosophila* muscle isoforms is due to the alternative exon encoded non-identical amino acids.

As part of an effort to understand how small changes in the alternative exon regions gives rise to functional myosin motor proteins with drastically different mechanical properties, we have developed a recombinant system for production of purified myosins using whole flies as the vehicle of expression (Caldwell, Melkani et al. 2012). As a first test case, we used this system to express and purify the embryonic isoform in adult flies and determined the X-ray crystal structure of a proteolytic fragment containing the entire motor domain to 2.2 Å resolution. This represents the first X-ray crystal structure of an insect myosin and the seventh species (after human, chicken, 3 mollusks, and the slime mold *Dictyostelium discoideum*) from which a myosin structure has been determined. The structure shows the alternative exon-encoded regions in the motor domain. It also provides interesting insight into a mechanism whereby pairs of myosin heads might work together to drive motion by the insect larvae.

5.2. Materials and Methods

(refer to Chapter 2)

5.3. Results and discussion

5.3.1. EMB motor domain preparation and X-ray crystal structure determination

The *Drosophila melanogaster* embryonic isoform of myosin II was expressed in transgenic adult flies using a system developed previously (Caldwell, Melkani et al. 2012). The *Drosophila melanogaster* indirect flight muscle system relies upon whole flies for the purpose of recombinant expression of histidine-tagged myosin proteins. An artificial gene encoding an N-terminal His-tag and the alternative exons specific for EMB (3a, 7a, 9b, 11c) along with the genomic region encoding the myosin rod was placed under the Actin88F promoter and the resulting plasmid was injected into fly embryos. The resulting fly line was crossed with a fly line null for endogenous myosin (in the indirect flight muscle and jump muscle) until a homozygous strain of flies expressing the His-tagged embryonic myosin heavy chain isoform was produced. The flies are viable but are incapable of flying and have the “wings up” and indented thorax phenotype common to muscle mutant lines (Wells, Edwards et al. 1996) (Figure 5.1).

The EMB isoform of *Drosophila* myosin was prepared via extraction from whole flies using a modification of standard protocols. Briefly, flies were homogenized and His-tagged myosin was extracted into high salt. The protein

Figure 5.1: *Drosophila melanogaster* 6 His-EMB transgenic fly

The female fly has a slight brown eye color (the eye color marker was included in the transposed transgene plasmid). The fly demonstrates the “wings up” phenotype common to muscle mutant fly lines (Wells, Edwards et al. 1996). Photo by Alex Wild

was purified by Ni-affinity chromatography. The resulting protein was treated to limited proteolysis with chymotrypsin resulting in cleavage of the motor domain from the rod and also removal of the His-tag. Rod fragments were precipitated in low salt and the motor domain was purified by size exclusion chromatography and crystallized.

X-ray diffraction data were collected in continuous mode on a Pilatus detector. The X-ray crystal structure was solved by molecular replacement using Balbes and MolRep software and refined with Refmac5 and Phenix. The resulting model, which contains two complete copies of the EMB motor domain each bound to its own separate essential light chain (ELC), has an R_{cryst} of 18.9% and R_{free} of 22.5% with exceptional stereochemistry for an asymmetric model of this size (Table 5.1).

5.3.2. Structure of the *Drosophila* myosin embryonic isoform

The *Drosophila* myosin embryonic isoform asymmetric unit contains two crystallographically distinct copies of a proteolytic S1-type fragment of the entire N-terminal motor domain. The first motor domain (chain A) begins at residue Val5 and ends at Glu805 while the other independent copy of the motor domain (chain C) begins at Ala9 and ends at Gln804. Each of the motor domains binds its own essential light chain (ELC)(chains B and D); chain B encompasses residues Met1 to Leu154 while chain D is complete from Pro5 to Lys155. No regulatory light chain (RLC) is contained in the crystal structure. This is likely

Table 5.1: Data collection and refinement statistics

	EMB
Data collection	
X-ray source	APS 24ID-C
Wavelength (Å)	0.9795
Space group	$P2_12_12_1$
Unit cell (Å)	
a	108.554
b	148.582
c	148.734
Molecules/asymm. unit	2
Resolution range (Å)[1]	105.1-2.23 (2.25-2.23)
R_{sym} (%)	9.0 (45.4)
Observations	523,304
Unique reflections	116,704
Completeness (%)	99.0 (91.2)
$<I/\sigma>$	11.0 (2.4)
Refinement	
Number of reflections	116,624
R_{cryst} (%)	18.9 (25.7)
R_{free} (%)[2]	22.5 (28.7)
Protein atoms (No H)	14,980
Solvent atoms	1,079
Hydrogen atoms	14,701
R.m.s.d.	
Bond lengths (Å)	0.003
Bond angles (°)	0.700
Ramachandran plot	
Favored	96.52%
Allowed	2.94%
Disallowed	0.54%
MolProbity score[3]	0.99

[1]Data in parentheses are for highest resolution shell
[2]Calculated against a cross-validation set of 5.01% of data selected at random prior to refinement
[3]Combines clashscore, rotamer, and Ramachandran evaluations in to a single score, normalized to the same scale as X-ray resolution (Chen, Arendall et al. 2010).

a consequence of the choice of protease in S1 fragment preparation. We employed α-chymotrypsin and found that it provided rapid and clean digestion of an active EMB motor domain fragment. Similar studies on other myosins, including the chicken skeletal muscle myosin, relied on the papain protease and yielded a longer C-terminal helical stalk bound to a complete regulatory light chain. It is possible that this difference in cutting by the two digestive enzymes might be indicative of some structural difference in the arrangement of accessory light chains on the EMB MHC and chicken skeletal myosin forms. However, the portion of the C-terminal neck between the essential and regulatory light chains has been shown to contain a bend. Furthermore, the high propensity of aromatic amino acid side chains in this neck region seems likely to make its unmasked portions ideal sites for proteolysis by chymotrypsin.

With the exception of the shorter C-terminal neck region and lack of the RLC, the EMB myosin structure closely resembles that of the chicken skeletal myosin (Rayment, Rypniewski et al. 1993). The molecule adopts a highly asymmetric structure with the long C-terminal α-helical neck extending from a large globular core. The longest dimension is approximately 130 Å. This is 35 Å shorter than the chicken skeletal muscle myosin structure and reflects the difference in the length of the C-terminal helix (Rayment, Rypniewski et al. 1993). When analyzed independently of the C-terminal neck, the primarily globular portion of the motor domain measures approximately 90 × 60 × 40 Å, with the 90 Å dimension nearly collinear with the overall longest dimension.

The relative paucity of ordered structural domains in such a large polypeptide as myosin makes describing the structure difficult. Early structural characterization of myosin relied upon limited proteolysis studies. After production of stable S1 fragments, additional incubation with the protease trypsin was found to further cleave the myosin protein into smaller 25, 50, and 20 kDa fragments (Applegate and Reisler 1983).

5.3.3. 25 kDa fragment structure

The EMB myosin motor domain exhibits the now familiar myosin fold. The N-terminal 25 kDa fragment begins near the base of the globular motor domain on the side of the C-terminal neck with a well-ordered random coil segment of more than twenty amino acids in length before the first α-helical secondary structure element forms between amino acids Leu21 and Ser29 (Figure 5.2 and 5.3). What then follows between amino acids Lys36 and Val80 is a well-ordered structural domain composed of five β-strands. This small domain is structurally similar to the well-recognized SH3 domain (Rayment, Rypniewski et al. 1993). However, there is no evidence of it functioning as a protein-protein interaction motif. Moreover, the domain is missing from several myosin type-I molecules, indicating that it is not required for motility (Kollmar, Durrwang et al. 2002). The SH3 domain has been implicated for the structural integrity and stability of the entire motor domain but it is not critical for the biological function of myosin II in *Dictyostelium* (Fujita-Becker, Tsiavaliaris et al. 2006). It remains to be seen what

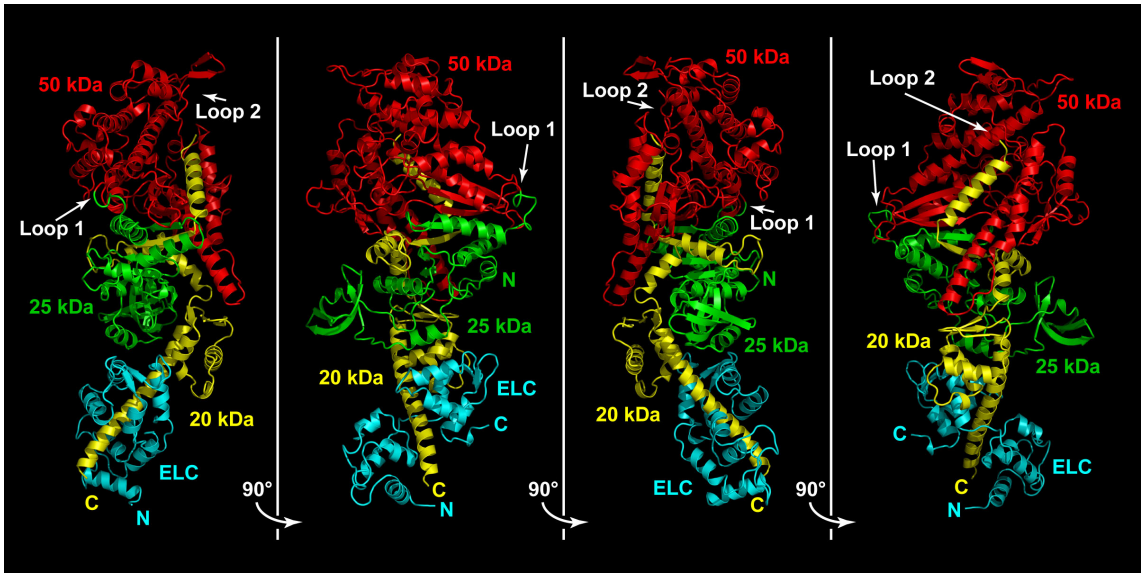

Figure 5.2: EMB myosin motor domain proteolytic fragments

The cartoon EMB myosin structure is shown in four views each sequentially rotated 90°. Myosin has two extremely proteolytically sensitive regions within the head. The fist of these “loop 1” is located about 25 kDa and the second “loop 2” about 75 kDa from the amino terminus. The cleavage of the loops results in the production of three fragments of the motor domain, an N-terminal 25 kDa fragment, a central 50 kDa fragment, and a C-terminal 20 kDa fragment. These fragments only dissociate under denaturing conditions and do not constitute independently folding domains (Sellers 1999)

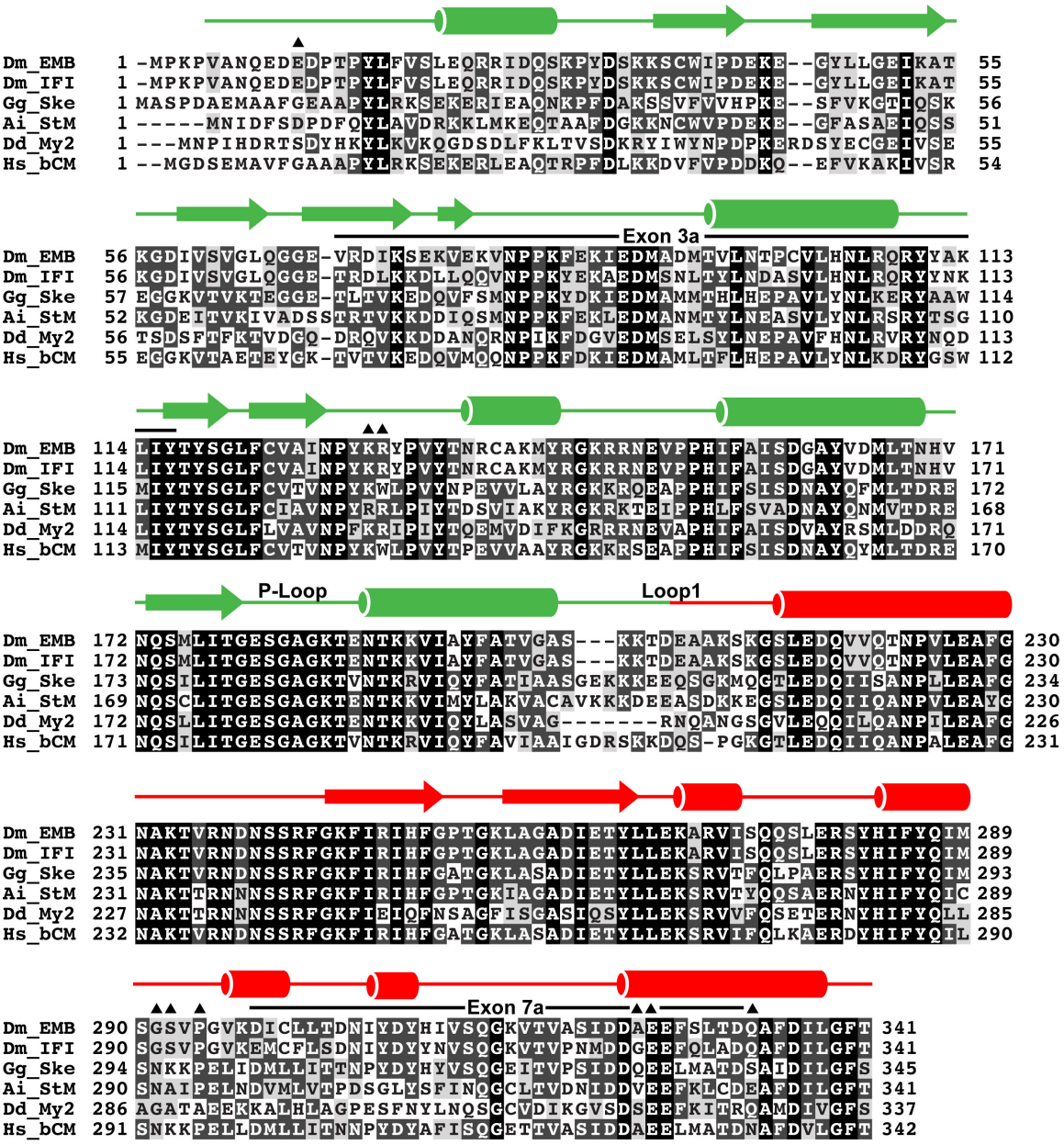

Figure 5.3: Structural alignment of primary amino acid sequences for various Myosins, continued

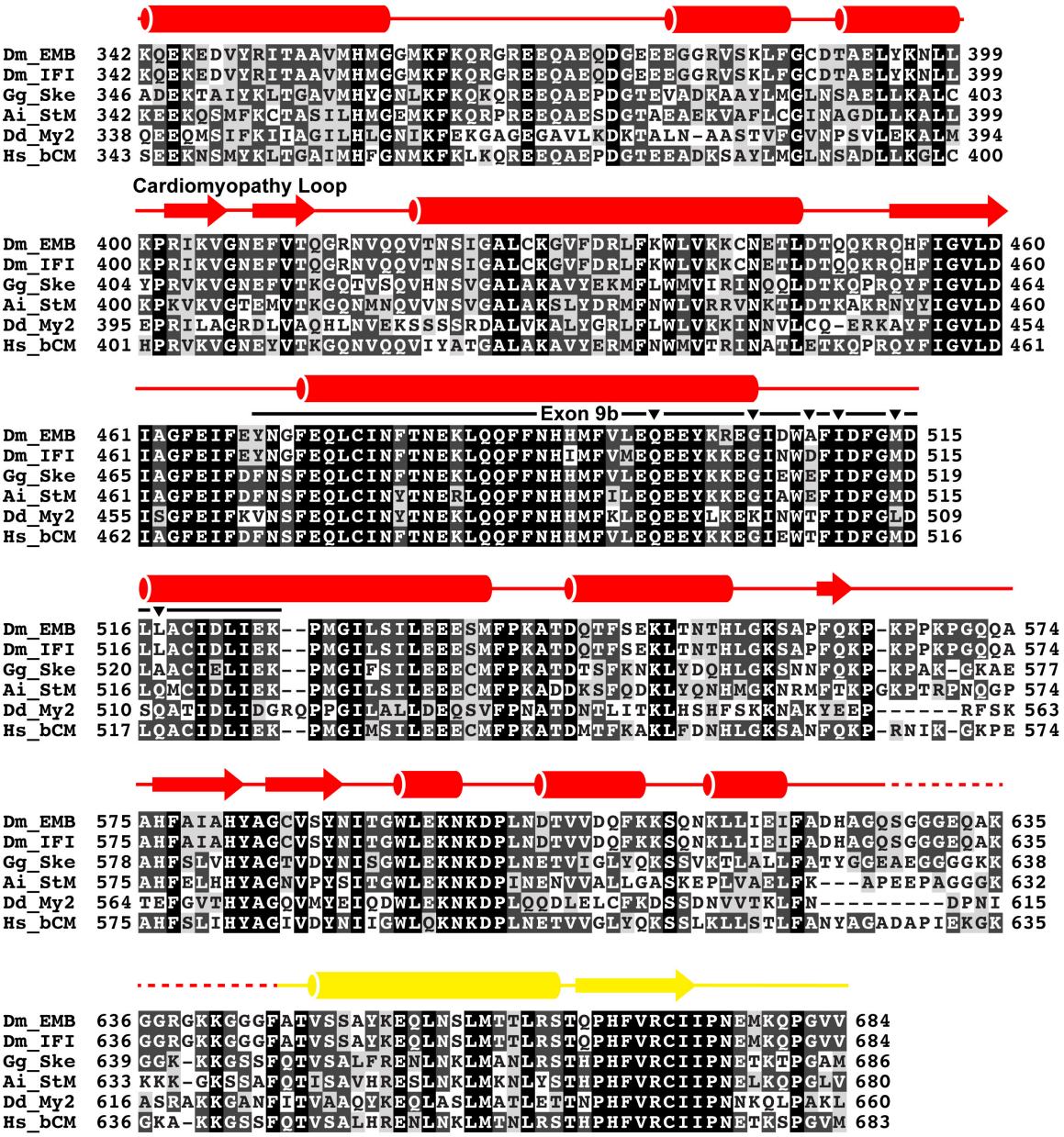

Figure 5.3: Structural alignment of primary amino acid sequences for various Myosins, continued

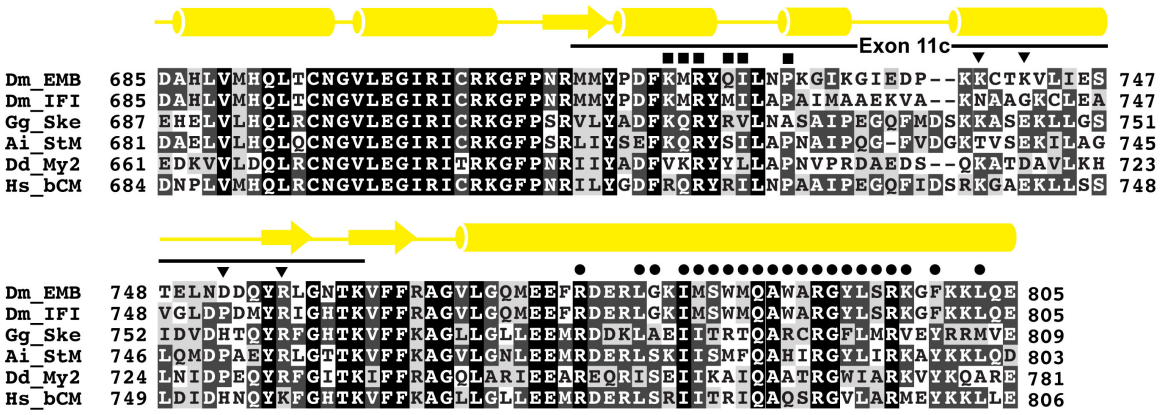

Figure 5.3: Structural alignment of primary amino acid sequences for various Myosins, continued

Key: (Dm_EMB-*Drosophila melanogaster* Embryonic Isoform; Dm_IFI-*Drosophila melanogaster* Indirect Flight Muscle Isoform; Gg_Ske-Chicken skeletal muscle myosin; Ai_StM-Scallop myosin; Dd_My2-*Dictyostelium discoideum* myosin; Hs_bCM-Human beta-Cardiac cell myosin). Numbering is given as well as secondary structure assignments (cylinders represent α-helices while arrows symbolize β-strands). The colors correspond with the proteolytic fragments of myosin (Green-25 kDa; Red-50 kDa; Yellow-20 kDa). The alternative exons specific to EMB are labeled with black bars above. Circles represent residues that mediate lever arm:ELC interactions. Squares denote residue positions that form converter domain:ELC interactions. Up and down triangles represent the positions at which the two myosin heavy chain monomers contact one another. The triangles for Chain A residues point up while the Chain C residue triangles point down.

role this domain plays in function of skeletal muscle.

The N-terminal SH3-like domain is followed by another well-ordered random coil segment of approximately 20 amino acids in length. Beginning with Thr99, one α-helical segment and a turn, position the first two of seven β-strands that together generate a mixed β-pleated sheet that form the core of the globular motor domain, known as the transducer (Coureux, Sweeney et al. 2004). These first two β-strands, composed of residues Tyr116-Ser119 and Phe122-Ile126, are anti-parallel and joined by a short turn. After the second of these β-strands, the polypeptide turns away from the core of the folded motor domain and employs a long stretch of roughly 40 amino acids to cover the β-sheet. Two solvent exposed α-helices are contained in this region. The first, spanning residues Asn137-Tyr143 comes within extremely close contact to the protein N-terminus. The second, longer α-helix within this stretch is composed of amino acids Ile155-Asn169. It is followed by a turn that immediately precedes, not the third, but the fourth β-strand of the core seven-stranded β-sheet. This fourth strand, composed of amino acids Gln173-Thr178, is one of the three central β-strands of the seven-stranded β-sheet. Each of these (strand 3, 4, and 5) derives from drastically different regions within the polypeptide primary sequence and they represent the only strands within the entire molecule that run parallel to one another.

After β-strand 4, the polypeptide once again turns back out to the protein surface and folds into a solvent exposed α-helix composed of amino acids

Lys185-Gly200. The ordered loop that connects β-strand 4 and the helix that follows it is known as the “phosphate binding loop” or “P-loop” (also know as the “Walker A motif”)(Walker, Saraste et al. 1982). It contains the signature GXXXXGK(T/S) sequence (wherein “X” denotes any amino acid) common to nucleotide binding proteins and its topology is essentially identical to that in the Ras protein and adenylate kinase (Rayment, Rypniewski et al. 1993). This subsequent helix is followed by a loop of approximately 15 amino acids in length that is highly solvent exposed. This loop has been referred to historically as “Loop 1” as it contains the first trypsin sensitive site(s) that separates the 25 and 50 kDa fragments. The amino acid sequence of this loop is highly charged and, consequently, its solvent accessibility and sensitivity to protease activity are not a surprise. In other structures, Loop 1 has not been well ordered enough for confident building into electron density maps (Rayment, Rypniewski et al. 1993). It is also significant to note that there are no amino acid recognition sites for chymotrypsin, the enzyme we used in preparing our EMB S1 fragments. Consequently, in our structure, we have succeeded in modeling this region. It does represent the portion of the model that exhibits the highest temperature (*B*) factors, which gives the insight that these atoms have the most freedom of movement in the molecule.

It seems obvious from the topology and placement of the 25 kDa fragment within the context of the entire myosin head structure that it does not form its own stable, independently folded domain. The SH3-like domain near the N-terminus

is the closest thing to an independent domain in the whole structure, and its functional significance remains to be discovered. Of greater interest, therefore, is the question of how the 25 kDa domain comes to adopt its final folded structure within the functioning myosin motor domain. This is especially interesting when one considers how β-strands 1, 2, and 4, but not stand 3, of the central 7-stranded myosin β-sheet are contributed by the N-terminal 25 kDa fragment. It is also interesting to note that the segment joining β-strands 2 and 4 is relatively long and that it collides with the protein N-terminus. It is possible, though admittedly high speculative, that this joining region that is composed of two loops and two α-helices in the domain structure, plays a role in the folding pathway of supplying a temporary anti-parallel β-strand 3. Upon further rearrangement, this strand might be ejected and replaced, projecting the resulting helices back toward the protein N-terminus. Such a folding pathway would seem, of a necessity, to require folding chaperones, which for myosin may be the UCS domain-containing protein UNC-45 (Barral, Hutagalung et al. 2002).

5.3.4. 50 kDa fragment structure

The 50 kDa fragment exhibits a complicated tertiary structure that does not contain isolated structural domains. The majority of the nucleotide binding residues and all of the known actin interacting surfaces are contained within the 50 kDa domain. The most notable structural feature of this large portion of the myosin head domain is a deep cleft that separates the 50 kDa fragment roughly

into two halves reviewed by Geeves and Holmes, 1999. These two portions are sometimes referred to as the “upper” and “lower” 50 kDa regions. They lie next to one another and, despite extensive contact through noncovalent interactions, are connected to one another through only one pass of polypeptide backbone, known as the strut (Sasaki, Ohkura et al. 2000). The upper and lower 50 kDa regions wrap around one another in a manner analogous to a pair of hands engaged in a handshake and, therefore, it is feasible that they could be “peeled” apart from one another leaving them connected only at the base through a single strand of polypeptide. In fact the opening of the cleft is thought to occur during release of myosin from actin, since it disrupts the actin binding site (Geeves and Holmes 1999).

The upper 50 kDa region begins with an α-helix encompassing amino acids Leu215-Gly230. This helix is strained so that it bends considerably and forms part of the nucleotide binding pocket. It ends in a buried loop that leads to β-strand 6 of the core seven-stranded β-sheet. Strand 6 is anti-parallel to its neighbors and is immediately followed in the structure by a tight turn and β-strand 7. Strand 7 terminates in a region of folded polypeptide that consists of four short α-helices connected by loops packed on to a helix-turn-helix motif. This portion of the upper 50 kDa region, composed of amino acids Leu266-Gly360, is the closest thing to a folded domain within this portion of the protein. The first of the final two helices of this “domain” forms the top of the nucleotide binding pocket.

The helical domain of the upper 50 kDa region is followed by a loop and pair of helices (helices HK and HL by conventional nomenclature see (Cope, Whisstock et al. 1996)) that cap the motor domain on the side of the protein that interacts with actin filaments (Geeves and Holmes 1999). The second of these helices is followed immediately by a two-stranded β-sheet composed of a pair of short anti-parallel β-strands connected by a tight turn. This sheet extends away from the rest of the folded globular head domain and constitutes the "cardiomyopathy loop", so named for the involvement of mutated residues in this region in heart disease pathologies. Residues from these regions provide the principle actin interaction surfaces.

The actin binding surfaces are followed in sequence by a long α-helix composed of amino acids Val416-Leu446. This α-helix passes straight through the core of the myosin upper 50 kDa region and terminates in a surface exposed ordered loop that turns inward to the core and becomes β-strand 5 of the central seven-stranded β-sheet. Strand 5, composed of amino acids Q453 and D460, is one of the three centrally positioned parallel β-strands along with the previously mentioned β-strand 4 from the 20 kDa region and strand 3 that will be discussed later.

A buried ordered loop composed of amino acids Asp460-Phe472 provides the only connection between the upper and lower portions of the 50 kDa region as reviewed in Geeves and Holmes, 1999. Its position near the base of the deep crevice that separates the two halves suggests that the upper and lower 50 kDa

regions could theoretically be separated one from another without significant disruption of either half. We also observe a significant amount of ordered water molecules decorating the surface of the protein all through the center of the crevice separating the 50 kDa upper and lower portions.

The lower 50 kDa region begins with a long α-helix composed of amino acids Phe472-Glu503 that reaches near the base of the myosin domain near that beginning of the C-terminal stalk. An ordered, solvent exposed loop then returns part of the way back along the bottom of the lower 50 kDa portion and becomes another long α-helix composed of amino acids Asp515-Met538. This α-helix is largely solvent exposed and is unique in that it contains a clear “bulge” in one of the helical turns at conserved residue Pro526. This helix ends with a turn that constitutes the bottom lip of the large crevice that separates the upper and lower portions of the 50 kDa fragment. These residues contribute with neighboring amino acids from the upper 50 kDa portion to mediate actin filament binding and the surface about the opening of the crevice is consequently referred to as the “actin binding cleft”.

A smaller α-helix composed of amino acids Asp544-His555, followed by a relatively long loop and a two-stranded anti-parallel β-sheet provide the surface-exposed “floor” of the lower 50 kDa region. This β-sheet precedes an extended stretch of polypeptide that spans amino acids Asn589-Ala646 that reaches across the 50 kDa fragment crevice and forms extensive noncovalent interactions between the lower and upper 50 kDa regions. This portion of the structure is

composed of three relatively short α-helical structures that are connected by extended loops. They come to rest on the upper 50 kDa region directly below the cardiomyopathy loop and likely support the upper 50 kDa actin binding surface conformation. Electron density for eighteen amino acids, Ser628-Phe645, is missing in maps generated from our X-ray diffraction data and the final refined model. This suggests that the loop, which contains a particularly high number of glycine and glutamine residues, exhibits flexibility and adopts multiple conformations in the crystal. Phe645, the final amino acid within this disordered stretch, is recognized by the specificity binding pocket of chymotrypsin. It is possible; therefore, that this loop is cut in at least some of the crystallized myosins and that might contribute to the poor electron density (Rayment, Rypniewski et al. 1993). What is known is that this loop is sensitive to cleavage by trypsin protease. This loop is known as “Loop 2”, which is involved in actin binding and forms the border between the 50 kDa and C-terminal 20 kDa myosins fragments (Knetsch, Uyeda et al. 1999).

5.3.5. 20 kDa fragment structure

The C-terminal 20 kDa fragment begins with an α-helix spanning amino acids Val648-Ser665. This helix abuts the lower 50 kDa region and lines the inside surface of the cleft that separates the upper and lower portions of the 50 kDa fragment. It is immediately followed by a β-strand that occupies the third position in the core 7-stranded β-sheet. This strand is interesting in that it and is

the first of three, strands 3 through 5, that run parallel to one another and occupies the central portion of the sheet.

A surface exposed loop follows β-strand 3. This loop caps one end of the nucleotide-binding pocket. Subsequently, the polypeptide chain forms two short α-helices that are nearly perpendicular to one another. The effect of the two α-helices is to pass over the 25 kDa fragment and orient the polypeptide toward the base of the globular motor domain. Contained within this pair of helices are Cys695 and Cys705 residues, which have been shown in chicken skeletal myosin to be more reactive than the other cysteine residues. These are, consequently, referred to as “SH1” and “SH2”, respectively (Rayment, Rypniewski et al. 1993). These residues can be chemically cross-linked by thiol reactive reagents. However, this covalent modification occurs only in the presence of nucleotide, when the SH1 helix is melted (Houdusse, Szent-Gyorgyi et al. 2000).

The segment that follows the reactive sulfhydryl groups consists of a small domain. The topology is that of a three-stranded anti-parallel β-sheet with three short α-helices joining the first and second strands, which occupy the outside positions in the sheet. A third β-strand immediately follows strand 2 and fills the central position in the β-sheet. This small domain has been named the “converter domain”.

The bottom of this domain interacts through close contacts with the Essential Light Chain. The 20 kDa fragment of the EMB isoform myosin heavy

chain continues as a long α-helix that begins at Val768 and ends with Gln804, the final amino acid residue built in the crystallographic model. This long helical stalk comprises the lever arm of the motor and provides the vast majority of surface contacts with the Essential Light Chain.

5.3.6. Essential light chain structure

Electron density from $2F_O$-F_C difference electron density maps calculated from the final refined model coordinates is excellent for both copies of the Essential Light Chain (ELC) in the asymmetric unit. The ELC is entirely α-helical in structure and wraps around the C-terminal stalk-like lever arm of the myosin heavy chain between amino acids Arg776-Leu803. As previously mentioned, it also makes contacts with several amino acids in the range of Lys720-Pro728 within the converter domain of the myosin heavy chain 20 kDa fragment.

The topology of the ELC resembles that of calmodulin and troponin (Rayment, Rypniewski et al. 1993). However, the central ELC portion that corresponds to the long helix that links the two small α-helical domains is collapsed as the two domains wrap around the myosin heavy chain lever arm. In fact, the interaction of the ELC with the myosin heavy chain lever arm α-helix closely resembles the complex of calmodulin with a helical target peptide from myosin light chain kinase (Meador, Means et al. 1992).

The primary amino acid sequence of the EMB ELC is homologous to, but bears significant differences from, the corresponding chain from the scallop myosin

structure. (Figure 5.4) However, most of the residues that contact the myosin heavy chain are identical or are conservative substitutions.

5.3.7. Myosin conformation

The orientation of the myosin head domain relative to the converter/lever arm is consistent with the EMB isoform adopting the post-rigor state conformation. This same conformation was observed in the first X-ray crystal structure of chicken skeletal myosin S1 (Rayment, Rypniewski et al. 1993). Overlaying, the two structures adopt nearly identical conformations. (Figure 5.5) The chicken myosin contains the extra length of C-terminal amino acid residues in the lever arm helix that associate with the Regulatory Light Chain.

5.3.8. Alternative exons

Each of the exons that are unique to EMB occupy surface-exposed positions in the structure (Figure 5.5). These are encoded by exon 3a (Val69-Tyr116), exon 7a (Asp298-Asp332), exon 9b (Tyr469-Lys525), and exon 11c (Tyr713-Lys761). Within these four exon-encoded regions there are 59 amino acid differences that are responsible for the distinct biomechanical properties of the *Drosophila* myosin EMB and IFI isoforms.

Exon 3a region begins within the small domain of the 25 kDa fragment and continues through the buried loop and α-helix that follow, ending at the beginning

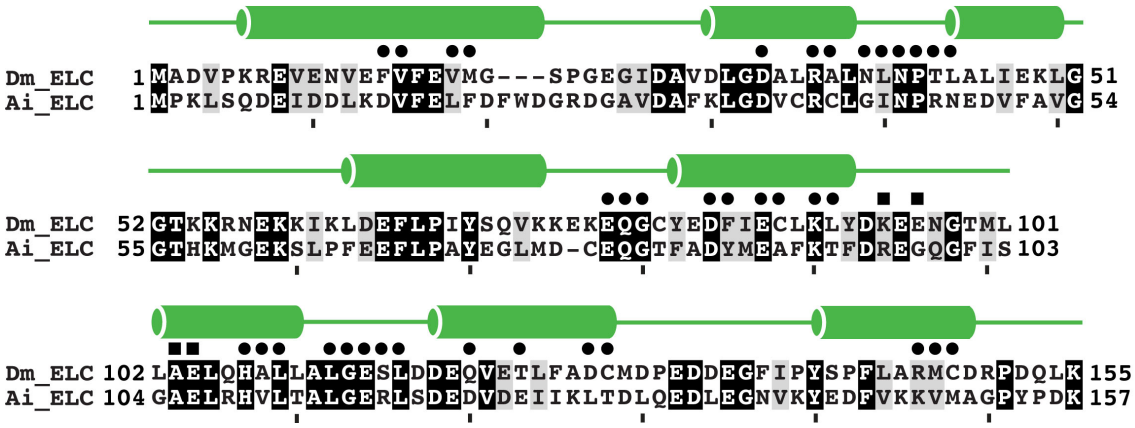

Figure 5.4: EMB ELC alignment with scallop ELC

Key: (Dm_ELC-*Drosophila melanogaster* Essential Light Chain; Ai_ELC-Scallop Essential Light Chain). Numbering is given as well as secondary structure assignments (cylinders represent α-helices). Circles represent residues that mediate ELC:lever arm interactions. Squares denote residue positions that form ELC:converter domain: interactions.

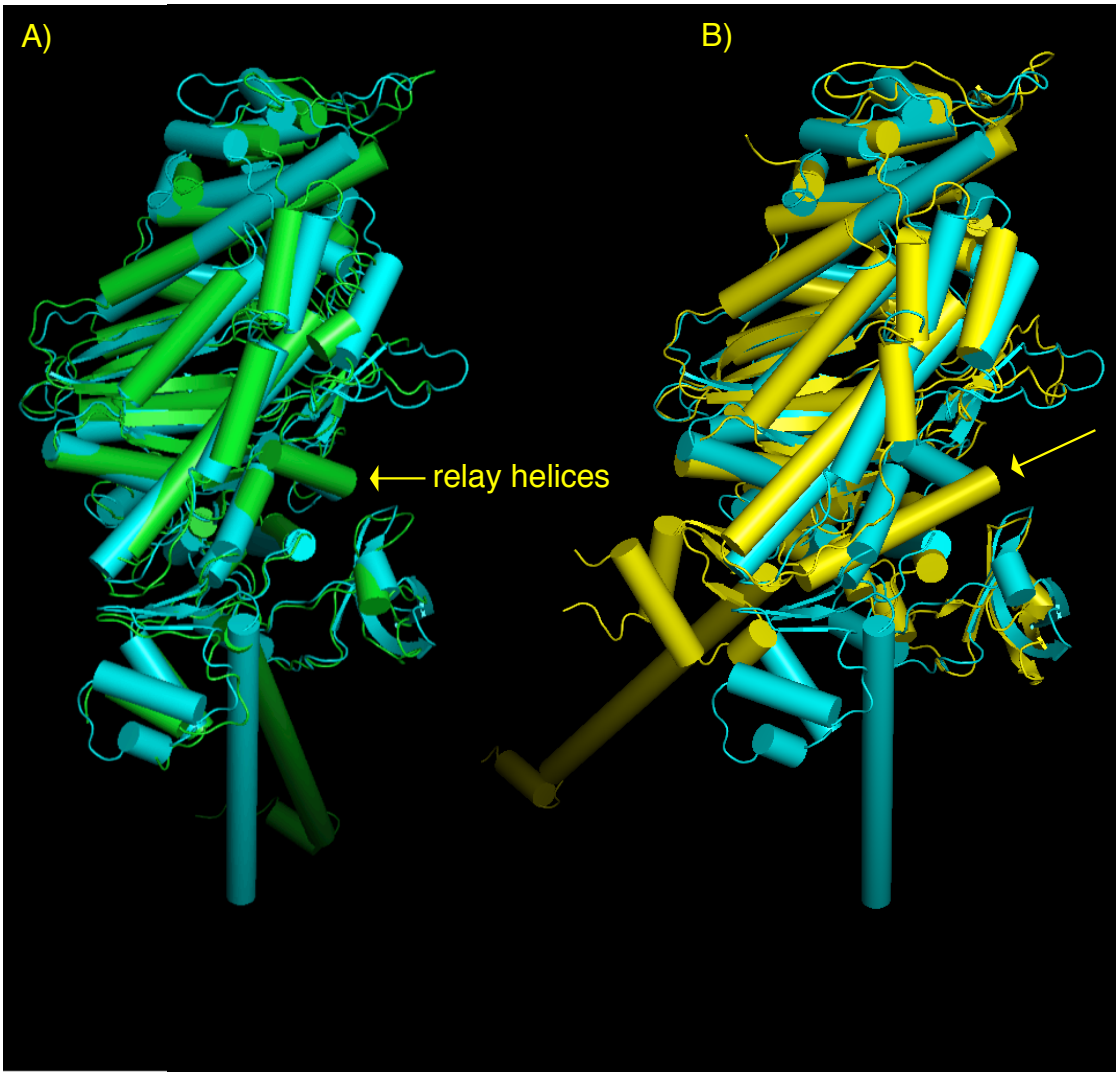

Figure 5.5: Overlay of EMB chain C with PDB structures 1QVI and 2MYS

A) The EMB chain C was aligned with the 2MYS, post-rigor chicken S1 structure sans the light chains. The RMSD was 3.038. The EMB lever arm was nearest to the chicken lever arm angle. The relay helices of both structures are in the kinked confirmation.
B) The EMB chain C was aligned with the 1QVI, pre-power stroke scallop S1 structure sans the light chains. The RMSD was 3.544. The EMB lever arm and converter domain are in vastly different positions. The relay helix of the scallop structure (shown with arrow) is not kinked in contrast to the relay helix in the EMB structure. Structure alignment and images done with PyMOL.

of the first β-strand of the core 7-stranded β-sheet. Eighteen amino acid differences are contained within this alternative exon. Lys76 within this region is a solvent-exposed residue. In other myosin heavy chains polar residues such as aspartic acid and glutamine occupy this position (Figure 5.3). However, the IFI isoform harbors a nonpolar leucine residue at position 76. It is currently unclear how the introduction of this relatively large and extremely nonpolar amino acid side chain in such a solvent exposed position might influence myosin activity. The exon 7a encoded region in the *Drosophila* EMB myosin isoform contains twelve amino acid differences from the same region in IFI. Amino acids encoded by this exon constitute an extended ordered surface loop that ends in the middle of an α-helix and that occupy the surface on top of the upper portion of the 50 kDa fragment. Among the amino acid difference is an interesting buried residue Ile311. This is one of several amino acid residues whose side chain is buried in the hydrophobic core that holds this loop in place over the largely helical upper portion of the 50 kDa fragment. This position is conserved as a phenylalanine, tyrosine, or leucine in other myosins. However, it is replaced by the small polar asparagine residue in IFI. Another curious replacement is the IFI amino acid glycine in the place of Ala325. This position initiates an α-helix that supports the actin binding portion of the upper 50 kDa region. Glycine is a notoriously poor helix initiating residue and, further, has the ability to increase flexibility within localized regions of structure.

The exon 9b region exhibits the least diversity between the EMB and IFI

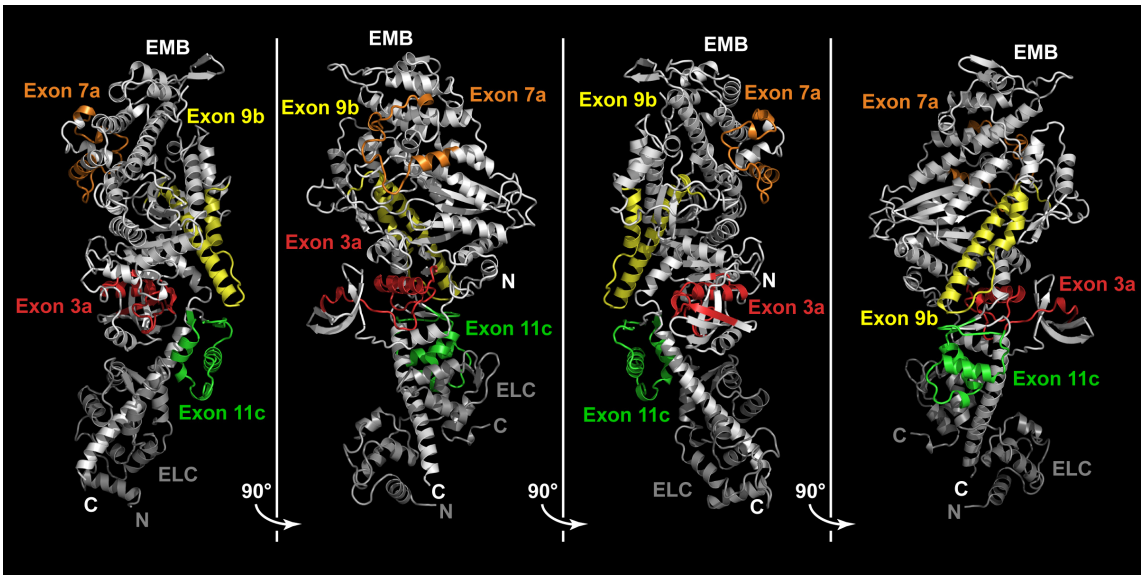

Figure 5.6: EMB model with alternative exons

The cartoon EMB myosin structure is shown in four views each sequentially rotated 90°. Each of the alternative exons are colored showing they occupy surface-exposed positions in the structure.

(exon 9a) isoforms with only five amino acid differences between the two. This region contains the relay domain that serves as a central communication pathway between the nucleotide binding pocket, the actin binding site and the converter domain (Bloemink, Dambacher et al. 2009). It contains the two α-helices from a portion of the polypeptide that follows β-strand 3 of the 7-stranded core β-sheet and the crossover from the upper to lower 50 kDa portion of the motor domain. Interestingly, the second helix from exon 9b ends right before the bulge in the helix that supports the actin binding loop from the lower portion of the 50 kDa fragment. Therefore, both exons 7a and 9b play a role in supporting the conformation of actin contacting surfaces.

The fourth and final alternative exon that engenders EMB with its unique properties is exon 11c. Twenty-six amino acid substitutions are made between the *Drosophila* EMB and IFI myosin isoforms that are encoded by this exon, including a stretch between Lys729-Pro752 in which 21 of 24 residues differ. exon 11c encodes the major portion of the small converter domain within the C-terminal 20 kDa fragment of myosin. It begins before the first of the three β-strands in the anti-parallel β-sheet, encodes for all three of the short helices and the second β-strand and ends at the beginning of the third and final β-strand. Most of the differences map to the loop that joins the two main α-helices on the back of the domain away from the rest of the structure. Near the beginning of this region there are two glycine residues within the EMB (Gly730 and Gly733) isoform while IFI contains only one glycine residue at position Gly742. It is

possible that the different placement of glycine residues in this region influences the flexibility and dynamics of the respective myosin isoforms.

The exon 11c region is also unique in that it contacts both the relay domain (exon 9b) and the ELC. Both the portions of the exon 11c region that mediate these contacts are highly conserved between isoforms. However, the differences in the converter domain (as a consequence of differences in EMB and IFI exon 11s) could influence myosin action at a distance through a network connecting the motor domain to the lever arm through the exons 9b and 11c regions along with the ELC.

5.3.9. Asymmetric dimer

The myosin EMB motor domain crystallizes as a dimer with two unique copies of the entire EMB motor domain with lever arm and ELC in in the asymmetric unit. Overall, the two copies are quite similar, with an RMSD after overlay of 0.5 Å. However, there are subtle differences in their structures. Most of the differences involve slight movement of whole of the lower 50 kDa portion relative to the rest of the structure in one of the EMB molecules relative to the other. While the changes are small and do not represent bona fide different conformational states, they do suggest hinge points from which bulk movement of portions of the protein originate.

The interaction between the two EMB molecules in the model is interesting. Both molecules stack next to one another such that they are nearly

parallel with their C-terminal lever arm and ELC both facing one direction and their actin binding surfaces poised next to one another at the other end. The two molecules are not identically disposed as one is rotated slightly about the long axis. The significance of this orientation is that it could represent a conformation adopted by a pair of dimeric myosin heavy chain motor domains in the myosin hexamer. In this quaternary structure, two myosins are known to interact with one another through their C-terminal rod domains leaving the motor domains and actin binding surfaces in close proximity at the opposite end. Moreover, as the characteristic of EMB isoform is slower kinetics with a greater mechanical strength (Swank, Bartoo et al. 2001, Swank, Knowles et al. 2002), the idea that two motor domains functioning together as a single unit might make sense (Tyska, Dupuis et al. 1999).

The surfaces on the two myosin heads that mediate their interaction is interesting as amino acids from three of the EMB-specific exons are involved in mediating contacts. The first molecule of the pair employs residues from exon 7a and contacts the second EMB motor domain through residues encoded by exons 9b and 11c. Close inspection of the residues that mediate the interaction do not reveal an extensive network of specific interactions nor is there a significant amount of surface area buried upon interaction. So, at present the physiological significance of the crystallographic EMB dimer is speculative at best.

References

Adams, M. D., S. E. Celniker, R. A. Holt, C. A. Evans, J. D. Gocayne, P. G. Amanatides, S. E. Scherer, P. W. Li, R. A. Hoskins, R. F. Galle, R. A. George, S. E. Lewis, S. Richards, M. Ashburner, S. N. Henderson, G. G. Sutton, J. R. Wortman, M. D. Yandell, Q. Zhang, L. X. Chen, R. C. Brandon, Y. H. Rogers, R. G. Blazej, M. Champe, B. D. Pfeiffer, K. H. Wan, C. Doyle, E. G. Baxter, G. Helt, C. R. Nelson, G. L. Gabor, J. F. Abril, A. Agbayani, H. J. An, C. Andrews-Pfannkoch, D. Baldwin, R. M. Ballew, A. Basu, J. Baxendale, L. Bayraktaroglu, E. M. Beasley, K. Y. Beeson, P. V. Benos, B. P. Berman, D. Bhandari, S. Bolshakov, D. Borkova, M. R. Botchan, J. Bouck, P. Brokstein, P. Brottier, K. C. Burtis, D. A. Busam, H. Butler, E. Cadieu, A. Center, I. Chandra, J. M. Cherry, S. Cawley, C. Dahlke, L. B. Davenport, P. Davies, B. de Pablos, A. Delcher, Z. Deng, A. D. Mays, I. Dew, S. M. Dietz, K. Dodson, L. E. Doup, M. Downes, S. Dugan-Rocha, B. C. Dunkov, P. Dunn, K. J. Durbin, C. C. Evangelista, C. Ferraz, S. Ferriera, W. Fleischmann, C. Fosler, A. E. Gabrielian, N. S. Garg, W. M. Gelbart, K. Glasser, A. Glodek, F. Gong, J. H. Gorrell, Z. Gu, P. Guan, M. Harris, N. L. Harris, D. Harvey, T. J. Heiman, J. R. Hernandez, J. Houck, D. Hostin, K. A. Houston, T. J. Howland, M. H. Wei, C. Ibegwam, M. Jalali, F. Kalush, G. H. Karpen, Z. Ke, J. A. Kennison, K. A. Ketchum, B. E. Kimmel, C. D. Kodira, C. Kraft, S. Kravitz, D. Kulp, Z. Lai, P. Lasko, Y. Lei, A. A. Levitsky, J. Li, Z. Li, Y. Liang, X. Lin, X. Liu, B. Mattei, T. C. McIntosh, M. P. McLeod, D. McPherson, G. Merkulov, N. V. Milshina, C. Mobarry, J. Morris, A. Moshrefi, S. M. Mount, M. Moy, B. Murphy, L. Murphy, D. M. Muzny, D. L. Nelson, D. R. Nelson, K. A. Nelson, K. Nixon, D. R. Nusskern, J. M. Pacleb, M. Palazzolo, G. S. Pittman, S. Pan, J. Pollard, V. Puri, M. G. Reese, K. Reinert, K. Remington, R. D. Saunders, F. Scheeler, H. Shen, B. C. Shue, I. Siden-Kiamos, M. Simpson, M. P. Skupski, T. Smith, E. Spier, A. C. Spradling, M. Stapleton, R. Strong, E. Sun, R. Svirskas, C. Tector, R. Turner, E. Venter, A. H. Wang, X. Wang, Z. Y. Wang, D. A. Wassarman, G. M. Weinstock, J. Weissenbach, S. M. Williams, WoodageT, K. C. Worley, D. Wu, S. Yang, Q. A. Yao, J. Ye, R. F. Yeh, J. S. Zaveri, M. Zhan, G. Zhang, Q. Zhao, L. Zheng, X. H. Zheng, F. N. Zhong, W. Zhong, X. Zhou, S. Zhu, X. Zhu, H. O. Smith, R. A. Gibbs, E. W. Myers, G. M. Rubin and J. C. Venter (2000). "The genome sequence of Drosophila melanogaster." Science **287**(5461): 2185-2195.

Adams, P. D., P. V. Afonine, G. Bunkoczi, V. B. Chen, I. W. Davis, N. Echols, J. J. Headd, L. W. Hung, G. J. Kapral, R. W. Grosse-Kunstleve, A. J. McCoy, N. W. Moriarty, R. Oeffner, R. J. Read, D. C. Richardson, J. S. Richardson, T. C. Terwilliger and P. H. Zwart (2010). "PHENIX: a comprehensive Python-based

system for macromolecular structure solution." Acta Crystallogr D Biol Crystallogr **66**(Pt 2): 213-221.

Allingham, J. S., R. Smith and I. Rayment (2005). "The structural basis of blebbistatin inhibition and specificity for myosin II." Nat Struct Mol Biol **12**(4): 378-379.

Altman, D., H. L. Sweeney and J. A. Spudich (2004). "The mechanism of myosin VI translocation and its load-induced anchoring." Cell **116**(5): 737-749.

Applegate, D. and E. Reisler (1983). "Protease-sensitive regions in myosin subfragment 1." Proc Natl Acad Sci U S A **80**(23): 7109-7112.

Arnold, K., L. Bordoli, J. Kopp and T. Schwede (2006). "The SWISS-MODEL workspace: a web-based environment for protein structure homology modelling." Bioinformatics **22**(2): 195-201.

Bárány, M., E. Gaetjens, K. Bárány and E. Karp (1964). "Comparative studies of rabit cardiac and skeletal myosins." Archives of Biochemistry and Biophysics **106**(0): 280-293.

Barral, J. M., A. H. Hutagalung, A. Brinker, F. U. Hartl and H. F. Epstein (2002). "Role of the myosin assembly protein UNC-45 as a molecular chaperone for myosin." Science **295**(5555): 669-671.

Barthmaier, P. and E. Fyrberg (1995). "Monitoring development and pathology of Drosophila indirect flight muscles using green fluorescent protein." Dev Biol **169**(2): 770-774.

Bauer, C. B., H. M. Holden, J. B. Thoden, R. Smith and I. Rayment (2000). "X-ray structures of the apo and MgATP-bound states of Dictyostelium discoideum myosin motor domain." J Biol Chem **275**(49): 38494-38499.

Bauer, C. B., P. A. Kuhlman, C. R. Bagshaw and I. Rayment (1997). "X-ray crystal structure and solution fluorescence characterization of Mg.2'(3')-O-(N-methylanthraniloyl) nucleotides bound to the Dictyostelium discoideum myosin motor domain." J Mol Biol **274**(3): 394-407.

Berg, J. S., B. C. Powell and R. E. Cheney (2001). "A millennial myosin census." Mol Biol Cell **12**(4): 780-794.

Berman, H. M., T. Battistuz, T. N. Bhat, W. F. Bluhm, P. E. Bourne, K. Burkhardt, Z. Feng, G. L. Gilliland, L. Iype, S. Jain, P. Fagan, J. Marvin, D. Padilla, V. Ravichandran, B. Schneider, N. Thanki, H. Weissig, J. D. Westbrook and C.

Zardecki (2002). "The Protein Data Bank." Acta Crystallogr D Biol Crystallogr **58**(Pt 6 No 1): 899-907.

Bernstein, S. and R. Milligan (1997). "Fine tuning a molecular motor: the location of alternative domains in the Drosophila myosin head." J Mol Biol **271**(1): 1-6.

Bernstein, S. I., K. Mogami, J. J. Donady and C. P. Emerson (1983). "Drosophila muscle myosin heavy chain encoded by a single gene in a cluster of muscle mutations." Nature **302**(5907): 393-397.

Bernstein, S. I., K. Mogami, J. J. Donady and C. P. Emerson, Jr. (1983). "Drosophila muscle myosin heavy chain encoded by a single gene in a cluster of muscle mutations." Nature **302**(5907): 393-397.

Bernstein, S. I., P. T. O'Donnell and R. M. Cripps (1993). "Molecular genetic analysis of muscle development, structure, and function in Drosophila." Int Rev Cytol **143**: 63-152.

Bischof, J., R. K. Maeda, M. Hediger, F. Karch and K. Basler (2007). "An optimized transgenesis system for Drosophila using germ-line-specific phi C31 integrases." Proceedings of the National Academy of Sciences of the United States of America **104**(9): 3312-3317.

Bischof, J., R. K. Maeda, M. Hediger, F. Karch and K. Basler (2007). "An optimized transgenesis system for Drosophila using germ-line-specific phiC31 integrases." Proc Natl Acad Sci U S A **104**(9): 3312-3317.

Bloemink, M. J., C. M. Dambacher, A. F. Knowles, G. C. Melkani, M. A. Geeves and S. I. Bernstein (2009). "Alternative exon 9-encoded relay domains affect more than one communication pathway in the Drosophila myosin head." J Mol Biol **389**(4): 707-721.

Bloemink, M. J., C. M. Dambacher, A. F. Knowles, G. C. Melkani, M. A. Geeves and S. I. Bernstein (2009). "Alternative Exon 9-Encoded Relay Domains Affect More than One Communication Pathway in the Drosophila Myosin Head." Journal of Molecular Biology **389**(4): 707-721.

Bloemink, M. J., G. C. Melkani, C. M. Dambacher, S. I. Bernstein and M. A. Geeves (2011). "Two Drosophila myosin transducer mutants with distinct cardiomyopathies have divergent ADP and actin affinities." J Biol Chem **286**(32): 28435-28443.

Blow, D. (2002). Outline of Crystallography for Biologists, Oxford University Press.

Bowker, B. C., D. R. Swartz, A. L. Grant and D. E. Gerrard (2004). "Method of isolation, rate of postmortem metabolism, and myosin heavy chain isoform composition influence ATPase activity of isolated porcine myofibrils." Meat Sci **66**(3): 743-752.

Bradu, A., L. Ma, J. W. Bloor and A. Podoleanu (2009). "Dual optical coherence tomography/fluorescence microscopy for monitoring of Drosophila melanogaster larval heart." J Biophotonics **2**(6-7): 380-388.

Bresnick, A. R. (1999). "Molecular mechanisms of nonmuscle myosin-II regulation." Curr Opin Cell Biol **11**(1): 26-33.

Caldwell, J. T., G. C. Melkani, T. Huxford and S. I. Bernstein (2012). "Transgenic expression and purification of myosin isoforms using the Drosophila melanogaster indirect flight muscle system." Methods **56**(1): 25-32.

Cammarato, A., C. H. Ahrens, N. N. Alayari, E. Qeli, J. Rucker, M. C. Reedy, C. M. Zmasek, M. Gucek, R. N. Cole, J. E. Van Eyk, R. Bodmer, B. O'Rourke, S. I. Bernstein and D. B. Foster (2011). "A Mighty Small Heart: The Cardiac Proteome of Adult Drosophila melanogaster." Plos One **6**(4).

Cammarato, A., C. M. Dambacher, A. F. Knowles, W. A. Kronert, R. Bodmer, K. Ocorr and S. I. Bernstein (2008). "Myosin transducer mutations differentially affect motor function, myofibril structure, and the performance of skeletal and cardiac muscles." Molecular Biology of the Cell **19**(2): 553-562.

Carpenter, J. M. (1950). "A new semisynthetic food medium for Drosophila." Drosophila Information Service **24**: 96-97.

Chen, V. B., W. B. Arendall, 3rd, J. J. Headd, D. A. Keedy, R. M. Immormino, G. J. Kapral, L. W. Murray, J. S. Richardson and D. C. Richardson (2010). "MolProbity: all-atom structure validation for macromolecular crystallography." Acta Crystallogr D Biol Crystallogr **66**(Pt 1): 12-21.

Chen, V. B., I. W. Davis and D. C. Richardson (2009). "KING (Kinemage, Next Generation): a versatile interactive molecular and scientific visualization program." Protein Sci **18**(11): 2403-2409.

Cheney, R. E., M. A. Riley and M. S. Mooseker (1993). "Phylogenetic analysis of the myosin superfamily." Cell Motil Cytoskeleton **24**(4): 215-223.

Cheung, A., J. A. Dantzig, S. Hollingworth, S. M. Baylor, Y. E. Goldman, T. J. Mitchison and A. F. Straight (2002). "A small-molecule inhibitor of skeletal muscle myosin II." Nat Cell Biol **4**(1): 83-88.

Chinthalapudi, K., M. H. Taft, R. Martin, S. M. Heissler, M. Preller, F. K. Hartmann, H. Brandstaetter, J. Kendrick-Jones, G. Tsiavaliaris, H. O. Gutzeit, R. Fedorov, F. Buss, H. J. Knolker, L. M. Coluccio and D. J. Manstein (2011). "Mechanism and specificity of pentachloropseudilin-mediated inhibition of myosin motor activity." J Biol Chem **286**(34): 29700-29708.

Choma, M. A., S. D. Izatt, R. J. Wessells, R. Bodmer and J. A. Izatt (2006). "Images in cardiovascular medicine: in vivo imaging of the adult Drosophila melanogaster heart with real-time optical coherence tomography." Circulation **114**(2): e35-36.

Chow, D., R. Srikakulam, Y. Chen and D. A. Winkelmann (2002). "Folding of the striated muscle myosin motor domain." J Biol Chem **277**(39): 36799-36807.

Chyb, S. and N. Gompel (2013). Atlas of Drosophila Morphology: Wild-type and Classical Mutants, Elsevier Science.

Cobb, M. (2002). "Timeline: exorcizing the animal spirits: Jan Swammerdam on nerve function." Nat Rev Neurosci **3**(5): 395-400.

Collaborative Computational Project, N. (1994). "The CCP4 suite: programs for protein crystallography." Acta Crystallogr D Biol Crystallogr **50**(Pt 5): 760-763.

Collier, V. L., W. A. Kronert, P. T. O'Donnell, K. A. Edwards and S. I. Bernstein (1990). "Alternative myosin hinge regions are utilized in a tissue-specific fashion that correlates with muscle contraction speed." Genes Dev **4**(6): 885-895.

Coluccio (2008). Myosins A Superfamily of Molecular Motors, Springer.

Coluccio, L. M. (2008). Myosins: A Superfamily of Molecular Motors, Springer London, Limited.

Consortium, H. G. S. (2006). "Insights into social insects from the genome of the honeybee Apis mellifera." Nature **443**(7114): 931-949.

Cope, M. J., J. Whisstock, I. Rayment and J. Kendrick-Jones (1996). "Conservation within the myosin motor domain: implications for structure and function." Structure **4**(8): 969-987.

Coureux, P. D., H. L. Sweeney and A. Houdusse (2004). "Three myosin V structures delineate essential features of chemo-mechanical transduction." EMBO J **23**(23): 4527-4537.

Coureux, P. D., A. L. Wells, J. Menetrey, C. M. Yengo, C. A. Morris, H. L. Sweeney and A. Houdusse (2003). "A structural state of the myosin V motor without bound nucleotide." Nature **425**(6956): 419-423.

Cripps, R. M., J. A. Suggs and S. I. Bernstein (1999). "Assembly of thick filaments and myofibrils occurs in the absence of the myosin head." EMBO J **18**(7): 1793-1804.

Crowe, J., B. S. Masone and J. Ribbe (1996). "One-step purification of recombinant proteins with the 6xHis tag and Ni-NTA resin." Methods Mol Biol **58**: 491-510.

Cuda, G., L. Fananapazir, N. D. Epstein and J. R. Sellers (1997). "The in vitro motility activity of beta-cardiac myosin depends on the nature of the beta-myosin heavy chain gene mutation in hypertrophic cardiomyopathy." J Muscle Res Cell Motil **18**(3): 275-283.

D.O.E. (2013). "Use of the Advanced Photon Source was supported by the U. S. Department of Energy, Office of Science, Office of Basic Energy Sciences, under Contract No. DE-AC02-06CH11357.".

Dalbey, R. E., J. Weiel and R. G. Yount (1983). "Forster energy transfer measurements of thiol 1 to thiol 2 distances in myosin subfragment 1." Biochemistry **22**(20): 4696-4706.

Dantzig, J. A., J. W. Walker, D. R. Trentham and Y. E. Goldman (1988). "Relaxation of muscle fibers with adenosine 5'-[gamma-thio]triphosphate (ATP[gamma S]) and by laser photolysis of caged ATP[gamma S]: evidence for Ca2+-dependent affinity of rapidly detaching zero-force cross-bridges." Proc Natl Acad Sci U S A **85**(18): 6716-6720.

Dominguez, R., Y. Freyzon, K. M. Trybus and C. Cohen (1998). "Crystal structure of a vertebrate smooth muscle myosin motor domain and its complex with the essential light chain: visualization of the pre-power stroke state." Cell **94**(5): 559-571.

Emerson, C. P., Jr. and S. I. Bernstein (1987). "Molecular genetics of myosin." Annu Rev Biochem **56**: 695-726.

Emsley, P. and K. Cowtan (2004). "Coot: model-building tools for molecular graphics." Acta Crystallogr D Biol Crystallogr **60**(Pt 12 Pt 1): 2126-2132.

Engelhardt, V. A., M.N. Ljubimova and R.A. Meitina (1941). "Chemistry and mechanics of the muscle studied on myosin threads." Compt. Rend. De l'acad. Sci. de l'USSR(30).

Engelhardt, W. A. and M. N. Liubimova (1939). "[Myosin and adenosine triphosphatase (Nature, 144, 688, Oct. 14, 1939)]." Mol Biol (Mosk) **28**(6): 1229-1230.

Falkenthal, S., M. Graham and J. Wilkinson (1987). "The indirect flight muscle of Drosophila accumulates a unique myosin alkali light chain isoform." Dev Biol **121**(1): 263-272.

Fedorov, R., M. Bohl, G. Tsiavaliaris, F. K. Hartmann, M. H. Taft, P. Baruch, B. Brenner, R. Martin, H. J. Knolker, H. O. Gutzeit and D. J. Manstein (2009). "The mechanism of pentabromopseudilin inhibition of myosin motor activity." Nat Struct Mol Biol **16**(1): 80-88.

Fisher, A., C. Smith, J. Thoden, R. Smith, K. Sutoh, H. Holden and I. Rayment (1995). "X-ray structures of the myosin motor domain of Dictyostelium discoideum complexed with MgADP.BeFx and MgADP.AlF4-." Biochemistry **34**(28): 8960-8972.

Fisher, A. J., C. A. Smith, J. B. Thoden, R. Smith, K. Sutoh, H. M. Holden and I. Rayment (1995). "X-ray structures of the myosin motor domain of Dictyostelium discoideum complexed with MgADP.BeFx and MgADP.AlF4." Biochemistry **34**(28): 8960-8972.

Frye, J. J., V. A. Klenchin, C. R. Bagshaw and I. Rayment (2010). "Insights into the importance of hydrogen bonding in the gamma-phosphate binding pocket of myosin: structural and functional studies of serine 236." Biochemistry **49**(23): 4897-4907.

Fujita-Becker, S., G. Tsiavaliaris, R. Ohkura, T. Shimada, D. J. Manstein and K. Sutoh (2006). "Functional characterization of the N-terminal region of myosin-2." J Biol Chem **281**(47): 36102-36109.

Geeves, M. A. (1991). "The dynamics of actin and myosin association and the crossbridge model of muscle contraction." Biochem J **274 (Pt 1)**: 1-14.

Geeves, M. A. and K. C. Holmes (1999). "Structural mechanism of muscle contraction." Annu Rev Biochem **68**: 687-728.

Geeves, M. A. and K. C. Holmes (2005). The Molecular Mechanism of Muscle Contraction. Advances in Protein Chemistry. M. S. John and A. D. P. David, Academic Press. **Volume 71:** 161-193.

George, E. L., M. B. Ober and C. P. Emerson, Jr. (1989). "Functional domains of the Drosophila melanogaster muscle myosin heavy-chain gene are encoded by alternatively spliced exons." Mol Cell Biol **9**(7): 2957-2974.

Gergely, J. (1950). "On the relationship between myosin and ATPase." Fed. Proc.(9).

Geyer, P. K. and E. A. Fyrberg (1986). "5'-flanking sequence required for regulated expression of a muscle-specific Drosophila melanogaster actin gene." Mol Cell Biol **6**(10): 3388-3396.

Gilmour, D. (1948). "Myosin and adenylpyrophosphatase in insect muscle." J Biol Chem **175**(1): 477.

Gourinath, S., D. M. Himmel, J. H. Brown, L. Reshetnikova, A. G. Szent-Gyorgyi and C. Cohen (2003). "Crystal structure of scallop myosin S1 in the pre-power stroke state to 2.6 a resolution: flexibility and function in the head." Structure **11**(12): 1621-1627.

Greenspan, R. J. (2004). Fly Pushing: The Theory and Practice of Drosophila Genetics, COLD SPRING HARBOR LABORATORY.

Guba, F. (1943). "Observations on myosin and actomyosin." Stud. Inst. Med. Chem. Univ. Szeged(III): 40-45.

Gulick, A., C. Bauer, J. Thoden, E. Pate, R. Yount and I. Rayment (2000). "X-ray structures of the Dictyostelium discoideum myosin motor domain with six non-nucleotide analogs." J Biol Chem **275**(1): 398-408.

Gulick, A. M., C. B. Bauer, J. B. Thoden and I. Rayment (1997). "X-ray structures of the MgADP, MgATPgammaS, and MgAMPPNP complexes of the Dictyostelium discoideum myosin motor domain." Biochemistry **36**(39): 11619-11628.

Hartman, M. A. and J. A. Spudich (2012). "The myosin superfamily at a glance." J Cell Sci **125**(Pt 7): 1627-1632.

Hastings, G. A. and C. P. Emerson, Jr. (1991). "Myosin functional domains encoded by alternative exons are expressed in specific thoracic muscles of Drosophila." J Cell Biol **114**(2): 263-276.

Higuchi, H. and S. Takemori (1989). "Butanedione monoxime suppresses contraction and ATPase activity of rabbit skeletal muscle." J Biochem **105**(4): 638-643.

Hill, J. A. and E. N. Olson, Eds. (2012). Muscle: Fundamental Biology and Mechanisms of Disease. London, Elsevier.

Himmel, D. M., S. Gourinath, L. Reshetnikova, Y. Shen, A. G. Szent-Gyorgyi and C. Cohen (2002). "Crystallographic findings on the internally uncoupled and near-rigor states of myosin: further insights into the mechanics of the motor." Proc Natl Acad Sci U S A **99**(20): 12645-12650.

Hiratsuka, T. (1983). "New ribose-modified fluorescent analogs of adenine and guanine nucleotides available as subtrates for various enzymes." Biochimica et Biophysica Acta (BBA) - Protein Structure and Molecular Enzymology **742**(3): 496-508.

Hiromi, Y. and Y. Hotta (1985). "Actin gene mutations in Drosophila; heat shock activation in the indirect flight muscles." EMBO J **4**(7): 1681-1687.

Honeybee Genome Sequencing, C. (2006). "Insights into social insects from the genome of the honeybee Apis mellifera." Nature **443**(7114): 931-949.

Houdusse, A., V. N. Kalabokis, D. Himmel, A. G. Szent-Gyorgyi and C. Cohen (1999). "Atomic structure of scallop myosin subfragment S1 complexed with MgADP: a novel conformation of the myosin head." Cell **97**(4): 459-470.

Houdusse, A., A. G. Szent-Gyorgyi and C. Cohen (2000). "Three conformational states of scallop myosin S1." Proc Natl Acad Sci U S A **97**(21): 11238-11243.

Huxley, A. F. (1957). "Muscle structure and theories of contraction." Prog Biophys Biophys Chem **7**: 255-318.

Huxley, A. F. and R. Niedergerke (1954). "Structural Changes in Muscle During Contraction: Interference Microscopy of Living Muscle Fibres." Nature **173**(4412): 971-973.

Huxley, A. F. and R. M. Simmons (1971). "Proposed mechanism of force generation in striated muscle." Nature **233**(5321): 533-538.

Huxley, H. and J. Hanson (1954). "Changes in the Cross-Striations of Muscle during Contraction and Stretch and their Structural Interpretation." Nature **173**(4412): 973-976.

Huxley, H. E. (1957). "The double array of filaments in cross-striated muscle." J Biophys Biochem Cytol **3**(5): 631-648.

Huxley, H. E. (1969). "The mechanism of muscular contraction." Science **164**(3886): 1356-1365.

Hynes, T. R., S. M. Block, B. T. White and J. A. Spudich (1987). "Movement of myosin fragments in vitro: domains involved in force production." Cell **48**(6): 953-963.

Jenkins, J. and M. Cook (2004). "Mosquito®: An Accurate Nanoliter Dispensing Technology." Journal of the Association for Laboratory Automation **9**(4): 257-261.

Josephson, R. K., J. G. Malamud and D. R. Stokes (2000). "Asynchronous muscle: a primer." J Exp Biol **203**(Pt 18): 2713-2722.

Kabsch, W. (2010). "XDS." Acta Crystallogr D Biol Crystallogr **66**(Pt 2): 125-132.

Kliche, W., S. Fujita-Becker, M. Kollmar, D. J. Manstein and F. J. Kull (2001). "Structure of a genetically engineered molecular motor." EMBO J **20**(1-2): 40-46.

Knetsch, M. L., T. Q. Uyeda and D. J. Manstein (1999). "Disturbed communication between actin- and nucleotide-binding sites in a myosin II with truncated 50/20-kDa junction." J Biol Chem **274**(29): 20133-20138.

Kollmar, M., U. Durrwang, W. Kliche, D. J. Manstein and F. J. Kull (2002). "Crystal structure of the motor domain of a class-I myosin." EMBO J **21**(11): 2517-2525.

Kristinsson, H. G. (2001). "EVALUATION OF DIFFERENT METHODS TO ISOLATE COD (GADUS MORHUA) MUSCLE MYOSIN." Journal of Food Biochemistry **25**(3): 249-256.

Kronert, W., C. Dambacher, A. Knowles, D. Swank and S. Bernstein (2008). "Alternative relay domains of Drosophila melanogaster myosin differentially affect ATPase activity, in vitro motility, myofibril structure and muscle function." J Mol Biol **379**(3): 443-456.

Kronert, W. A., C. M. Dambacher, A. F. Knowles, D. M. Swank and S. I. Bernstein (2008). "Alternative relay domains of Drosophila melanogaster myosin differentially affect ATPase activity, in vitro motility, myofibril structure and muscle function." Journal of Molecular Biology **379**(3): 443-456.

Kronert, W. A., C. M. Dambacher, A. F. Knowles, D. M. Swank and S. I. Bernstein (2008). "Alternative relay domains of Drosophila melanogaster myosin differentially affect ATPase activity, in vitro motility, myofibril structure and muscle function." J Mol Biol **379**(3): 443-456.

Kronert, W. A., G. C. Melkani, A. Melkani and S. I. Bernstein (2010). "Mutating the converter-relay interface of Drosophila myosin perturbs ATPase activity, actin motility, myofibril stability and flight ability." J Mol Biol **398**(5): 625-632.

Kronert, W. A., G. C. Melkani, A. Melkani and S. I. Bernstein (2012). "Alternative relay and converter domains tune native muscle myosin isoform function in Drosophila." J Mol Biol **416**(4): 543-557.

Kronert, W. A., P. T. O'Donnell, A. Fieck, A. Lawn, J. O. Vigoreaux, J. C. Sparrow and S. I. Bernstein (1995). "Defects in the Drosophila myosin rod permit sarcomere assembly but cause flight muscle degeneration." J Mol Biol **249**(1): 111-125.

Kull, F. J. and S. A. Endow (2013). "Force generation by kinesin and myosin cytoskeletal motor proteins." J Cell Sci **126**(Pt 1): 9-19.

Laemmli, U. K. (1970). "Cleavage of structural proteins during the assembly of the head of bacteriophage T4." Nature **227**(5259): 680-685.

Levine, J. D. and R. J. Wyman (1973). "Neurophysiology of flight in wild-type and a mutant Drosophila." Proc Natl Acad Sci U S A **70**(4): 1050-1054.

Littlefield, K., D. Swank, B. Sanchez, A. Knowles, D. Warshaw and S. Bernstein (2003). "The converter domain modulates kinetic properties of Drosophila myosin." Am J Physiol Cell Physiol **284**(4): C1031-1038.

Littlefield, K. P., D. M. Swank, B. M. Sanchez, A. F. Knowles, D. M. Warshaw and S. I. Bernstein (2003). "The converter domain modulates kinetic properties of Drosophila myosin." Am J Physiol Cell Physiol **284**(4): C1031-1038.

Littlefield, K. P., A. B. Ward, J. S. Chappie, M. K. Reedy, S. I. Bernstein, R. A. Milligan and M. C. Reedy (2008). "Similarities and differences between frozen-hydrated, rigor acto-S1 complexes of insect flight and chicken skeletal muscles." J Mol Biol **381**(3): 519-528.

Lohmann, K. (1929). "Über die Pyrophosphatfraktion im Muskel." Naturwissenschaften **17**(31): 624-625.

Lompre, A. M., J. J. Mercadier, C. Wisnewsky, P. Bouveret, C. Pantaloni, A. D'Albis and K. Schwartz (1981). "Species- and age-dependent changes in the relative amounts of cardiac myosin isoenzymes in mammals." Dev Biol **84**(2): 286-290.

Long, F., A. A. Vagin, P. Young and G. N. Murshudov (2008). "BALBES: a molecular-replacement pipeline." Acta Crystallogr D Biol Crystallogr **64**(Pt 1): 125-132.

Lowey, S., L. M. Lesko, A. S. Rovner, A. R. Hodges, S. L. White, R. B. Low, M. Rincon, J. Gulick and J. Robbins (2008). "Functional effects of the hypertrophic

cardiomyopathy R403Q mutation are different in an alpha- or beta-myosin heavy chain backbone." J Biol Chem **283**(29): 20579-20589.

Lucas-Lopez, C., J. S. Allingham, T. Lebl, C. P. Lawson, R. Brenk, J. R. Sellers, I. Rayment and N. J. Westwood (2008). "The small molecule tool (S)-(-)-blebbistatin: novel insights of relevance to myosin inhibitor design." Org Biomol Chem **6**(12): 2076-2084.

Lymn, R. W. and E. W. Taylor (1971). "Mechanism of adenosine triphosphate hydrolysis by actomyosin." Biochemistry **10**(25): 4617-4624.

Malik, F. I., J. J. Hartman, K. A. Elias, B. P. Morgan, H. Rodriguez, K. Brejc, R. L. Anderson, S. H. Sueoka, K. H. Lee, J. T. Finer, R. Sakowicz, R. Baliga, D. R. Cox, M. Garard, G. Godinez, R. Kawas, E. Kraynack, D. Lenzi, P. P. Lu, A. Muci, C. Niu, X. Qian, D. W. Pierce, M. Pokrovskii, I. Suehiro, S. Sylvester, T. Tochimoto, C. Valdez, W. Wang, T. Katori, D. A. Kass, Y. T. Shen, S. F. Vatner and D. J. Morgans (2011). "Cardiac myosin activation: a potential therapeutic approach for systolic heart failure." Science **331**(6023): 1439-1443.

Manstein, D. J. and D. M. Hunt (1995). "Overexpression of myosin motor domains in Dictyostelium: screening of transformants and purification of the affinity tagged protein." J Muscle Res Cell Motil **16**(3): 325-332.

Manstein, D. J., H. P. Schuster, P. Morandini and D. M. Hunt (1995). "Cloning vectors for the production of proteins in Dictyostelium discoideum." Gene **162**(1): 129-134.

Margossian, S. S. and S. Lowey (1982). [7] Preparation of myosin and its subfragments from rabbit skeletal muscle. Methods in Enzymology. L. W. C. Dixie W. Frederiksen, Academic Press. **Volume 85:** 55-71.

Margossian, S. S. and S. Lowey (1982). "Preparation of myosin and its subfragments from rabbit skeletal muscle." Methods Enzymol **85 Pt B**: 55-71.

Marygold, S. J., P. C. Leyland, R. L. Seal, J. L. Goodman, J. Thurmond, V. B. Strelets and R. J. Wilson (2013). "FlyBase: improvements to the bibliography." Nucleic Acids Res **41**(Database issue): D751-757.

McLachlan, A. D. and J. Karn (1982). "Periodic charge distributions in the myosin rod amino acid sequence match cross-bridge spacings in muscle." Nature **299**(5880): 226-231.

McPherson, A. (1995). "INCREASING THE SIZE OF MICROCRYSTALS BY FINE SAMPLING OF PH LIMITS." Journal of Applied Crystallography **28**: 362-365.

Meador, W. E., A. R. Means and F. A. Quiocho (1992). "Target enzyme recognition by calmodulin: 2.4 A structure of a calmodulin-peptide complex." Science **257**(5074): 1251-1255.

Menetrey, J., A. Bahloul, A. L. Wells, C. M. Yengo, C. A. Morris, H. L. Sweeney and A. Houdusse (2005). "The structure of the myosin VI motor reveals the mechanism of directionality reversal." Nature **435**(7043): 779-785.

Miller, B., M. Bloemink, M. Nyitrai, S. Bernstein and M. Geeves (2007). "A variable domain near the ATP-binding site in Drosophila muscle myosin is part of the communication pathway between the nucleotide and actin-binding sites." J Mol Biol **368**(4): 1051-1066.

Miller, B. M., M. J. Bloemink, M. Nyitrai, S. I. Bernstein and M. A. Geeves (2007). "A variable domain near the ATP-binding site in Drosophila muscle myosin is part of the communication pathway between the nucleotide and actin-binding sites." J Mol Biol **368**(4): 1051-1066.

Miller, B. M., M. Nyitrai, S. I. Bernstein and M. A. Geeves (2003). "Kinetic analysis of Drosophila muscle myosin isoforms suggests a novel mode of mechanochemical coupling." J Biol Chem **278**(50): 50293-50300.

Miller, B. M., S. Zhang, J. A. Suggs, D. M. Swank, K. P. Littlefield, A. F. Knowles and S. I. Bernstein (2005). "An alternative domain near the nucleotide-binding site of Drosophila muscle myosin affects ATPase kinetics." J Mol Biol **353**(1): 14-25.

Mooseker, M. S. and B. J. Foth (2008). The structural and functional diversity of the myosin family of actin-based molecular motors. Myosins: A Superfamily of Molecular Motors. L. M. Coluccio, Springer. **7:** 1-34.

Mueller, H. and S. V. Perry (1962). "The degradation of heavy meromyosin by trypsin." Biochem J **85**: 431-439.

Murshudov, G. N., P. Skubak, A. A. Lebedev, N. S. Pannu, R. A. Steiner, R. A. Nicholls, M. D. Winn, F. Long and A. A. Vagin (2011). "REFMAC5 for the refinement of macromolecular crystal structures." Acta Crystallogr D Biol Crystallogr **67**(Pt 4): 355-367.

Na, J., L. P. Musselman, J. Pendse, T. J. Baranski, R. Bodmer, K. Ocorr and R. Cagan (2013). "A Drosophila model of high sugar diet-induced cardiomyopathy." PLoS Genet **9**(1): e1003175.

Niemann, H. H., M. L. Knetsch, A. Scherer, D. J. Manstein and F. J. Kull (2001). "Crystal structure of a dynamin GTPase domain in both nucleotide-free and GDP-bound forms." EMBO J **20**(21): 5813-5821.

Nongthomba, U., S. Pasalodos-Sanchez, S. Clark, J. D. Clayton and J. C. Sparrow (2001). "Expression and function of the Drosophila ACT88F actin isoform is not restricted to the indirect flight muscles." J Muscle Res Cell Motil **22**(2): 111-119.

Null, B., C. W. Liu, M. Hedehus, S. Conolly and R. W. Davis (2008). "High-resolution, in vivo magnetic resonance imaging of Drosophila at 18.8 Tesla." PLoS One **3**(7): e2817.

Odronitz, F. and M. Kollmar (2007). "Drawing the tree of eukaryotic life based on the analysis of 2,269 manually annotated myosins from 328 species." Genome Biol **8**(9): R196.

Odronitz, F. and M. Kollmar (2008). "Comparative genomic analysis of the arthropod muscle myosin heavy chain genes allows ancestral gene reconstruction and reveals a new type of 'partially' processed pseudogene." BMC Mol Biol **9**: 21.

Onishi, H., T. Ohki, N. Mochizuki and M. Morales (2002). "Early stages of energy transduction by myosin: roles of Arg in switch I, of Glu in switch II, and of the salt-bridge between them." Proc Natl Acad Sci U S A **99**(24): 15339-15344.

Pak, W. L., Grabowski, S. R (1986). The Genetics and biology of Drosophila, Academic Press.

Pandey, U. B. and C. D. Nichols (2011). "Human disease models in Drosophila melanogaster and the role of the fly in therapeutic drug discovery." Pharmacol Rev **63**(2): 411-436.

Parker, V. P., S. Falkenthal and N. Davidson (1985). "Characterization of the myosin light-chain-2 gene of Drosophila melanogaster." Mol Cell Biol **5**(11): 3058-3068.

Patterson, B. and J. A. Spudich (1995). "A novel positive selection for identifying cold-sensitive myosin II mutants in Dictyostelium." Genetics **140**(2): 505-515.

Patterson, B. and J. A. Spudich (1996). "Cold-sensitive mutations of Dictyostelium myosin heavy chain highlight functional domains of the myosin motor." Genetics **143**(2): 801-810.

Peckham, M., J. E. Molloy, J. C. Sparrow and D. C. White (1990). "Physiological properties of the dorsal longitudinal flight muscle and the tergal depressor of the trochanter muscle of Drosophila melanogaster." J Muscle Res Cell Motil **11**(3): 203-215.

Preller, M., S. Bauer, N. Adamek, S. Fujita-Becker, R. Fedorov, M. A. Geeves and D. J. Manstein (2011). "Structural basis for the allosteric interference of myosin function by reactive thiol region mutations G680A and G680V." J Biol Chem **286**(40): 35051-35060.

Preller, M., K. Chinthalapudi, R. Martin, H. J. Knolker and D. J. Manstein (2011). "Inhibition of Myosin ATPase activity by halogenated pseudilins: a structure-activity study." J Med Chem **54**(11): 3675-3685.

Qian, L. and R. Bodmer (2012). "Probing the polygenic basis of cardiomyopathies in Drosophila." J Cell Mol Med **16**(5): 972-977.

Ramanath, S., Q. Wang, S. I. Bernstein and D. M. Swank (2011). "Disrupting the myosin converter-relay interface impairs Drosophila indirect flight muscle performance." Biophys J **101**(5): 1114-1122.

Rayment, I., H. Holden, M. Whittaker, C. Yohn, M. Lorenz, K. Holmes and R. Milligan (1993). "Structure of the actin-myosin complex and its implications for muscle contraction." Science **261**(5117): 58-65.

Rayment, I., W. Rypniewski, K. Schmidt-Bäse, R. Smith, D. Tomchick, M. Benning, D. Winkelmann, G. Wesenberg and H. Holden (1993). "Three-dimensional structure of myosin subfragment-1: a molecular motor." Science **261**(5117): 50-58.

Rayment, I., W. R. Rypniewski, K. Schmidt-Base, R. Smith, D. R. Tomchick, M. M. Benning, D. A. Winkelmann, G. Wesenberg and H. M. Holden (1993). "Three-dimensional structure of myosin subfragment-1: a molecular motor." Science **261**(5117): 50-58.

Reedy, M. C. and C. Beall (1993). "Ultrastructure of developing flight muscle in Drosophila. I. Assembly of myofibrils." Dev Biol **160**(2): 443-465.

Reedy, M. C., B. Bullard and J. O. Vigoreaux (2000). "Flightin is essential for thick filament assembly and sarcomere stability in Drosophila flight muscles." J Cell Biol **151**(7): 1483-1500.

Reiter, L. T., L. Potocki, S. Chien, M. Gribskov and E. Bier (2001). "A systematic analysis of human disease-associated gene sequences in Drosophila melanogaster." Genome Research **11**(6): 1114-1125.

Resetar, A. M. and J. M. Chalovich (1995). "Adenosine 5'-(gamma-thiotriphosphate): an ATP analog that should be used with caution in muscle contraction studies." Biochemistry **34**(49): 16039-16045.

Resnicow, D. I., J. C. Deacon, H. M. Warrick, J. A. Spudich and L. A. Leinwand (2010). "Functional diversity among a family of human skeletal muscle myosin motors." Proc Natl Acad Sci U S A **107**(3): 1053-1058.

Reubold, T. F., S. Eschenburg, A. Becker, F. J. Kull and D. J. Manstein (2003). "A structural model for actin-induced nucleotide release in myosin." Nat Struct Biol **10**(10): 826-830.

Risal, D., S. Gourinath, D. M. Himmel, A. G. Szent-Gyorgyi and C. Cohen (2004). "Myosin subfragment 1 structures reveal a partially bound nucleotide and a complex salt bridge that helps couple nucleotide and actin binding." Proc Natl Acad Sci U S A **101**(24): 8930-8935.

Rozek, C. E. and N. Davidson (1983). "Drosophila has one myosin heavy-chain gene with three developmentally regulated transcripts." Cell **32**(1): 23-34.

Rupp, B. (2003). "Maximum-likelihood crystallization." Journal of Structural Biology **142**(1): 162-169.

Sasaki, N., R. Ohkura and K. Sutoh (2000). "Insertion or deletion of a single residue in the strut sequence of Dictyostelium myosin II abolishes strong binding to actin." J Biol Chem **275**(49): 38705-38709.

Schoenberg, M. (1989). "Effect of adenosine triphosphate analogues on skeletal muscle fibers in rigor." Biophys J **56**(1): 33-41.

Sellers, J. (1999). Myosins, OUP Oxford.

Sellers, J. R. (2000). "Myosins: a diverse superfamily." Biochim Biophys Acta **1496**(1): 3-22.

Silva, R., J. C. Sparrow and M. A. Geeves (2003). "Isolation and kinetic characterisation of myosin and myosin S1 from the Drosophila indirect flight muscles." J Muscle Res Cell Motil **24**(8): 489-498.

Slayter, H. S. and S. Lowey (1967). "Substructure of the myosin molecule as visualized by electron microscopy." Proc Natl Acad Sci U S A **58**(4): 1611-1618.

Smith, C. A. and I. Rayment (1995). "X-ray structure of the magnesium(II)-pyrophosphate complex of the truncated head of Dictyostelium discoideum myosin to 2.7 A resolution." Biochemistry **34**(28): 8973-8981.

Smith, C. A. and I. Rayment (1996). "X-ray structure of the magnesium(II).ADP.vanadate complex of the Dictyostelium discoideum myosin motor domain to 1.9 A resolution." Biochemistry **35**(17): 5404-5417.

Straight, A. F., A. Cheung, J. Limouze, I. Chen, N. J. Westwood, J. R. Sellers and T. J. Mitchison (2003). "Dissecting temporal and spatial control of cytokinesis with a myosin II Inhibitor." Science **299**(5613): 1743-1747.

Suggs, J. A., A. Cammarato, W. A. Kronert, M. Nikkhoy, C. M. Dambacher, A. Megighian and S. I. Bernstein (2007). "Alternative S2 hinge regions of the myosin rod differentially affect muscle function, myofibril dimensions and myosin tail length." J Mol Biol **367**(5): 1312-1329.

Swank, D., A. Knowles, W. Kronert, J. Suggs, G. Morrill, M. Nikkhoy, G. Manipon and S. Bernstein (2003). "Variable N-terminal regions of muscle myosin heavy chain modulate ATPase rate and actin sliding velocity." J Biol Chem **278**(19): 17475-17482.

Swank, D., A. Knowles, J. Suggs, F. Sarsoza, A. Lee, D. Maughan and S. Bernstein (2002). "The myosin converter domain modulates muscle performance." Nat Cell Biol **4**(4): 312-316.

Swank, D. M. (2012). "Mechanical analysis of Drosophila indirect flight and jump muscles." Methods **56**(1): 69-77.

Swank, D. M., M. L. Bartoo, A. F. Knowles, C. Iliffe, S. I. Bernstein, J. E. Molloy and J. C. Sparrow (2001). "Alternative exon-encoded regions of Drosophila myosin heavy chain modulate ATPase rates and actin sliding velocity." J Biol Chem **276**(18): 15117-15124.

Swank, D. M., J. Braddock, W. Brown, H. Lesage, S. I. Bernstein and D. W. Maughan (2006). "An alternative domain near the ATP binding pocket of Drosophila myosin affects muscle fiber kinetics." Biophys J **90**(7): 2427-2435.

Swank, D. M., A. F. Knowles, W. A. Kronert, J. A. Suggs, G. E. Morrill, M. Nikkhoy, G. G. Manipon and S. I. Bernstein (2003). "Variable N-terminal regions of muscle myosin heavy chain modulate ATPase rate and actin sliding velocity." J Biol Chem **278**(19): 17475-17482.

Swank, D. M., W. A. Kronert, S. I. Bernstein and D. W. Maughan (2004). "Alternative N-terminal regions of Drosophila myosin heavy chain tune muscle kinetics for optimal power output." Biophys J **87**(3): 1805-1814.

Swank, D. M., L. Wells, W. A. Kronert, G. E. Morrill and S. I. Bernstein (2000). "Determining structure/function relationships for sarcomeric myosin heavy chain

by genetic and transgenic manipulation of Drosophila." Microsc Res Tech **50**(6): 430-442.

Szent-Györgyi, A. (1945). "Studies on muscle." Acta Physiol Scand **9**: 25.

Szent-Gyorgyi, A. G. (1953). "Meromyosins, the subunits of myosin." Arch Biochem Biophys **42**(2): 305-320.

Szent-Gyorgyi, A. G. (2004). "The early history of the biochemistry of muscle contraction." J Gen Physiol **123**(6): 631-641.

Tardiff, J. C. (2005). "Sarcomeric proteins and familial hypertrophic cardiomyopathy: linking mutations in structural proteins to complex cardiovascular phenotypes." Heart Fail Rev **10**(3): 237-248.

Taylor, M. V. (2006). Comparison of muscle development in Drosophila and vertebrates. Muscle Development in Drosophila. H. Sink. Georgetown, TX, Landes Bioscience**:** 169-203.

Terwilliger, T. C., R. W. Grosse-Kunstleve, P. V. Afonine, N. W. Moriarty, P. H. Zwart, L. W. Hung, R. J. Read and P. D. Adams (2008). "Iterative model building, structure refinement and density modification with the PHENIX AutoBuild wizard." Acta Crystallogr D Biol Crystallogr **64**(Pt 1): 61-69.

The PyMOL Molecular Graphics System. (2011).

Titus, M. A., G. Ashiba and A. G. Szent-Gyorgyi (1989). "SH-1 modification of rabbit myosin interferes with calcium regulation." J Muscle Res Cell Motil **10**(1): 25-33.

Trybus, K. M. (1994). "Regulation of expressed truncated smooth muscle myosins. Role of the essential light chain and tail length." J Biol Chem **269**(33): 20819-20822.

Tyska, M. J., D. E. Dupuis, W. H. Guilford, J. B. Patlak, G. S. Waller, K. M. Trybus, D. M. Warshaw and S. Lowey (1999). "Two heads of myosin are better than one for generating force and motion." Proc Natl Acad Sci U S A **96**(8): 4402-4407.

Tyska, M. J. and D. M. Warshaw (2002). "The myosin power stroke." Cell Motil Cytoskeleton **51**(1): 1-15.

Vagin, A. and A. Teplyakov (2010). "Molecular replacement with MOLREP." Acta Crystallogr D Biol Crystallogr **66**(Pt 1): 22-25.

Vogel, S. and A. de Ferrari (2001). Prime mover: A Natural History of Muscle, W W Norton & Company Incorporated.

Walker, J. E., M. Saraste, M. J. Runswick and N. J. Gay (1982). "Distantly related sequences in the alpha- and beta-subunits of ATP synthase, myosin, kinases and other ATP-requiring enzymes and a common nucleotide binding fold." EMBO J **1**(8): 945-951.

Wang, Q., C. L. Moncman and D. A. Winkelmann (2003). "Mutations in the motor domain modulate myosin activity and myofibril organization." J Cell Sci **116**(Pt 20): 4227-4238.

Weber, H. H. (1935). "Der feinbau und die mechanischen eigenschaften des myosin-fadens.
." Arch. Physiol. **235**: 205-233.

Weiss, A. and L. A. Leinwand (1996). "The mammalian myosin heavy chain gene family." Annu Rev Cell Dev Biol **12**: 417-439.

Weiss, A., S. Schiaffino and L. A. Leinwand (1999). "Comparative sequence analysis of the complete human sarcomeric myosin heavy chain family: implications for functional diversity." J Mol Biol **290**(1): 61-75.

Wells, L., K. A. Edwards and S. I. Bernstein (1996). "Myosin heavy chain isoforms regulate muscle function but not myofibril assembly." EMBO J **15**(17): 4454-4459.

Yang, C., S. Ramanath, W. A. Kronert, S. I. Bernstein, D. W. Maughan and D. M. Swank (2008). "Alternative versions of the myosin relay domain differentially respond to load to influence Drosophila muscle kinetics." Biophys J **95**(11): 5228-5237.

Yang, C. X., S. Ramanath, W. A. Kronert, S. I. Bernstein, D. W. Maughan and D. M. Swank (2008). "Alternative Versions of the Myosin Relay Domain Differentially Respond to Load to Influence Drosophila Muscle Kinetics." Biophysical Journal **95**(11): 5228-5237.

Yang, Y., S. Gourinath, M. Kovács, L. Nyitray, R. Reutzel, D. Himmel, E. O'Neall-Hennessey, L. Reshetnikova, A. Szent-Györgyi, J. Brown and C. Cohen (2007). "Rigor-like structures from muscle myosins reveal key mechanical elements in the transduction pathways of this allosteric motor." Structure **15**(5): 553-564.

Zhang, S. and S. I. Bernstein (2001). "Spatially and temporally regulated expression of myosin heavy chain alternative exons during Drosophila embryogenesis." Mech Dev **101**(1-2): 35-45.